

B E R I C H T E

aus dem

INSTITUT FÜR MEERESKUNDE

an der

CHRISTIAN-ALBRECHTS-UNIVERSITÄT · KIEL

Nr. 20b

Inverse Analysis of the

Trimooored

Internal Wave Experiment (IWEX)

Part 2

by

J. Willebrand<sup>1)</sup>, P. Müller<sup>2)</sup>, D.J. Olbers<sup>2)</sup>

1) Institut für Meereskunde an der Universität Kiel

2) Institut für Geophysik, Universität Hamburg  
Max-Planck-Institut für Meteorologie, Hamburg

DOI 10.3289/IFM\_BER\_206

-----  
1977

TABLE CAPTIONS

- I.1 : Current meter array: depths, instruments, N-profile
- I.2 : Mean data set: frequencies, edofs, 95% conf. limit and bias for zero true coherence
- I.3 : Number of spectra used in the analysis
  
- II.1 : Symmetry and isotropy relations for propagating waves
- II.2 : Number of independent moments and relations for propagating waves
- II.3 : Consistency and isotropy relations for standing modes
- II.4 : Number of independent moments and relations for standing modes
- II.5 : Fundamental invariants, structure of cross spectral matrix and invariance relations for various transformation classes
  
- III.1 : Properties of various metrics
  
- IV.1 : Number of different cross-spectral components and number of independent consistency relations
- IV.2 : Results of consistency tests
  
- V.1 : Models of internal wave spectrum
- V.2 : Normalization factor  $I(t,s)$  and conversion factor  $J(t,s)$  for various values of  $t$  and  $s$

FIGURE CAPTIONS

- I.1 : Location of IWEX (from Briscoe, 1975)
  - I.2 : N-profile and array geometry
  - I.3 : (a) Low-passed temperatures (courtesy of C. Frankignoul)  
(b) Low-passed current vectors (from Frankignoul and Joyce, 1977)
  - I.4 : Vertical wavenumber spectrum of vertical displacement (from Hayes, 1975)
  - I.5 : Time variability of energy (inertial, tidal and internal wave continuum)
  - I.6 : Histogram of sensor separations
  - I.7 : Autospectra at C6: (a) east, (b) north, (c) up (courtesy of M. Briscoe)
  - I.8 : Average rotary autospectra: (a) current, (b) displacement
  - I.9 : Examples of coherences and phases as function of frequency: (a) slant east, (b) slant up, (c) horizontal east, (d) horizontal up (courtesy of M. Briscoe)
  - I.10 : Examples of coherences and phases as function of separation for  $\omega_3$  :  
(a) slant separation, (b) horizontal separation
  - I.11 : Same for  $\omega_6$
  - I.12 : Same for  $\omega_{13}$
  - I.13 : Same for  $\omega_{20}$
  - I.14 : Same for  $\omega_{28}$
  - I.15 : Up coherences as a function of frequency for various slant separations on leg A
- 
- III.1 : Sketch of data space
  - III.2 : Reduction factor
- 
- IV.1 : Consistency tests: zero model, white noise, finestructure. Also included are the equivalent degrees of freedom (edof)
  - IV.2 : Consistency tests: basic assumptions of GM model
  - IV.3 : Consistency tests: homogeneity and WKB-scaling
  - IV.4 : Consistency tests: homogeneity and WKB-scaling for  $\zeta$  and  $u, v$  separately
  - IV.5 : Consistency tests: symmetric and isotropic field of propagating waves
  - IV.6 : Consistency tests: horizontal isotropy
  - IV.7 : Consistency tests: vertical symmetry
  - IV.8 : Averaged coherences between rotary velocity components
  - IV.9 : Consistency tests: propagating waves
  - IV.10 : Normalized mean scaled autospectra  $P_{\zeta\zeta}$  and  $P_{++} + P_{--}$
  - IV.11 : Normalized mean scaled autospectra  $P_{\zeta\zeta}$ ,  $P_{++}$  and  $P_{--}$
  - IV.12 : Phases  $\phi_{+\zeta}$  and  $\phi_{-\zeta}$  of mean cross-spectra
  - IV.13 : Consistency tests: standing/propagating waves (discriminating tests)
  - IV.14 : Consistency tests: standing/propagating waves (all tests)

FIGURES:

- IV.15 : Consistency tests: isotropic field of standing modes
- IV.16 : Consistency tests: combination of standing and propagating waves
- IV.17 : Consistency tests:  $D_3^{ij} = 0$  and  $D_4^{ij} = 0$
- IV.18 : Consistency tests:  $D_1^{ij} = 0$  for arbitrary and zero separations
- IV.19 : Consistency tests:  $D_1^{ij} = 0$  for slant and horizontal separations
- IV.20 : Consistency tests: propagating waves contaminated by white noise
- IV.21 : Consistency tests: propagating waves contaminated by finestructure
- IV.22 : Consistency tests: internal waves contaminated by coherent noise
- IV.23 : Consistency tests: IWEX model class
  
- V.1 : Hybrid IWEX model: Internal wave energies
- V.2 : Vertical asymmetry  $E^\uparrow - E^\downarrow$  for displacements and current separately
- V.3 : Wavenumber distribution model: (a) for  $s = 1$  and various  $t$ ,  
(b) for  $t = 2$  and various  $s$
- V.4 : Vertical model coherences for  $s = 2$  and  $t = 2, 3, 4$  and  $5$ : (a) for constant equivalent bandwidth, (b) for constant bandwidth scale parameter
- V.5 : Slant up coherence for  $\omega_6$ ,  $\omega_8$  and  $\omega_{18}$
- V.6 : Hybrid IWEX model: equivalent mode number (bandwidth)
- V.7 : IWEX dispersion relation (courtesy of M. Briscoe)
- V.8 : Horizontal wavenumber spectrum of vertical displacement (from Katz, 1975)
- V.9 : Sketch of reciprocal relation between wavenumber spectrum and coherence
- V.10 : Horizontal up coherence for  $\omega_4$ ,  $\omega_{11}$ ,  $\omega_{21}$  and  $\omega_{28}$
- V.11 : Same as V.10, logarithmical presentation
- V.12 : Hybrid IWEX model: high-wavenumber slope
- V.13 : Slant normalized cospectrum for  $\omega_5$ ,  $\omega_9$  and  $\omega_{18}$
- V.14 : Hybrid IWEX model: peak mode number
- V.15 : Modes of IWEX profile for  $\omega_{15}$  (courtesy of F. Schott)
- V.16 : Hybrid IWEX model: peak shape parameter
- V.17 : Relation between model isotropy parameter and beamwidth
- V.18 : Model coherence  $\gamma_{+-}$  as function of beamwidth
- V.19 : Coherences and phases at C6
- V.20 : Hybrid IWEX model: mean propagation direction and isotropy parameter (beamwidth)
- V.21 : Inverse fit for pure internal wave model, slant and horizontal coherence for  $\omega_{26}$
- V.22 : Coherence disparity in frequency domain, full circles  $\gamma_{00}$ , open circles  $\gamma_{--}$ , triangles  $\gamma_{++}$
- V.23 : Horizontal coherences for  $\omega_{21}$ , full circle  $u_{00}$ , open circle  $u_{u-}$
- V.24 : Slant coherences for  $\omega_{21}$ , full circle  $u_{00}$ , open circle  $u_{u-}$

FIGURES:

- V.25 : Hybrid IWEX model: finestructure ratio
- V.26 : Hybrid IWEX model: finestructure correlation scale
- V.27 : Hybrid IWEX model: energy of internal wave field and current contamination
- V.28 : Hybrid IWEX model: horizontal coherence drop of current contamination
- V.29 : Inverse fit of slant coherence at  $\omega_{26}$
- V.30 : Sketch of energy and coherence disparities
- V.31 : Total wave energy for ups and currents separately
- V.32 : Parameters of the hybrid IWEX model, (a) internal wave field, (b) up-contamination, (c) current contamination
- V.33 : Consistency of IWEX model; distance squared between model and data point with expectation value and 95% confidence limit
- V.34 : Consistency of IWEX model; normalized distance squared with 95% confidence limit
- V.35 : Parameter correlations: (a)  $E^\uparrow - E^\downarrow$ ,  $E^\uparrow - \delta_f$ ,  $E^\downarrow - \delta_f$ , (b)  $E^\uparrow - E_{\text{cont}}$ ,  $E^\downarrow - E_{\text{cont}}$  (c)  $E^\uparrow - j_e$ ,  $E_{\text{cont}} - j_e$ , (d)  $j_e - j_p$ ,  $j_e - t$ , (e)  $E^\uparrow - q$ ,  $E^\downarrow - q$  (f)  $q - \varphi_0$ ,  $j_e - q$ ,  $E_{\text{cont}} - t$
- V.36 : Sections through the minimum of  $\epsilon^2(x_\alpha)$ .

Depth (m)	Level	Leg A	Leg B	Leg C	N (cph)
603.6	1	VACM <sup>+</sup>		VACM	2.54
605.7	2	VACM	VACM	VACM	2.54
610.6	4	VACM <sup>+</sup>	VACM <sup>+</sup>		2.55
639.5	5	VACM <sup>+</sup>	VACM <sup>+</sup>	VACM <sup>+</sup>	2.60
730.6	6	VACM	VACM	VACM <sup>+</sup>	2.76
1014.4	8	VACM			2.07
1023.1	10	VACM	VACM <sup>+</sup>	VACM <sup>+</sup>	2.05
2050.4	14	850	850	850	0.66

TABLE I.1 Current meter array (from Briscoe 1975). Asterices indicate instruments used for mean data set of horizontal currents.  
N from Knorr cruise 34 mean.

Frequency No.	cpn	Period h	Average over original frequencies	Equiv. degrees of freedom	Bias for zero true coherence	C <sub>95</sub> for zero true coherence
3	.0400	25.0	1	48	.20	.35
4	.0533	18.8	1	48	.20	.35
5	.0667	15.0	1	48	.20	.35
6	.0800	12.5	1	48	.20	.35
7	.0933	10.7	1	48	.20	.35
8	.1067	9.4	1	48	.20	.35
9	.1200	8.3	1	48	.20	.35
10	.1333	7.5	1	48	.20	.35
11	.1466	6.8	2	64	.18	.30
12	.1733	5.8	2	64	.18	.30
13	.2000	5.0	2	64	.18	.30
14	.2266	4.4	2	64	.18	.30
15	.2600	3.8	3	84	.15	.27
16	.3000	3.3	3	84	.15	.27
17	.3400	2.9	3	84	.15	.27
18	.3866	2.6	4	105	.14	.24
19	.4400	2.3	4	105	.14	.24
20	.5000	2.0	5	126	.13	.22
21	.5733	1.74	6	148	.12	.20
22	.6600	1.52	7	170	.11	.19
23	.7600	1.32	8	193	.10	.18
24	.8667	1.15	8	193	.10	.18
25	.9866	1.01	10	237	.09	.16
26	1.1333	.88	12	281	.08	.15
27	1.3000	.77	13	303	.08	.14
28	1.487	.67	15	347	.08	.13
29	1.700	.59	17	392	.07	.12
30	1.947	.51	20	458	.07	.12

1  
2  
1

TABLE I.2: Mean data set: frequencies, edofs, 95% conf. limit and bias for zero true coherence.

frequency interval	3 - 21	22 - 29	30
total number of spectra	1444	1225	729
number of autospectra	38	35	27
number of cross-spectra	1406	1190	702
Number of cross-spectra with vertical separation	1218	1008	562
Number of cross-spectra with purely horizontal separation	134	128	98
Number of cross-spectra with no separation	54	54	42

TABLE I.3: Number of spectra used in the analysis



	slant separation	horizontal separation	vertical separation	no separation $M_m = M_m^*$
Symmetry		$M_1^{ij} = 0$ $M_{-1}^{ij} = 0$	$\Im m \{ M_0^{ij} \} = 0$ $M_1^{ij} + [M_{-1}^{ij}]^* = 0$ $M_2^{ij} - [M_{-2}^{ij}]^* = 0$	$M_1 = 0$
Isotropy	$e^{-i\gamma} M_{-1}^{ij} - e^{i\gamma} M_1^{ij} = 0$ $e^{-2i\gamma} M_{-2}^{ij} - e^{2i\gamma} M_2^{ij} = 0$	$\Im m \{ M_0^{ij} \} = 0$ $M_1^{ij} + [M_{-1}^{ij}]^* = 0$ $\Re e \{ e^{-i\gamma} M_{-1}^{ij} \} = 0$ $M_2^{ij} - [M_{-2}^{ij}]^* = 0$ $\Im m \{ e^{-2i\gamma} M_{-2}^{ij} \} = 0$	$M_1^{ij} = 0$ $M_{-1}^{ij} = 0$ $M_2^{ij} = 0$ $M_{-2}^{ij} = 0$	$M_1 = 0$ $M_2 = 0$
Symmetry and isotropy	$\Im m \{ M_0^{ij} \} = 0$ $M_1^{ij} - [M_{-1}^{ij}]^* = 0$ $\Im m \{ e^{-i\gamma} M_{-1}^{ij} \} = 0$ $M_2^{ij} - [M_{-2}^{ij}]^* = 0$ $\Im m \{ e^{-2i\gamma} M_{-2}^{ij} \} = 0$	$\Im m \{ M_0^{ij} \} = 0$ $M_1^{ij} = 0$ $M_{-1}^{ij} = 0$ $M_2^{ij} - [M_{-2}^{ij}]^* = 0$ $\Im m \{ e^{-2i\gamma} M_{-2}^{ij} \} = 0$	$\Im m \{ M_0^{ij} \} = 0$ $M_1^{ij} = 0$ $M_{-1}^{ij} = 0$ $M_2^{ij} = 0$ $M_{-2}^{ij} = 0$	$M_1 = 0$ $M_2 = 0$
Non-vanishing moments in case of symmetry and isotropy	$\Re e \{ M_0^{ij} \}$ $\Re e \{ e^{-i\gamma} M_{-1}^{ij} \}$ $\Re e \{ e^{-2i\gamma} M_{-2}^{ij} \}$	$\Re e \{ M_0^{ij} \}$ $\Re e \{ e^{-2i\gamma} M_{-2}^{ij} \}$	$\Re e \{ M_0^{ij} \}$ $\Re e \{ M_0^{ij} \} = \int d\alpha E(\omega, \alpha) J_0(\alpha r_{ij}) \cos \theta_{ij}$ $\Re e \{ e^{-i\gamma} M_{-1}^{ij} \} = - \int d\alpha E(\omega, \alpha) J_1(\alpha r_{ij}) \sin \theta_{ij}$ $\Re e \{ e^{-2i\gamma} M_{-2}^{ij} \} = - \int d\alpha E(\omega, \alpha) J_2(\alpha r_{ij}) \cos \theta_{ij}$	$\Re e \{ M_0 \}$

TABLE II.1 Symmetry and isotropy relations for propagating waves.

	slant separation	horizontal separation	vertical separation	no separation
different cross spectral components	18	18	18	9
independent consistency relations	8	8	8	4
independent wave moments	10	10	10	5
independent relations satisfied by a symmetric wave field	0	4	5	2
independent relations satisfied by an isotropic wave field	4	7	8	4
independent relations satisfied by a symmetric and isotropic wave field	7	8	9	4
non-vanishing moments in case of symmetry and isotropy	3	-2	1	1

TABLE II.2. Number of independent moments and relations for propagating waves.

	slant separation	horizontal separation	vertical separation	no separation $R_{\nu\mu} = R_{\mu\nu}^*$
Consistency relations	$(\omega+f)^2 R_{+0}^{ii} - (\omega-f)^2 R_{-1}^{ii} = 0$	$(\omega+f)^2 R_{+0}^{ij} - (\omega-f)^2 R_{-1}^{ij} = 0$ $(\omega-f) R_{-0}^{ij} + (\omega+f) R_{+0}^{ij} = 0$ $(\omega+f) R_{+0}^{ij} + (\omega-f) R_{-0}^{ij} = 0$	$(\omega+f)^2 R_{+0}^{ii} - (\omega-f)^2 R_{-1}^{ii} = 0$ $(\omega-f) [R_{-0}^{ij}]^* + (\omega+f) R_{+0}^{ij} = 0$ $(\omega+f) [R_{+0}^{ij}]^* + (\omega-f) R_{-0}^{ij} = 0$ $\text{Im} \{ R_{+0}^{ii} \} = 0$ $\text{Im} \{ R_{-1}^{ij} \} = 0$ $R_{-1}^{ii} - [R_{+0}^{ij}] = 0$	$(\omega+f)^2 P_{+0} - (\omega-f)^2 P_{-1} = 0$ $(\omega+f) R_{+0} + (\omega-f) R_{-0} = 0$
Independent moments	$M_0^{00}$ $M_0^{++}$ $M_1^{+0}$ $M_{-1}^{+0}$ $M_1^{++}$ $M_{-1}^{0+}$ $M_2^{++}$ $M_{-2}^{++}$	$M_0^{00}$ $M_0^{++}$ $M_1^{+0}$ $M_{-1}^{+0}$  $M_2^{++}$ $M_{-2}^{++}$	$\text{Re} \{ M_0^{00} \}$ $\text{Re} \{ M_0^{++} \}$ $M_1^{+0}$  $M_1^{++}$  $M_2^{++}$	$\text{Re} \{ M_0^{00} \}$ $\text{Re} \{ M_0^{++} \}$ $M_1^{+0}$    $M_2^{++}$
Isotropy relations	$\text{Im} \{ M_0^{00} \} = 0$ $\text{Im} \{ M_0^{++} \} = 0$ $M_1^{+0} + [M_{-1}^{+0}]^* = 0$ $M_1^{++} + [M_{-1}^{0+}]^* = 0$ $M_2^{++} - [M_{-2}^{++}]^* = 0$ $\text{Re} \{ e^{-i4} M_{-1}^{+0} \} = 0$ $\text{Re} \{ e^{i4} M_{-1}^{0+} \} = 0$ $\text{Im} \{ e^{-2i4} M_{-2}^{++} \} = 0$	$\text{Im} \{ M_0^{00} \} = 0$ $\text{Im} \{ M_0^{++} \} = 0$ $M_1^{+0} + [M_{-1}^{+0}]^* = 0$ $M_2^{++} - [M_{-2}^{++}]^* = 0$ $\text{Re} \{ e^{-i4} M_{-1}^{+0} \} = 0$  $\text{Im} \{ e^{-2i4} M_{-2}^{++} \} = 0$	$M_1^{+0} = 0$ $M_1^{++} = 0$ $M_2^{++} = 0$	$M_1^{+0} = 0$   $M_2^{++} = 0$
Non-vanishing moments in case of isotropy	$\text{Re} \{ M_0^{00} \}$ $\text{Re} \{ M_0^{++} \}$ $\text{Im} \{ e^{-i4} M_{-1}^{+0} \}$ $\text{Im} \{ e^{-i4} M_{-1}^{0+} \}$ $\text{Re} \{ e^{-2i4} M_{-2}^{++} \}$	$\text{Re} \{ M_0^{00} \}$ $\text{Re} \{ M_0^{++} \}$ $\text{Im} \{ e^{-i4} M_{-1}^{+0} \}$  $\text{Re} \{ e^{-2i4} M_{-2}^{++} \}$	$\text{Re} \{ M_0^{00} \}$ $\text{Re} \{ M_0^{++} \}$	$\text{Re} \{ M_0^{00} \}$ $\text{Re} \{ M_0^{++} \}$

$$\begin{aligned} \text{Re} \{ M_0^{00} \} &= \int d\alpha \tilde{E}(\omega, \alpha) \tilde{\eta}_0(x_3^i) \tilde{\eta}_0(x_3^j) \mathcal{J}_0(\alpha \tau_{ij}) \\ \text{Re} \{ M_0^{++} \} &= \int d\alpha \tilde{E}(\omega, \alpha) \tilde{\eta}_+(x_3^i) \tilde{\eta}_+(x_3^j) \mathcal{J}_0(\alpha \tau_{ij}) \\ \text{Im} \{ e^{-i4} M_{-1}^{+0} \} &= - \int d\alpha \tilde{E}(\omega, \alpha) \tilde{\eta}_+(x_3^i) \tilde{\eta}_0(x_3^j) \mathcal{J}_1(\alpha \tau_{ij}) \\ \text{Im} \{ e^{-i4} M_{-1}^{0+} \} &= - \int d\alpha \tilde{E}(\omega, \alpha) \tilde{\eta}_0(x_3^i) \tilde{\eta}_+(x_3^j) \mathcal{J}_1(\alpha \tau_{ij}) \\ \text{Re} \{ e^{-2i4} M_{-2}^{++} \} &= - \int d\alpha \tilde{E}(\omega, \alpha) \tilde{\eta}_+(x_3^i) \tilde{\eta}_+(x_3^j) \mathcal{J}_2(\alpha \tau_{ij}) \end{aligned}$$

TABLE II.3 Consistency and isotropy relations for standing modes.

	slant separation	horizontal separation	vertical separation	no separation
different cross spectral components	18	18	18	9
independent consistency relations	2	6	10	3
independent wave moments	16	12	8	6
independent isotropy relations	11	8	6	4
non-vanishing moments in case of isotropy	5	4	2	2

TABLE II.4 Number of independent moments and relations for standing modes.

Name	Transformation class	fundamental invariants	cross-spectral matrix	invariance relations
3-dimensional isotropy	arbitrary rotations and reflections or arbitrary rotations	$a_m b_m$	$A_{mn} = A \delta_{mn}$	$P_{11} + P_{22} - 2P_{33} = 0$ $Q_{12} = 0$ $P_{11} - P_{22} = P_{12} = 0$ $P_{13} = Q_{13} = P_{23} = Q_{23} = 0$
horizontal isotropy and symmetry	rotations about $\vec{\lambda} = (0,0,1)$ and reflections at $\vec{\lambda}$	$a_m b_m, a_m \lambda_m, b_m \lambda_m$	$A_{mn} = A \delta_{mn} + B \lambda_m \lambda_n$	$Q_{12} = 0$ $P_{11} - P_{22} = P_{12} = 0$ $P_{13} = Q_{13} = P_{23} = Q_{23} = 0$
horizontal isotropy	rotation about $\vec{\lambda} = (0,0,1)$ without reflections	$a_m b_m, a_m \lambda_m, b_m \lambda_m, \epsilon_{mno} a_m b_n \lambda_o$	$A_{mn} = A \delta_{mn} + B \lambda_m \lambda_n + C \epsilon_{mno} \lambda_o$	$P_{11} - P_{22} = P_{12} = 0$ $P_{13} = Q_{13} = P_{23} = Q_{23} = 0$
vertical symmetry	reflection at the plane $\vec{\lambda} = (0,1,0)$ , $\vec{\mu} = (1,0,0)$	$a_m b_m, a_m \gamma_m, b_m \gamma_m, a_m \mu_m, b_m \mu_m$	$A_{mn} = A \delta_{mn} + B \gamma_m \gamma_n + C \gamma_m \mu_n + D \mu_m \gamma_n + E \mu_m \mu_n$	$P_{13} = Q_{13} = P_{23} = Q_{23} = 0$

TABLE II.5 Fundamental invariants, structure of cross spectral matrix and invariance relations for various transformation classes. Here a and b represent arbitrary unit vectors and A,B,C,D and E arbitrary constants.

METRIC	$\langle \epsilon^2 \rangle$	VAR[ $\epsilon^2$ ]	$L_{\text{eff}}$
$W_{\epsilon\epsilon'} = S_{\epsilon\epsilon'}^{-1}$	L	$2L$	L
$W_{\epsilon\epsilon'}^{(a)} = \delta_{\epsilon\epsilon'} \frac{1}{S_{\epsilon\epsilon'}}$	L	$2 \sum_{\epsilon, \epsilon'} C_{\epsilon\epsilon'}$	$\frac{L^2}{\sum_{\epsilon, \epsilon'} C_{\epsilon\epsilon'}}$
$W_{\epsilon\epsilon'}^{(b)} = \delta_{\epsilon\epsilon'} \frac{1}{S_{\epsilon\epsilon'}} \sum_k C_{\epsilon k}$	$\sum_{\epsilon, \epsilon'} C_{\epsilon\epsilon'}^{-1}$	$2 \sum_{\epsilon, \epsilon'} C_{\epsilon\epsilon'}^{-1}$	$\sum_{\epsilon, \epsilon'} C_{\epsilon\epsilon'}^{-1}$
$W_{\epsilon\epsilon'}^{\text{INEX}} = \delta_{\epsilon\epsilon'} \frac{k_\epsilon}{S_{\epsilon\epsilon'}}$	$\sum_\epsilon k_\epsilon$	$2 \sum_{\epsilon, \epsilon'} C_{\epsilon\epsilon'} k_\epsilon k_{\epsilon'}$	$\frac{\sum_{\epsilon, \epsilon'} k_\epsilon k_{\epsilon'}}{\sum_{\epsilon, \epsilon'} C_{\epsilon\epsilon'} k_\epsilon k_{\epsilon'}}$

$S$  = covariance matrix  
 $L$  = number of data  
 $C_{\epsilon\epsilon'} = \frac{S_{\epsilon\epsilon'} S_{\epsilon\epsilon'}}{S_{\epsilon\epsilon'} S_{\epsilon\epsilon'}}$ ,  $k_\epsilon = (\sum_{\epsilon'} C_{\epsilon\epsilon'})^{-1}$

TABLE III.1 Properties of various metrics.

	Fig.	FREQUENCY INTERVAL			
		3 - 21	22 - 29	30	
Number of different cross spectral components		1444	1225	729	
Zero model	IV.1	1444	1225	729	
White noise	IV.1	1406	1190	702	
Finestructure	IV.1	1218	1008	562	
Basic assumptions of the Garrett and Munk model	IV.2	854	797	492	
Homogeneity and WKB-scaling	$\left\{ \begin{array}{l} UV\xi \\ UV \\ \xi \end{array} \right.$	IV.3	83	80	60
		IV.4	32	32	24
		IV.4	19	16	12
Propagating waves, vert. symmetric, hor. isotropic	IV.5	771	717	432	
Hor. isotropy	IV.6	54	54	42	
Vert. symmetry	IV.7	36	36	28	
Propagating waves	IV.9	324	324	196	
Standing modes	$\left\{ \begin{array}{l} \text{Discriminating tests} \\ \text{All tests} \end{array} \right.$	IV.13	38	38	30
		IV.14	119	119	79
Standing modes hor. isotropic	IV.15	690	636	323	
Combination of standing and prop. waves	IV.16	81	81	49	
$D_3^{ij}, D_4^{ij} = 0$	IV.17	162	162	98	
$D_1^{ij} = 0$	$\left\{ \begin{array}{l} \text{total} \\ \text{no sep.} \\ \text{slant sep.} \\ \text{hor. sep.} \end{array} \right.$	IV.18	81	81	49
		IV.18	9	9	7
		IV.19	62	62	33
		IV.19	10	10	9
Prop. waves contaminated by white noise	IV.20	306	306	182	
Prop. waves contaminated by finestructure	IV.21	286	286	166	
Prop. waves contaminated by coherent noise	IV.22	243	243	147	
IWEX model class	IV.23	224	224	132	

TABLE IV.1 Number of different cross spectral components and number of different consistency relations.

	Fig.	Low frequency band		Medium frequency band	High frequency band
		inertial fr. f	tidal fr. M <sub>2</sub>		
Basic assumption of the Garrett and Munk model	IV.2	?	strongly violated	slightly violated	strongly violated
Homogeneity and WKB-scaling	IV.3	satisfied	satisfied	satisfied	strongly violated (partly due to proximity of turning point)
Prop. waves, hor. isotropic, vert. symmetric	IV.5	?	strongly violated	slightly violated	strongly violated
Hor. isotropy	IV.6	strongly violated	strongly violated	satisfied	slightly violated
Vert. symmetry	IV.7	strongly violated	strongly violated	satisfied	slightly violated
Prop. waves	IV.9	?	strongly violated	slightly violated	strongly violated
Standing modes	IV.14	?	strongly violated	satisfied	satisfied
Comb. of standing and prop. waves	IV.16	?	strongly violated	satisfied	satisfied
$D_3^{ij}, D_4^{ij} = 0$	IV.17	satisfied	satisfied	satisfied	slightly violated (partly due to proximity of turning point)
$D_1^{ij} = 0$	IV.18	strongly violated	strongly violated	slightly violated	strongly violated
Prop. waves contaminated by finestructure	IV.21	?	strongly violated	slightly violated	strongly violated
Prop. waves contaminated by coherent noise	IV.22	?	slightly violated	satisfied	slightly violated (partly due to proximity of turning point)
IWEX model class	IV.23	satisfied	slightly violated	satisfied	slightly violated (partly due to proximity of turning point)

TABLE IV.2 Results of consistency tests.



	GM 72	GM 75	CW
$j_*$	20	6	3
$j_e$	20	11	10
$t$	$\infty$	5/2	2
$s$	$\infty$	1	2
$d$	0	0	0
$I(t,s)$	1	3/2	$2/\pi$
$J(t,s)$	1	1.8	$\pi$

TABLE V.1: Models of internal wave spectrum

$t \rightarrow$

$J(t,s)$	1.300	1.500	1.700	2.000	2.200	2.500	3.000	3.500	4.000
1.000	17.778	8.000	4.898	3.000	2.361	1.778	1.250	0.960	0.778
1.100	16.968	7.800	4.861	3.043	2.424	1.854	1.332	1.041	0.856
1.200	16.320	7.632	4.824	3.074	2.473	1.917	1.402	1.112	0.926
1.300	15.792	7.488	4.789	3.096	2.512	1.968	1.461	1.173	0.986
1.500	14.985	7.255	4.723	3.123	2.567	2.045	1.555	1.272	1.088
1.700	14.402	7.076	4.666	3.156	2.602	2.100	1.624	1.349	1.167
2.000	13.784	6.875	4.594	3.142	2.633	2.153	1.698	1.432	1.257
2.500	13.137	6.650	4.503	3.134	2.655	2.202	1.772	1.521	1.355
3.000	12.743	6.504	4.438	3.121	2.660	2.226	1.814	1.574	1.415
4.000	12.302	6.330	4.353	3.095	2.656	2.243	1.854	1.629	1.481
5.000	12.070	6.234	4.302	3.075	2.647	2.247	1.870	1.654	1.513
7.000	11.844	6.136	4.247	3.049	2.633	2.244	1.881	1.674	1.540
10.000	11.708	6.074	4.210	3.029	2.620	2.238	1.882	1.681	1.552

$S \downarrow$

$I(t,s)$	1.500	1.700	2.000	2.500	3.000	3.500	4.000
1.000	0.500	0.700	1.000	1.500	2.000	2.500	3.000
1.100	0.473	0.652	0.914	1.337	1.885	2.448	3.049
1.200	0.453	0.616	0.850	1.218	1.700	2.265	2.914
1.300	0.437	0.588	0.801	1.127	1.595	2.114	2.798
1.500	0.413	0.548	0.730	1.000	1.443	1.940	2.667
1.700	0.397	0.520	0.683	0.916	1.318	1.814	2.544
2.000	0.381	0.493	0.637	0.835	1.200	1.714	2.432
2.500	0.366	0.466	0.592	0.757	1.100	1.629	2.332
3.000	0.357	0.451	0.566	0.713	1.027	1.555	2.244
4.000	0.347	0.435	0.539	0.668	0.963	1.490	2.167
5.000	0.342	0.427	0.526	0.645	0.914	1.432	2.100
7.000	0.338	0.420	0.514	0.625	0.870	1.381	2.044
10.000	0.336	0.416	0.507	0.613	0.833	1.338	2.000

TABLE V.2 Normalization factor  $I(t,s)$  and conversion factor  $J(t,s)$  for various values of  $t$  and  $s$ .

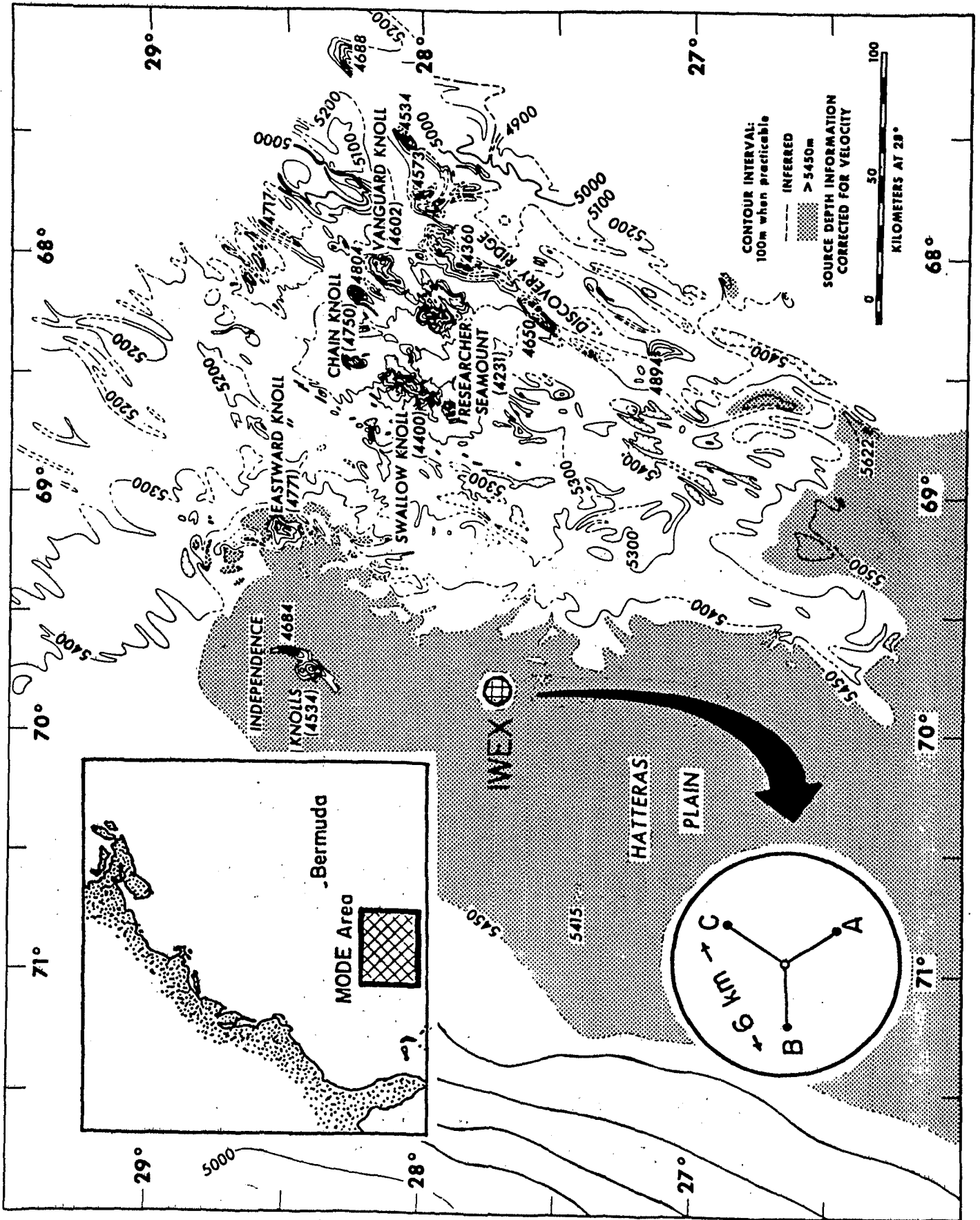


Fig. I.1

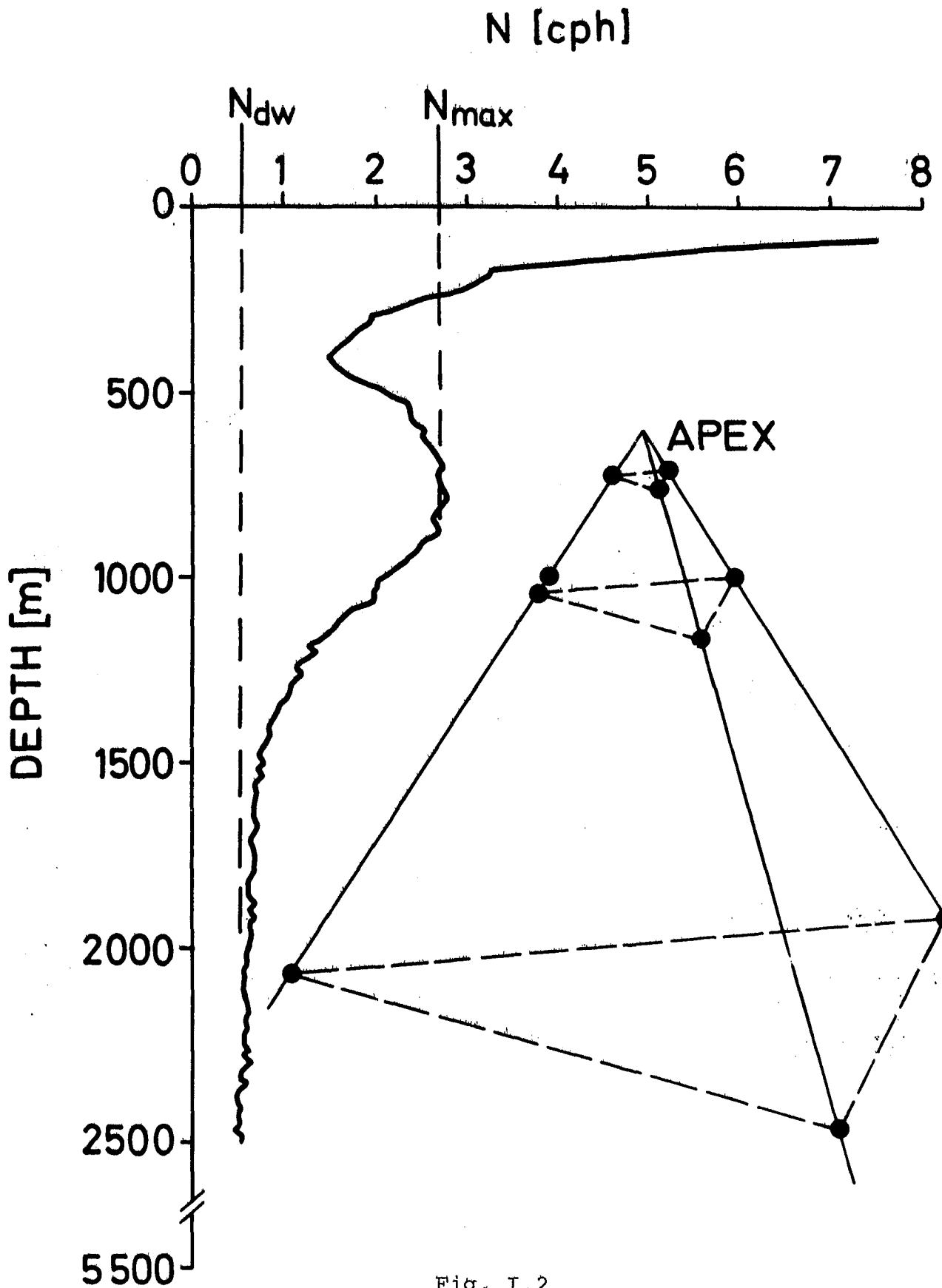


Fig. I.2

### LOW PASSED TEMPERATURE

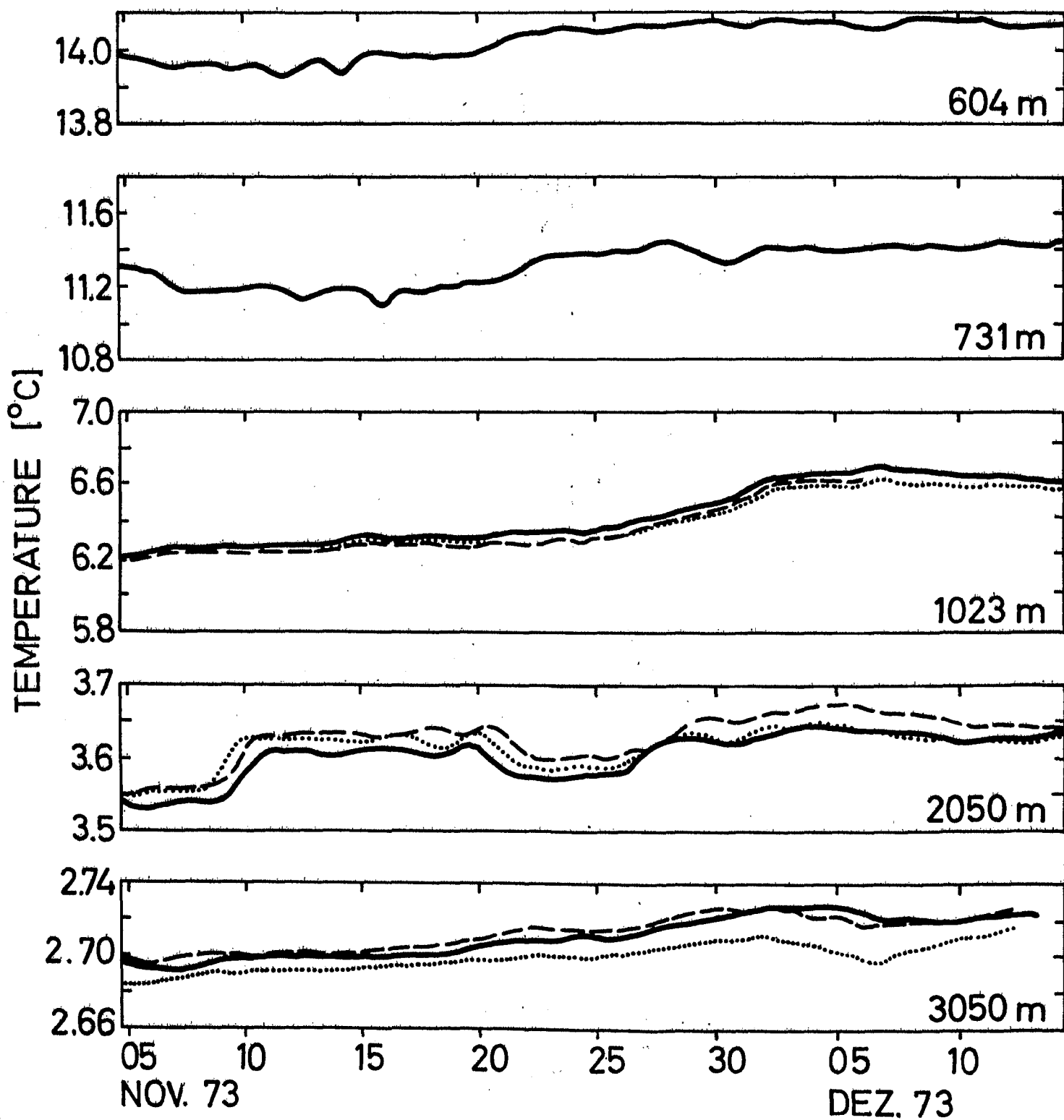


Fig. I.3a

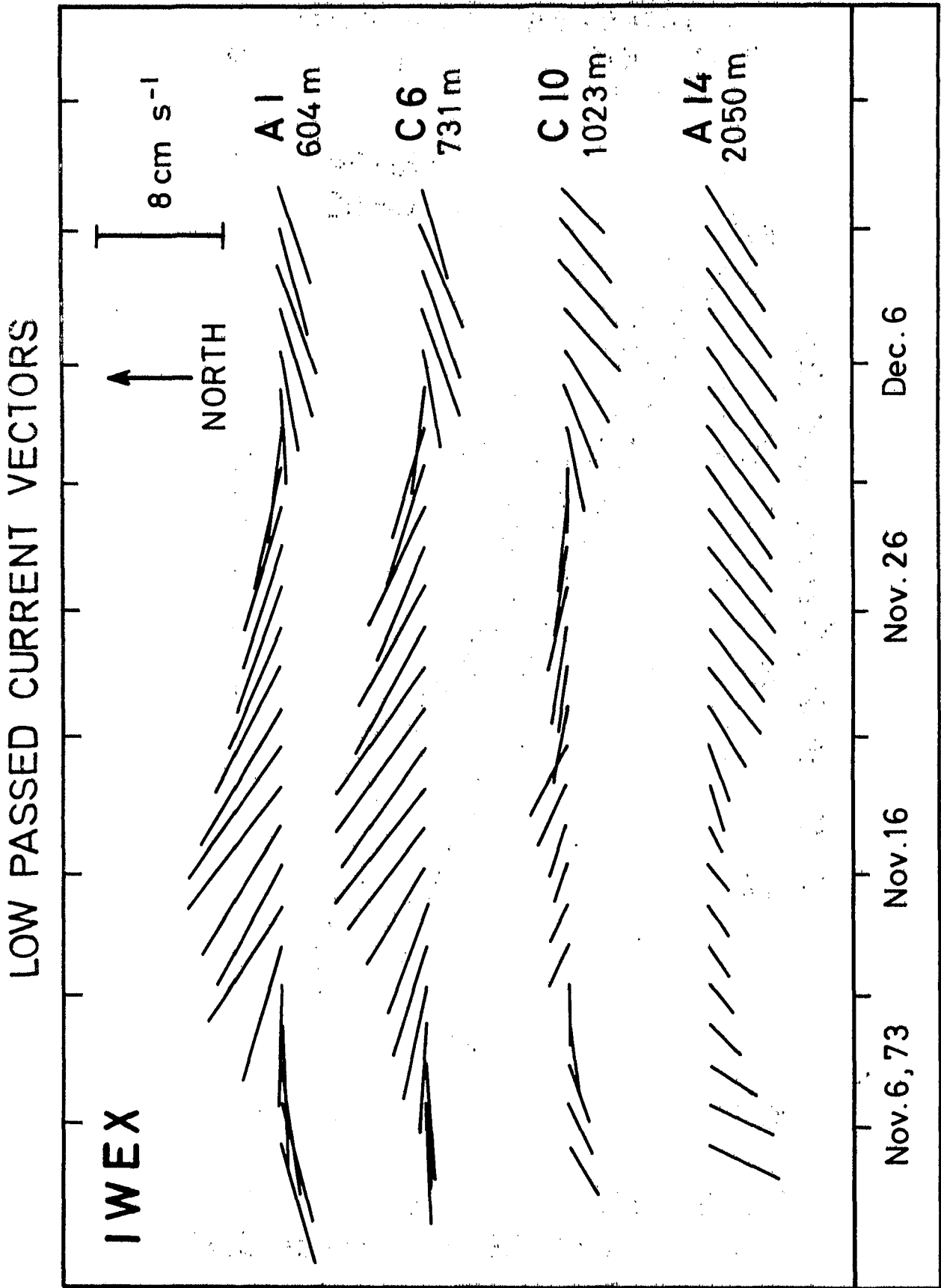


Fig. I.3b

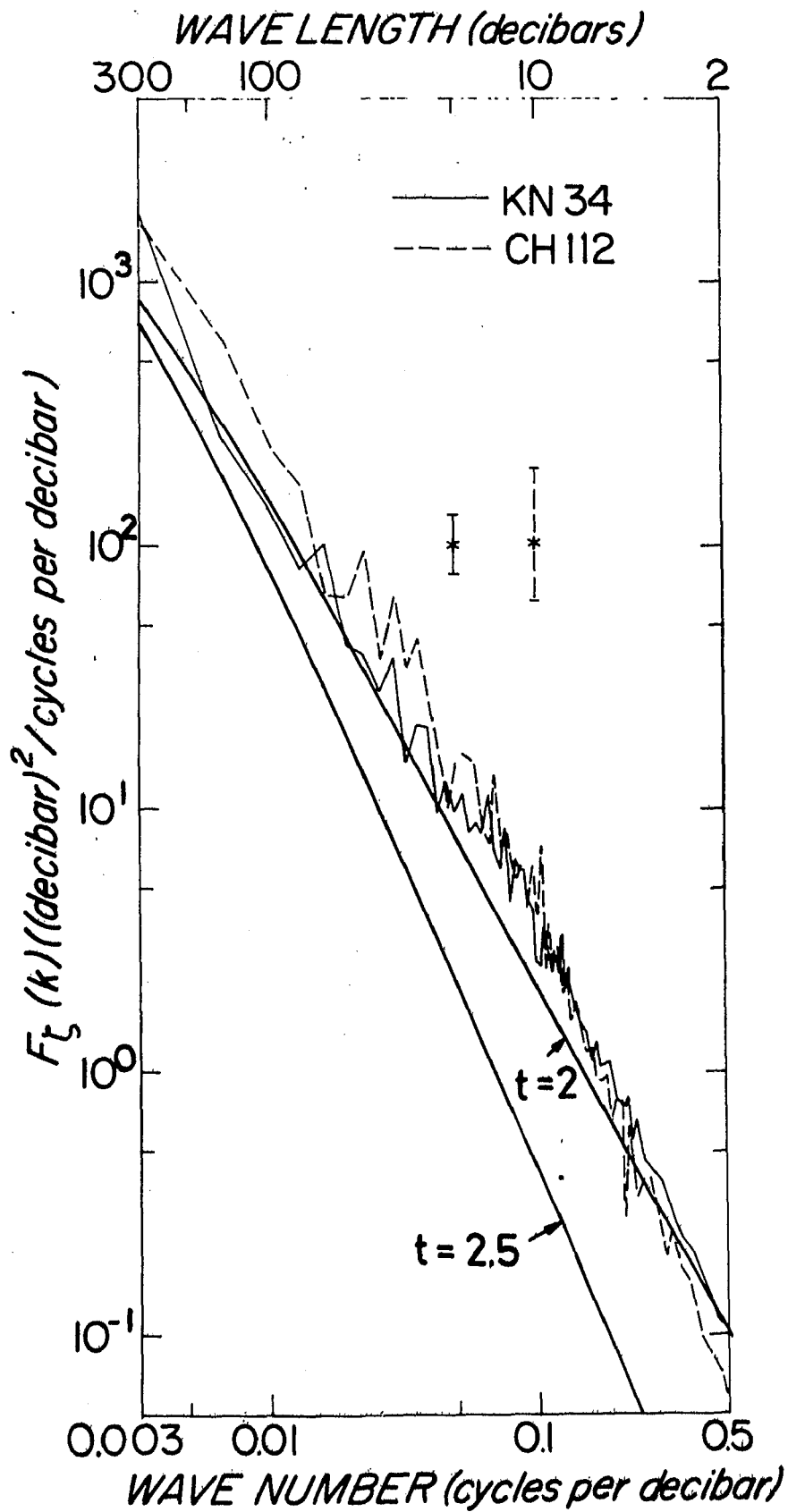


Fig. 1.4

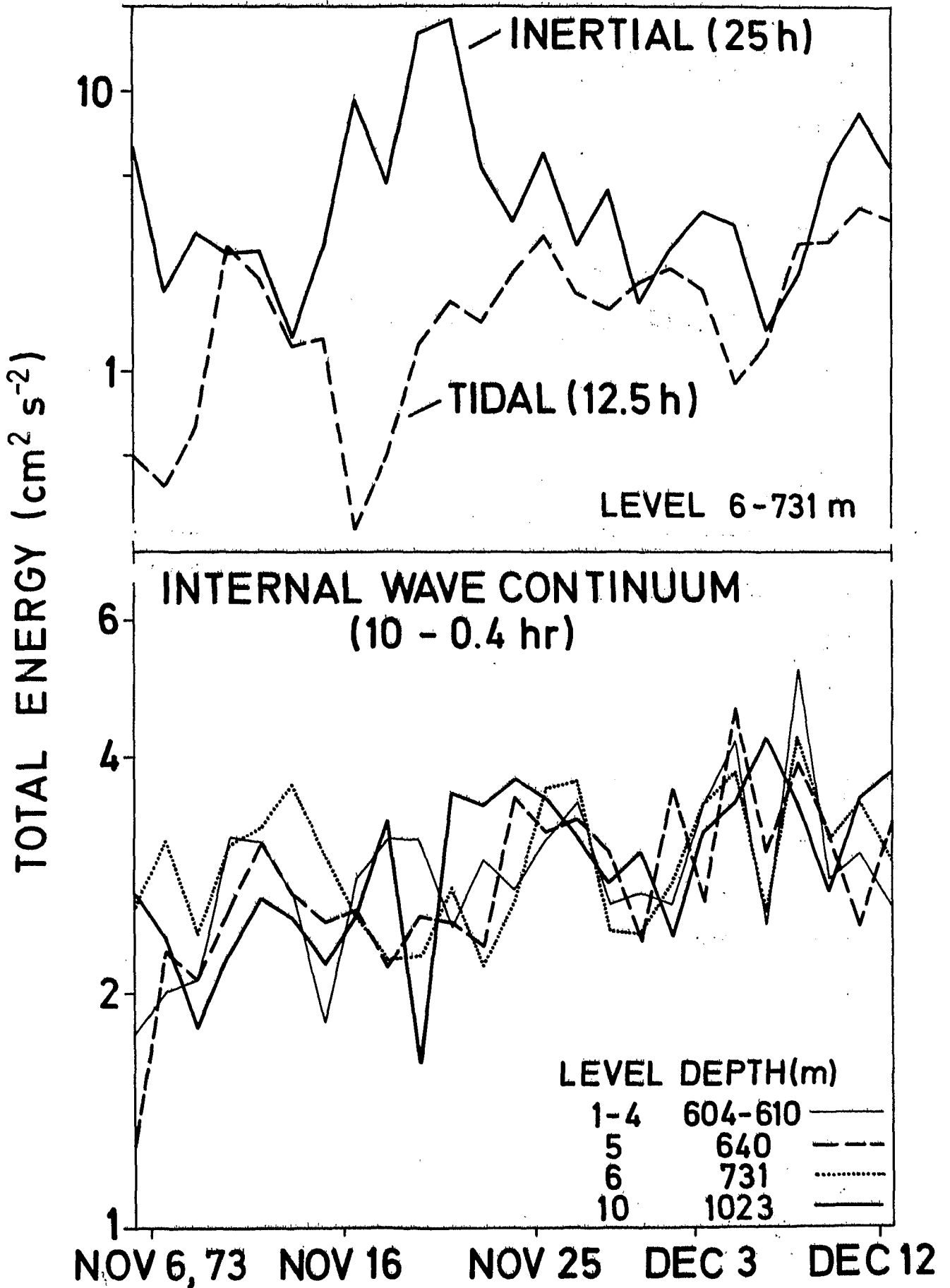


Fig. I.5



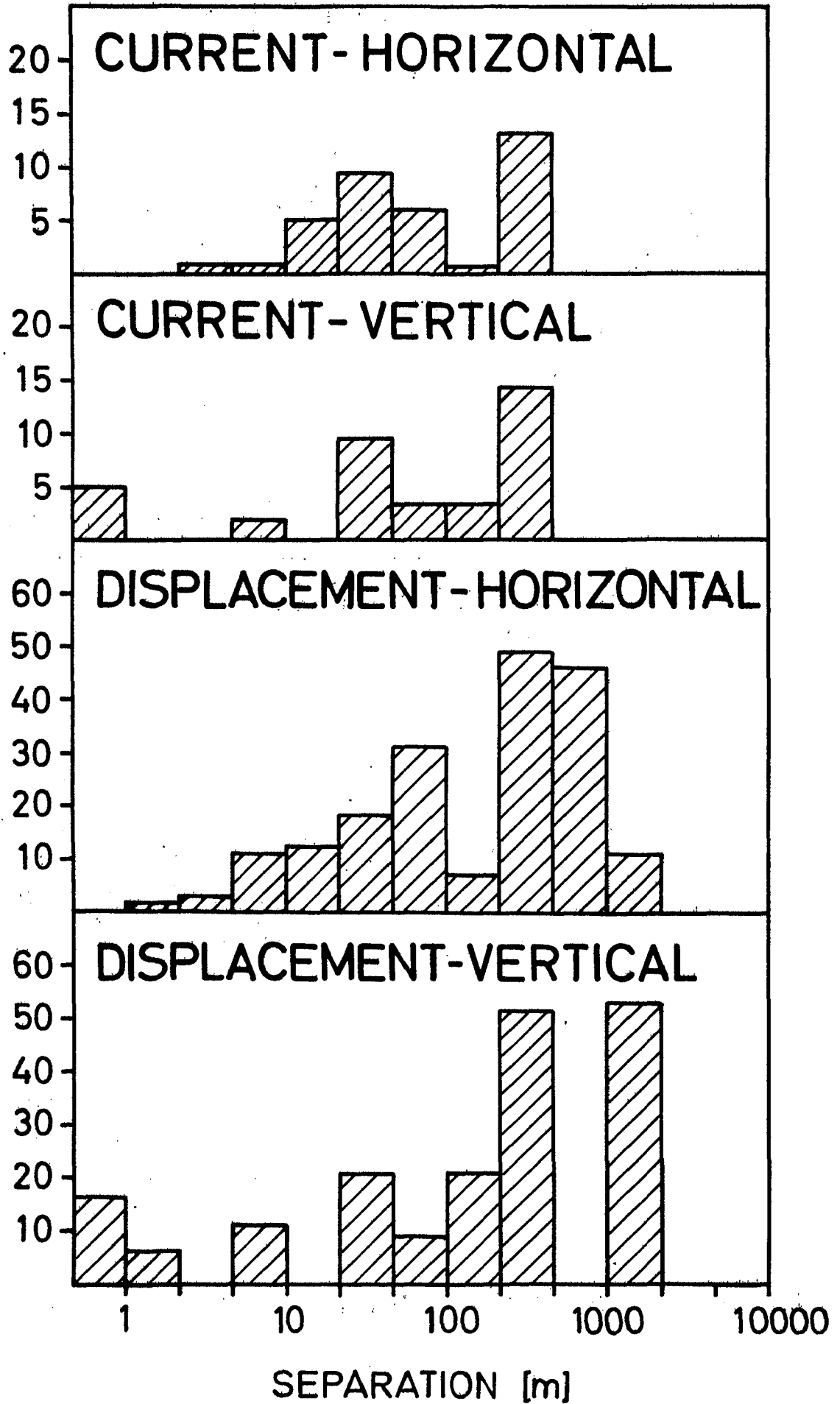


Fig. I.6

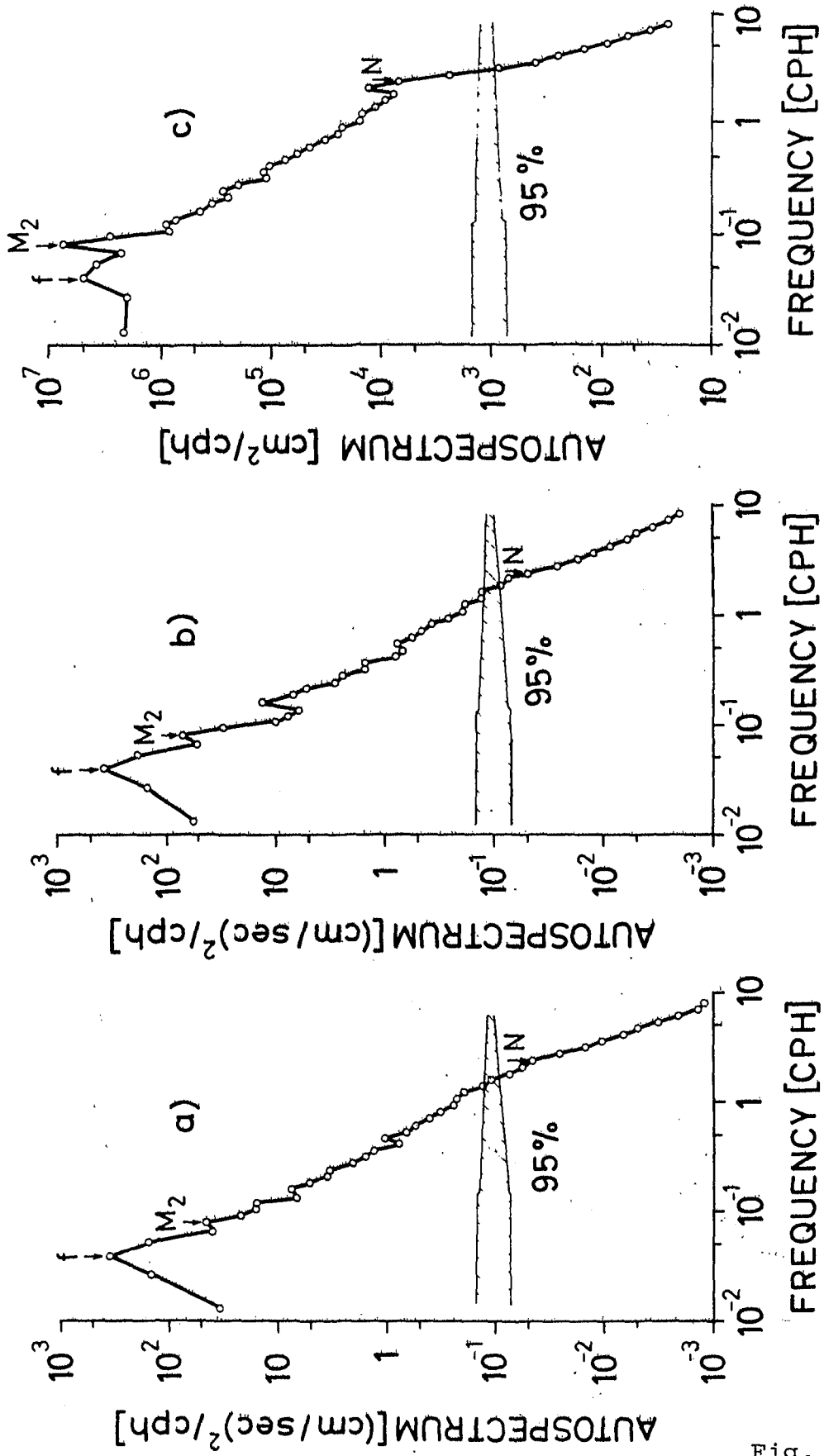


Fig. I.7

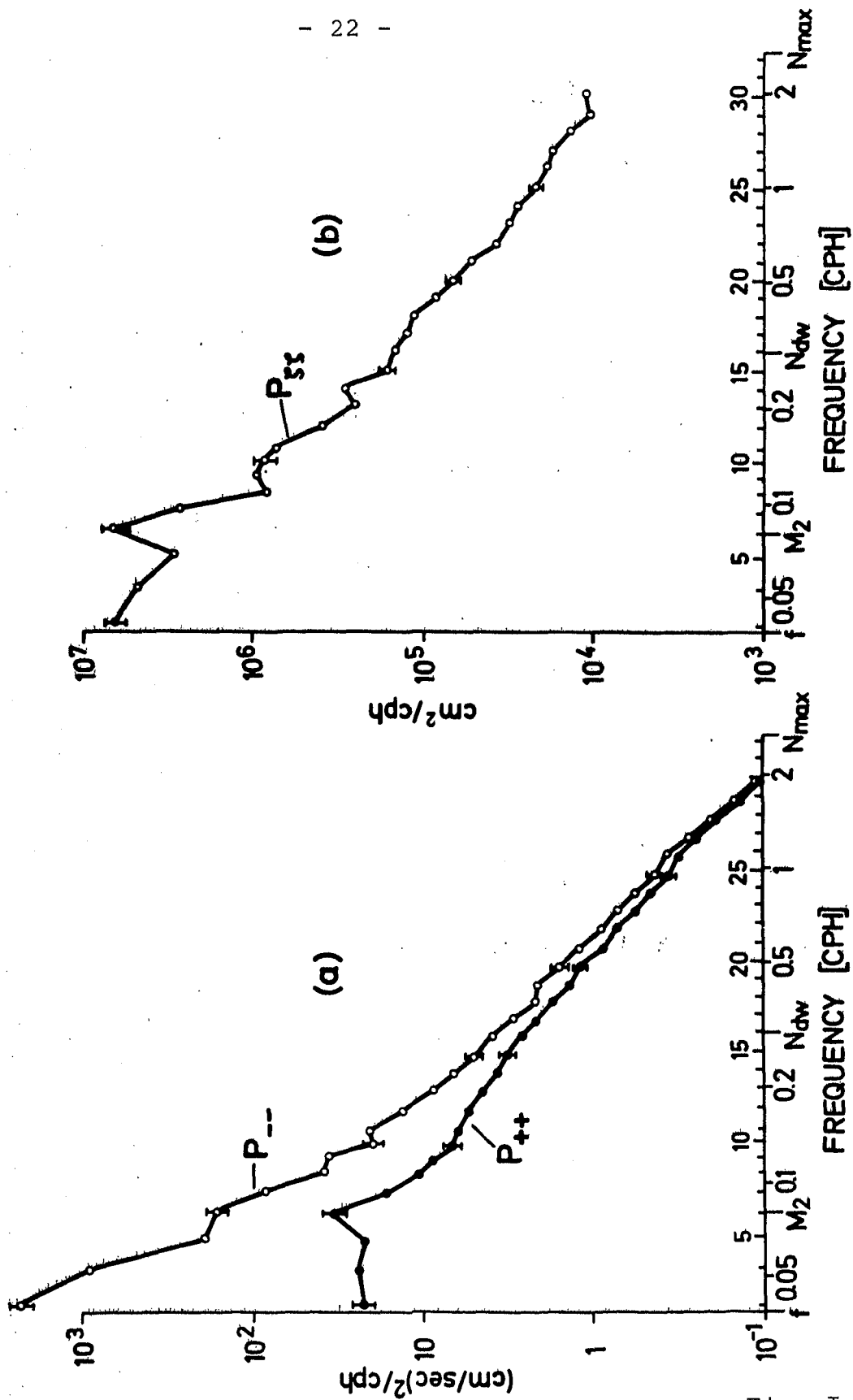


Fig. I.8

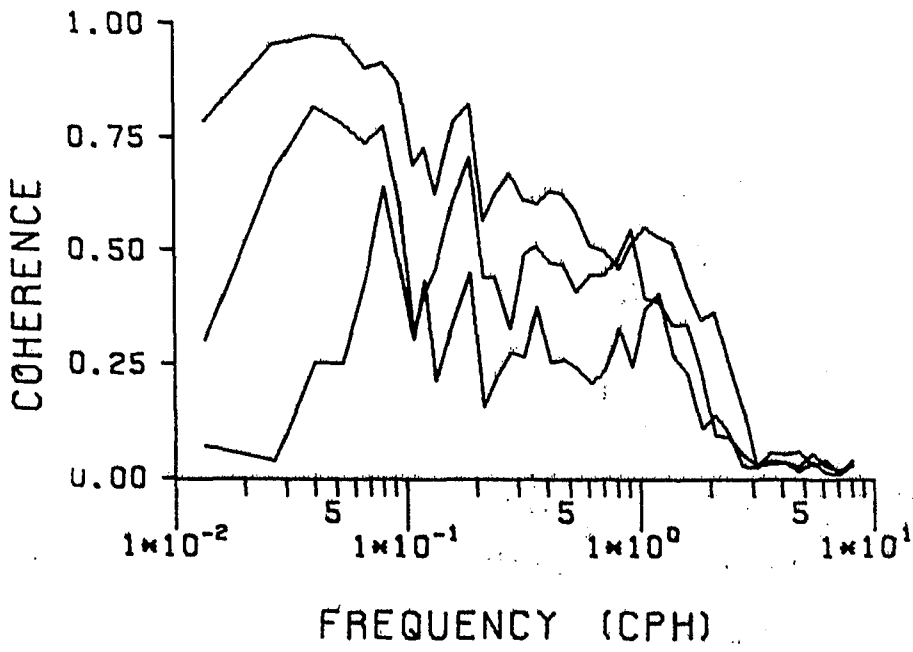
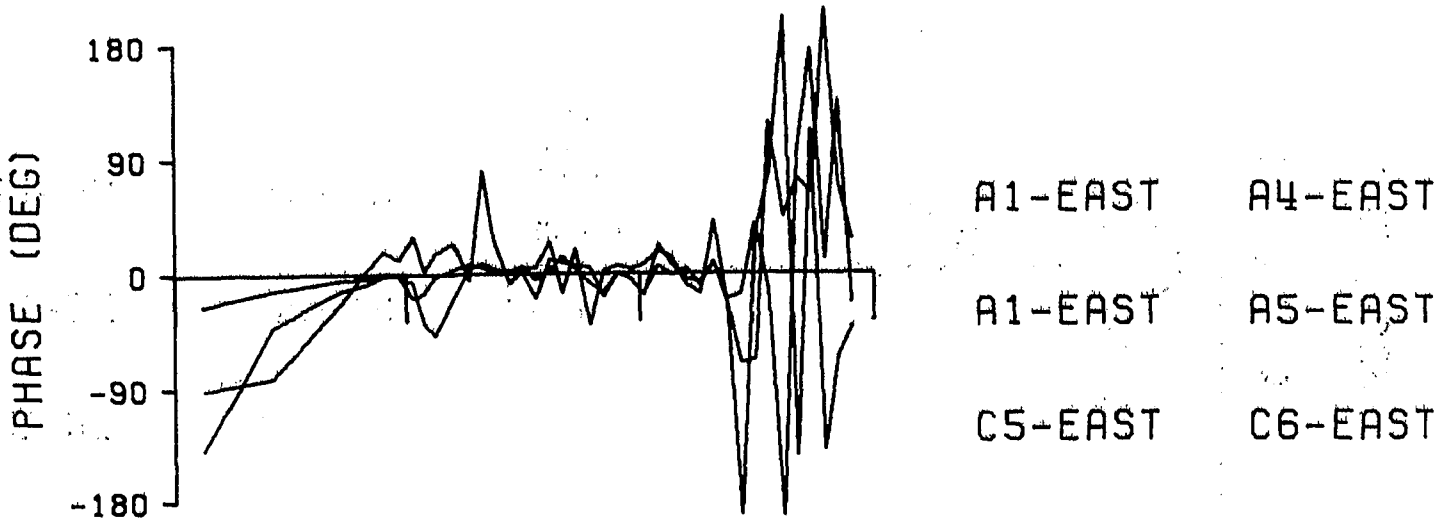
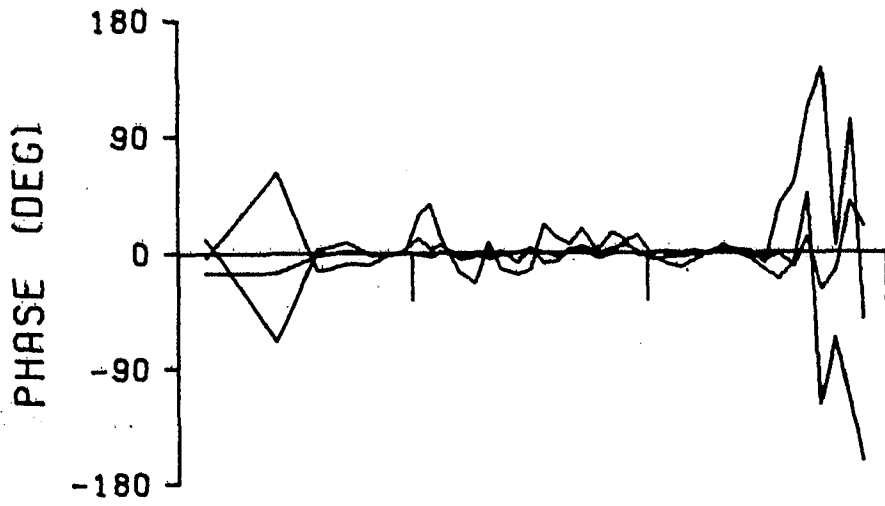


Fig. I.9a



A1-UP

A4-UP

A1-UP

A5-UP

C5-UP

C6-UP

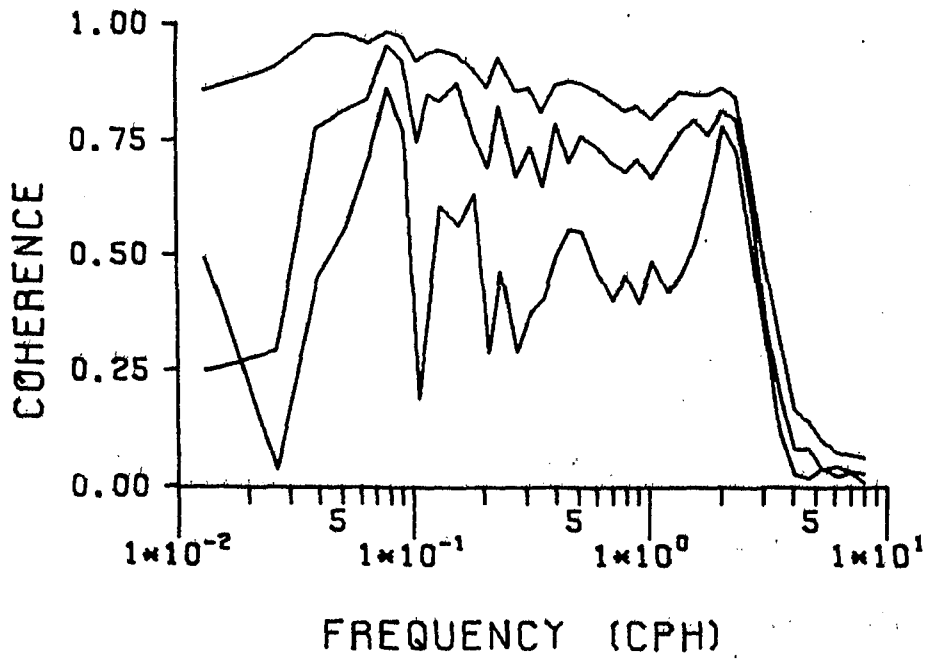


Fig. I.9b

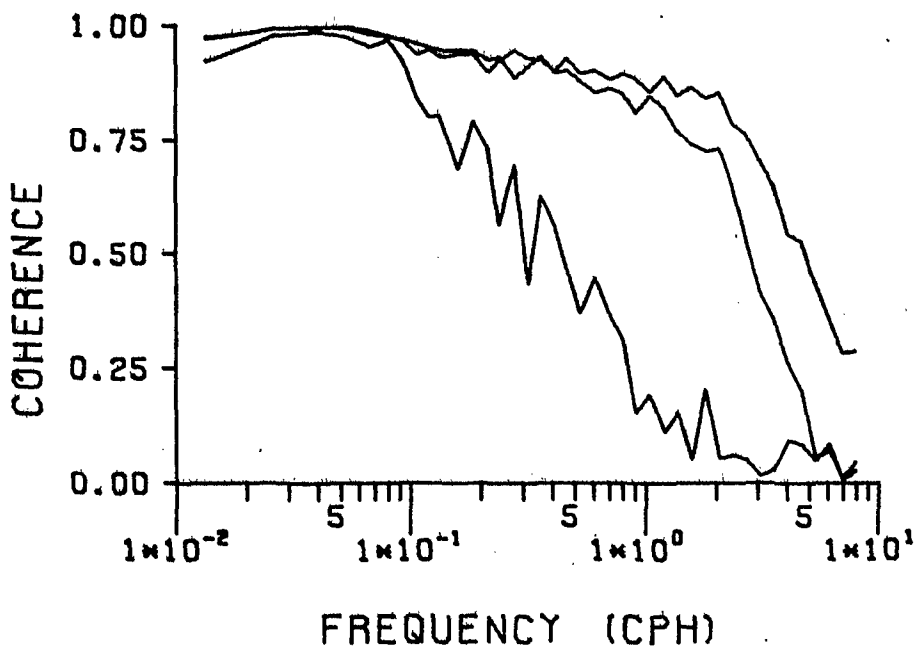
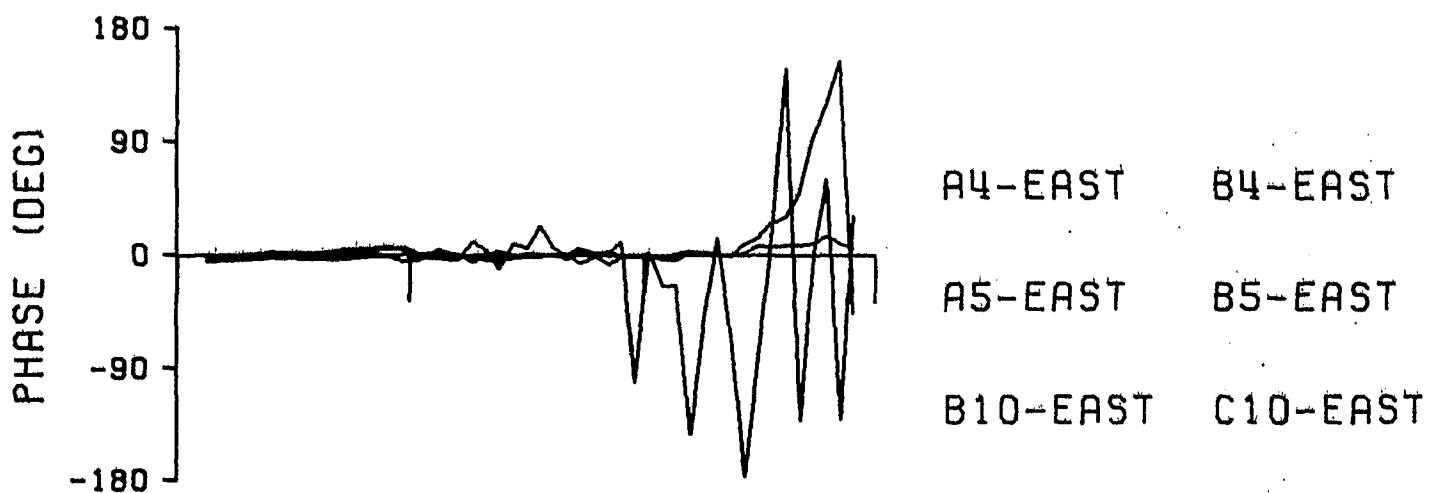
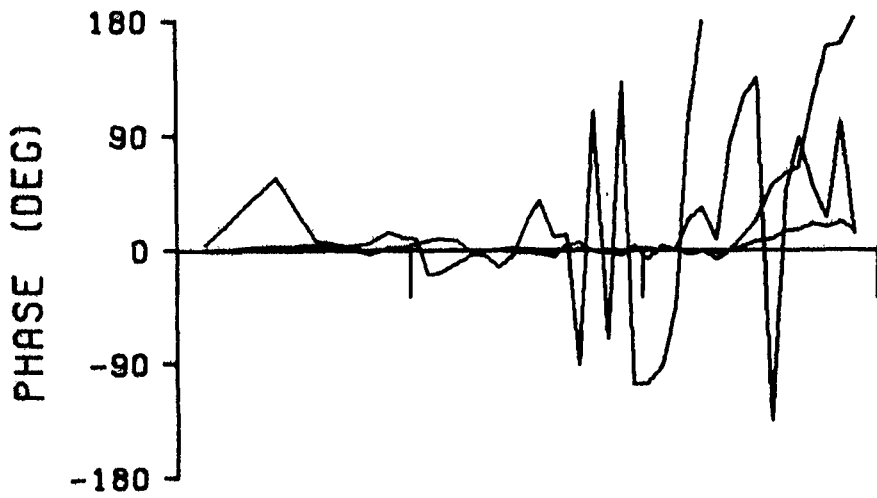


Fig. I.9c



A4-UP

B4-UP

A5-UP

B5-UP

A10-UP

B10-UP

A14-UP

B14-UP

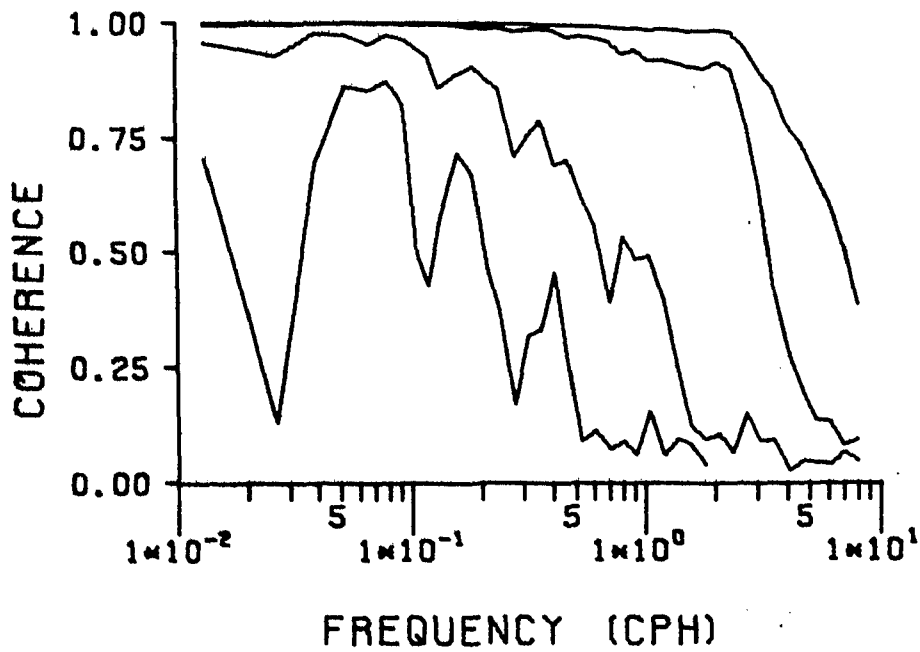


Fig. I.9d

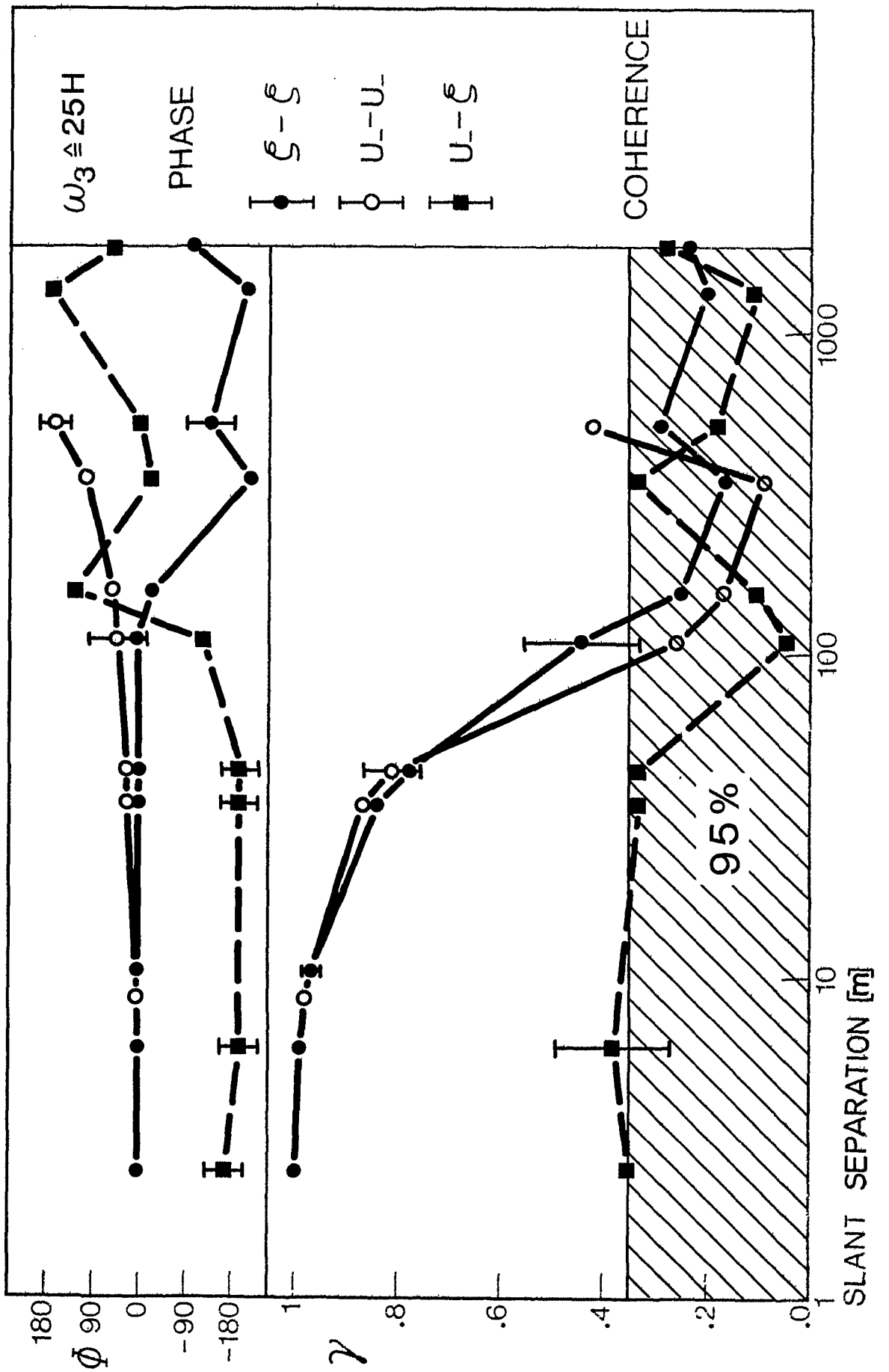


Fig. I.10a



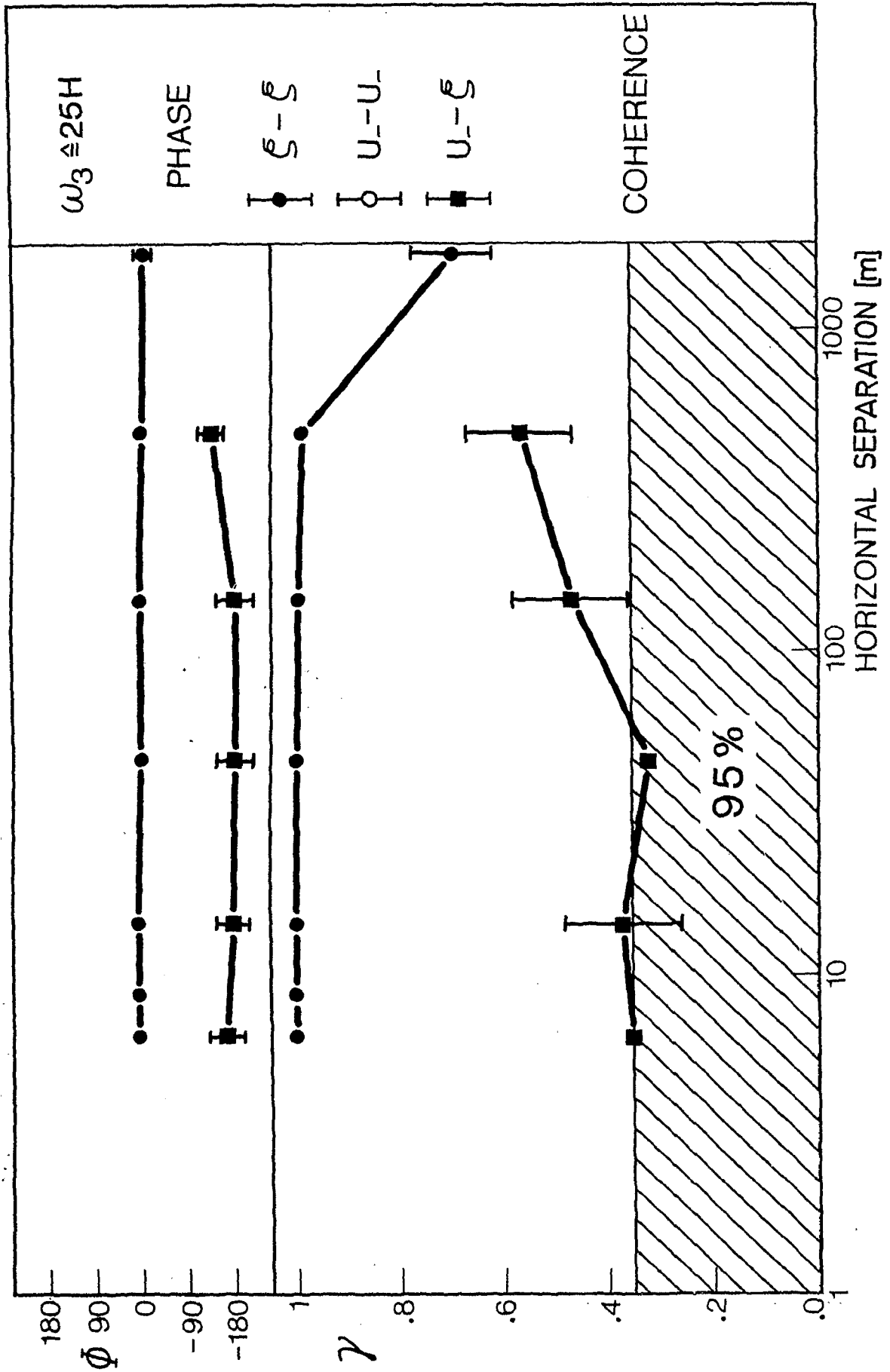


Fig. I.10b

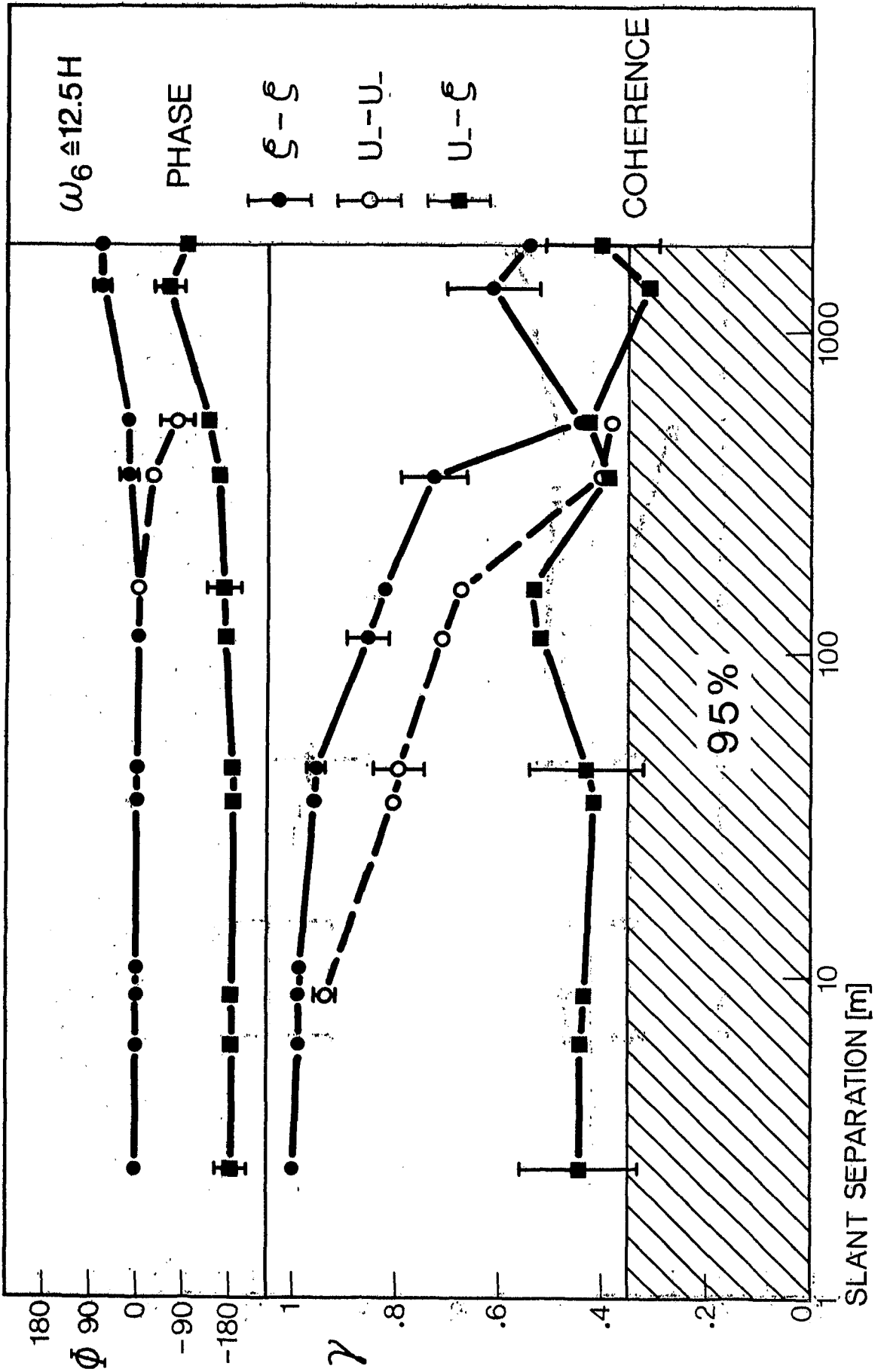


Fig. I.11a

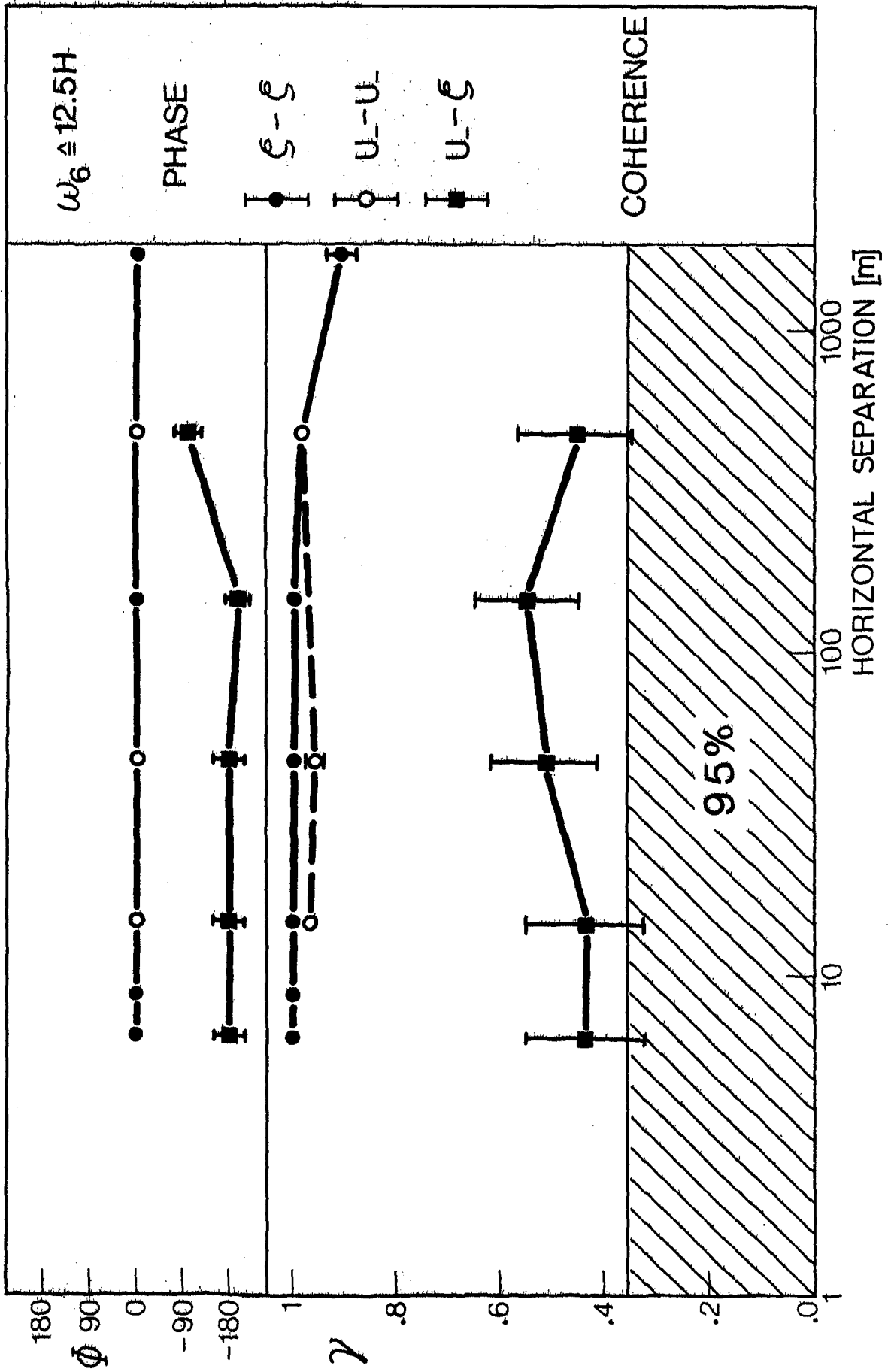


Fig. I.11b

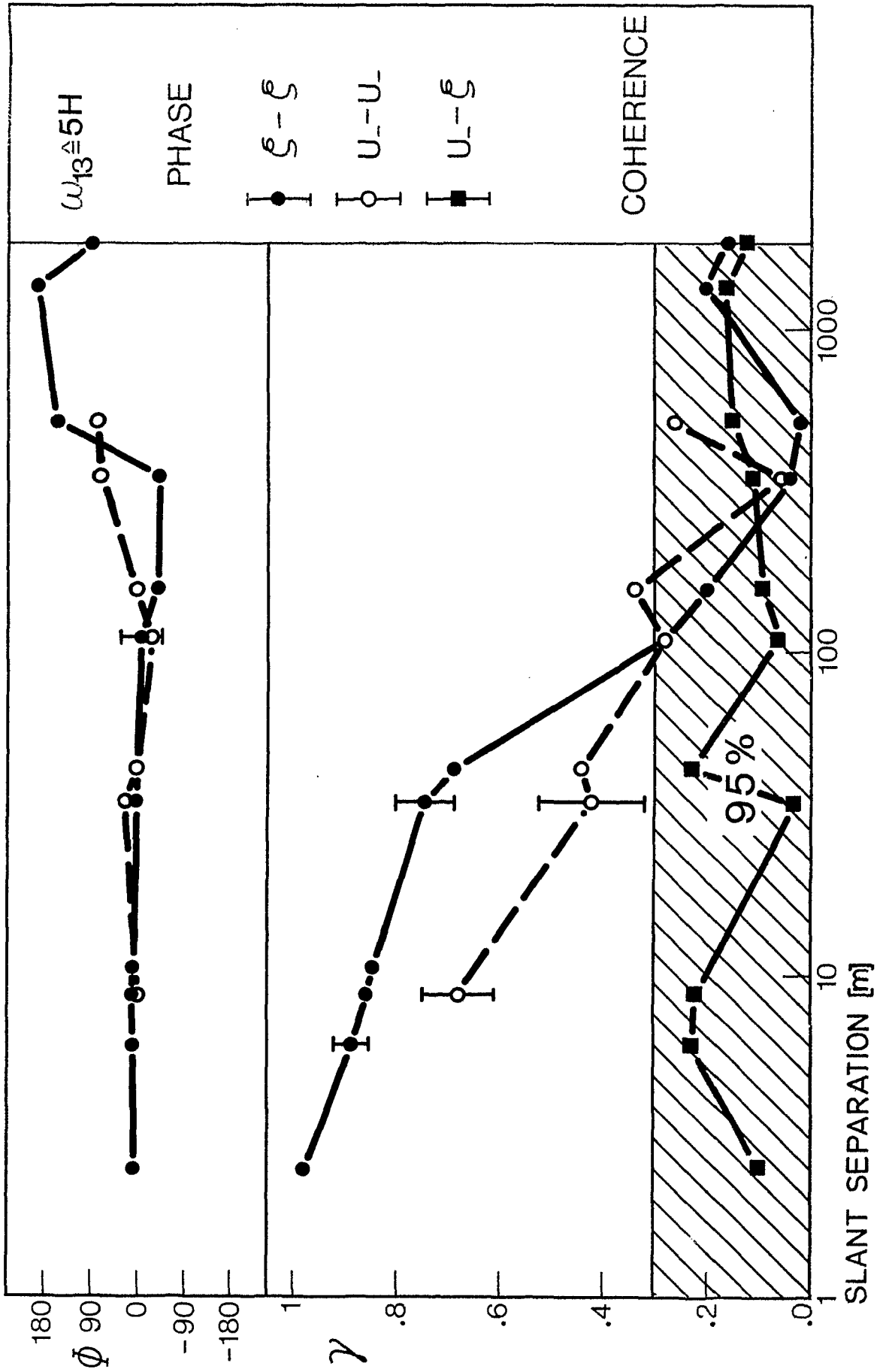


Fig. I.12a

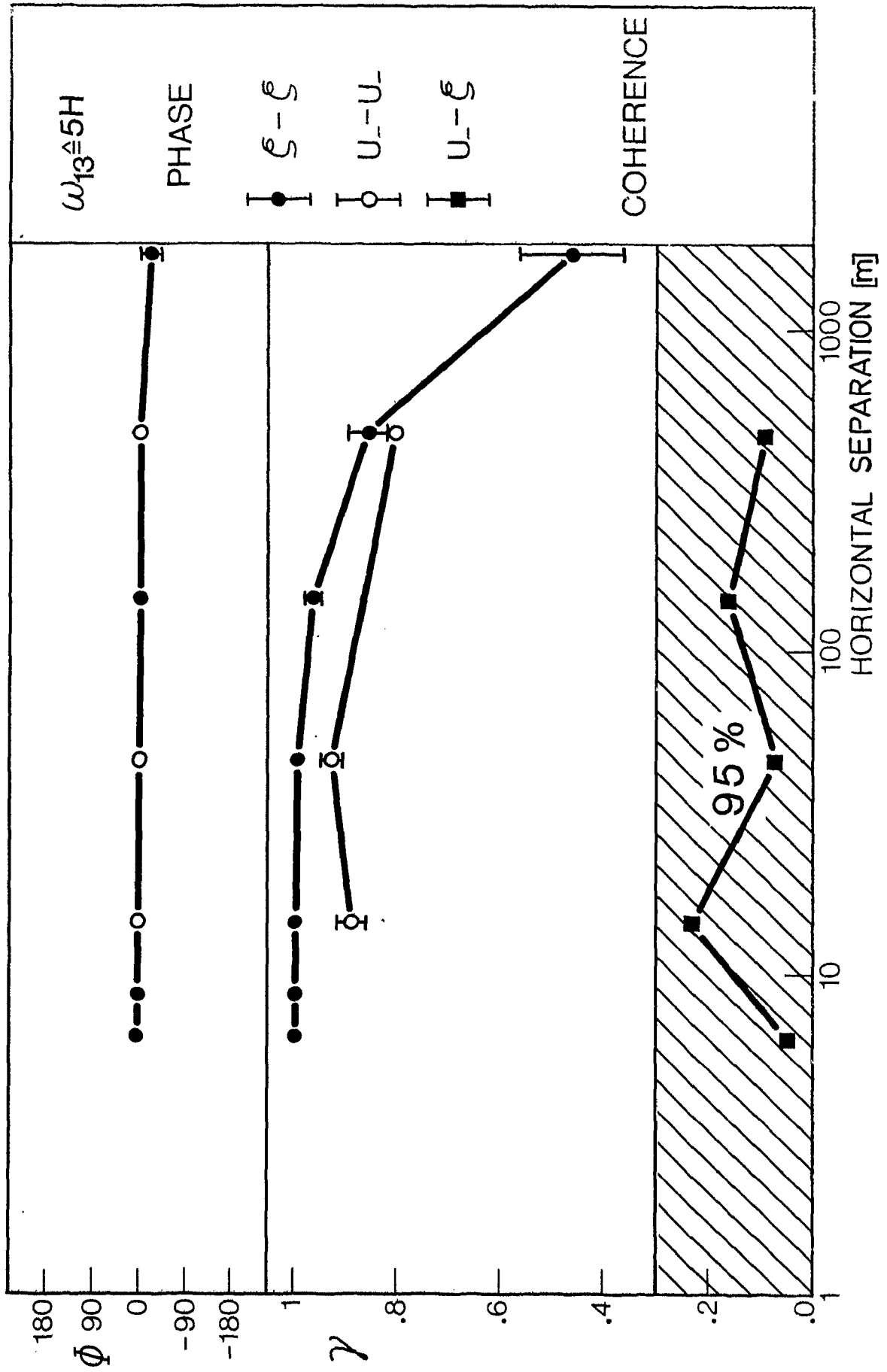


Fig. I.12b

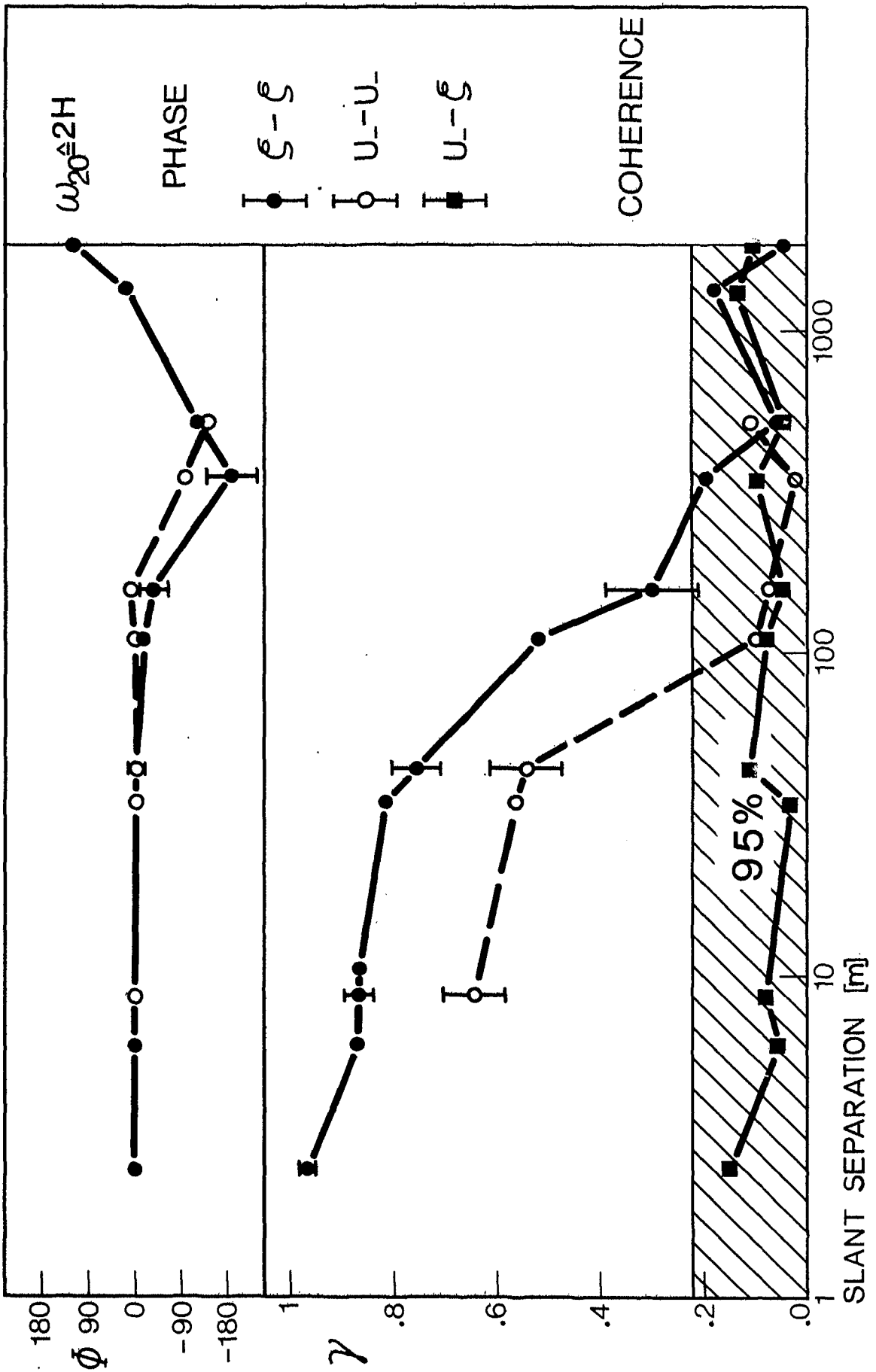


Fig. I.13a

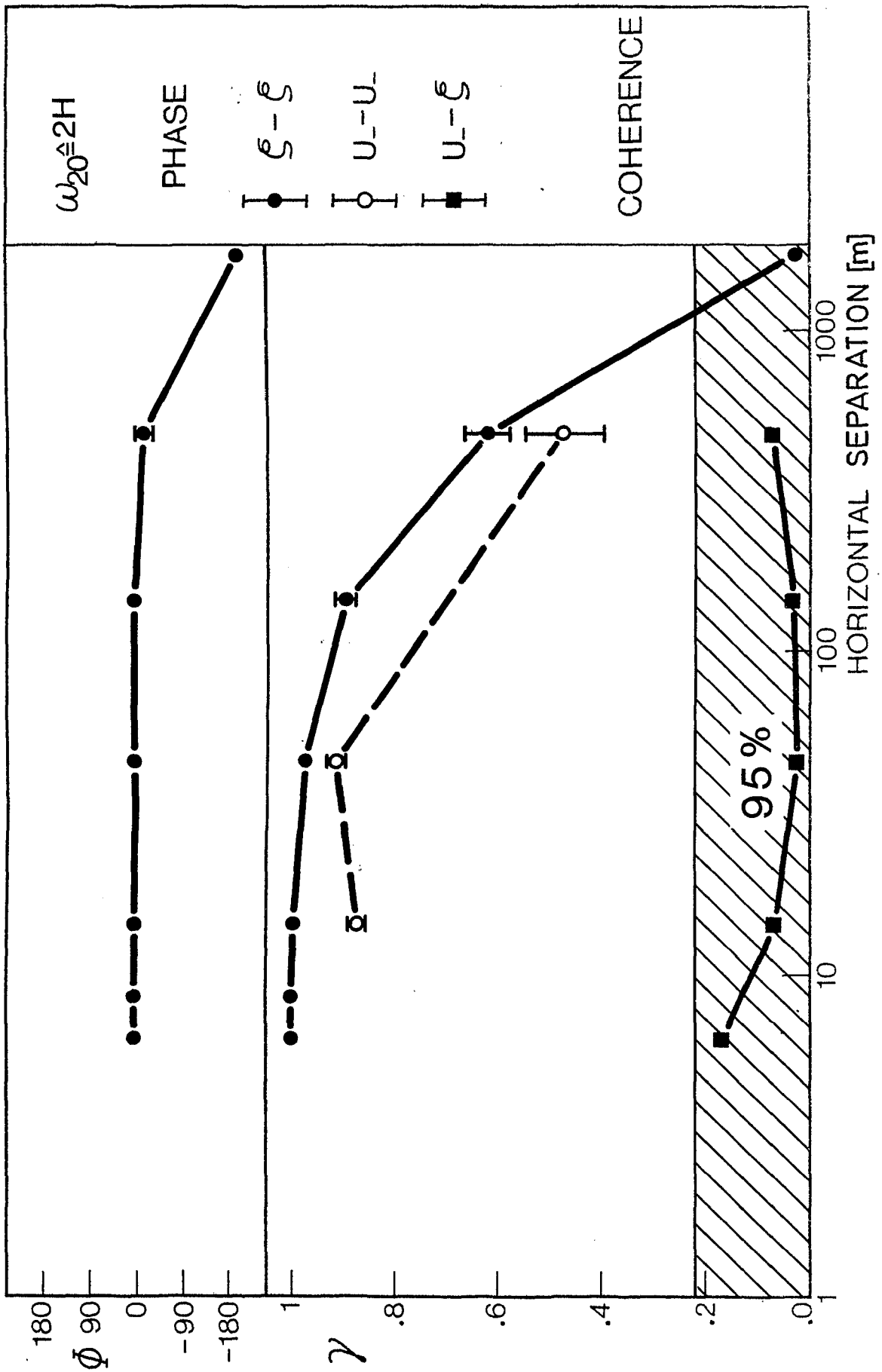


Fig. I.13b

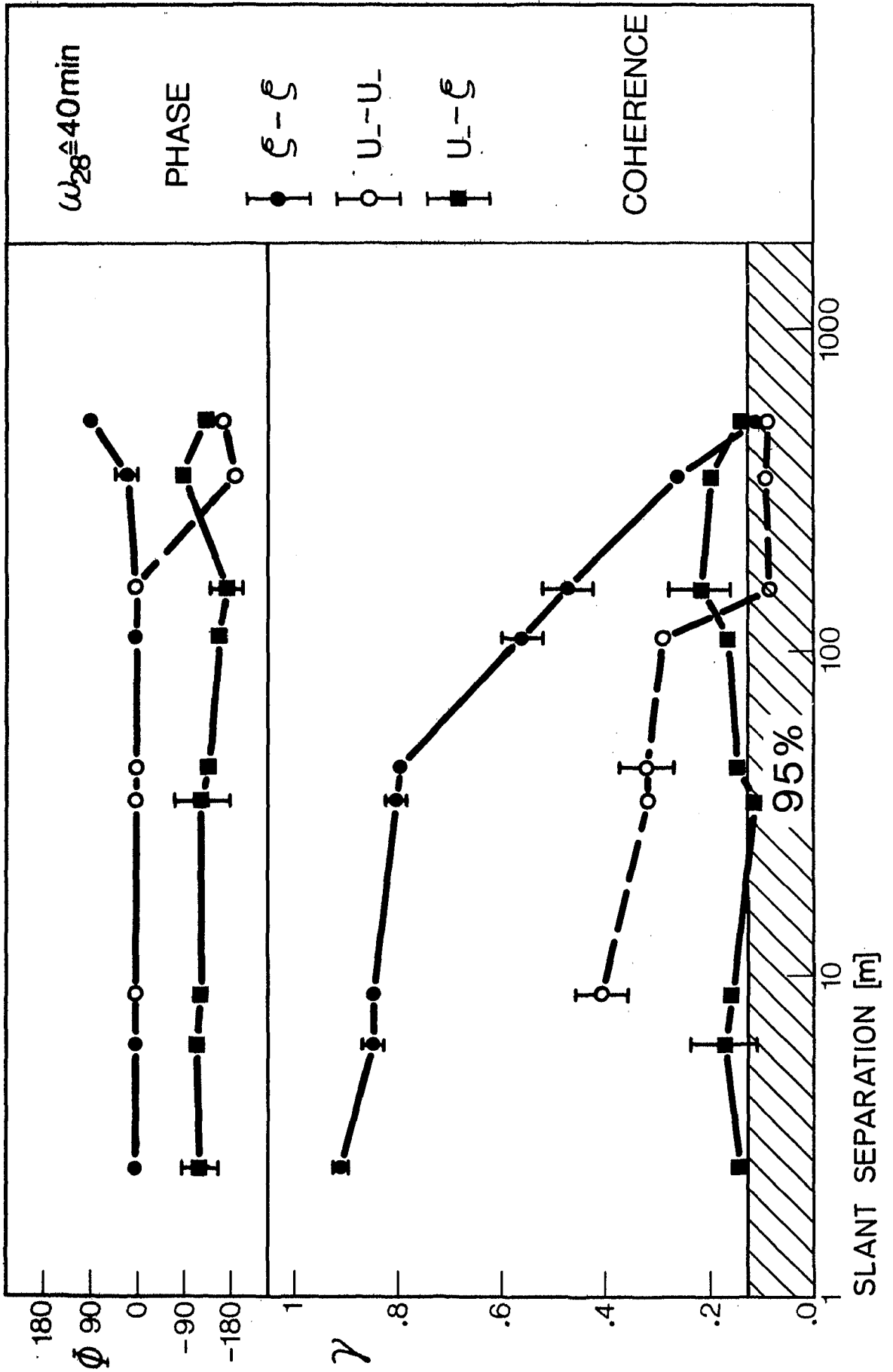


Fig. I.14a



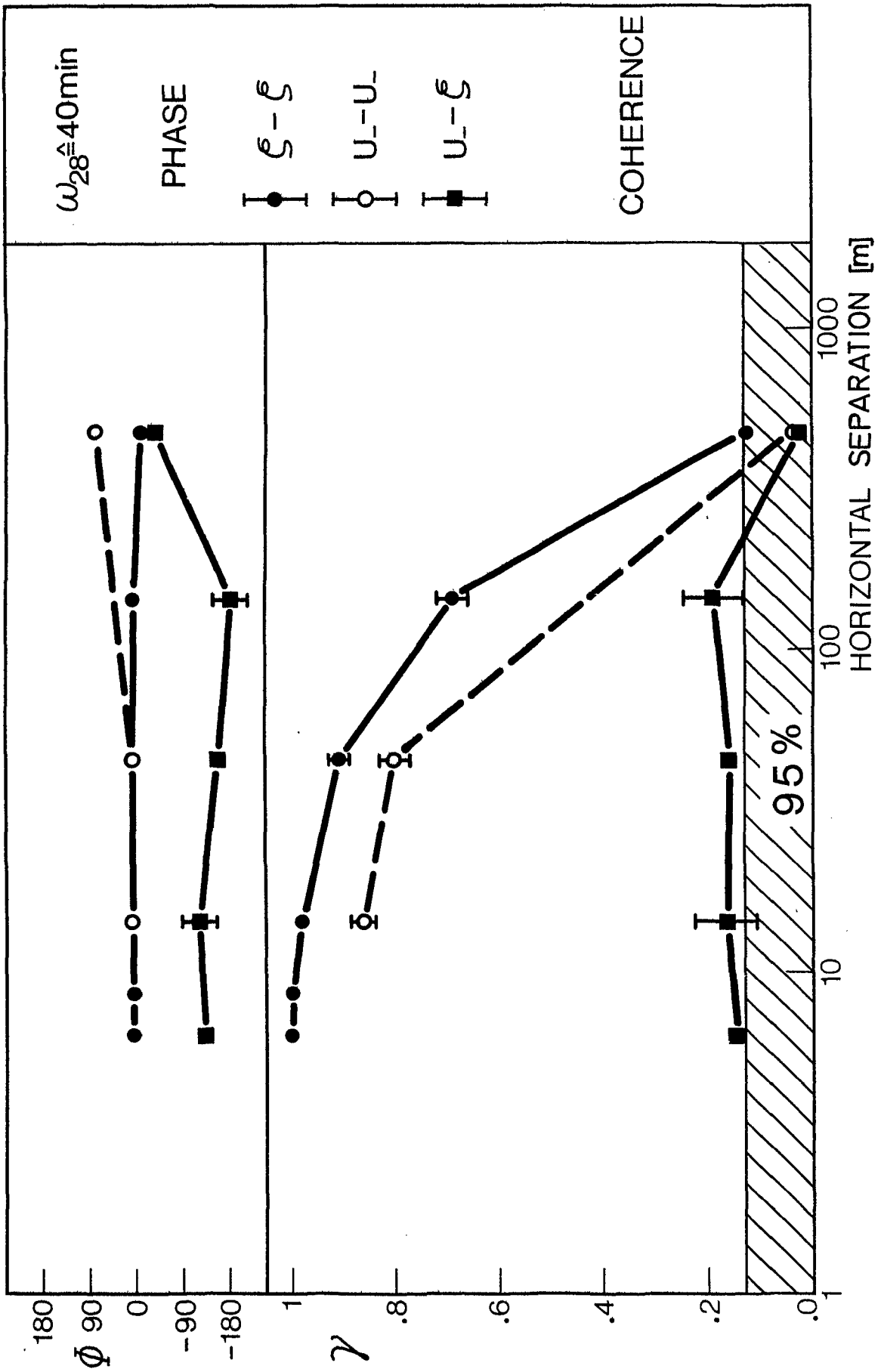


Fig. I.14b

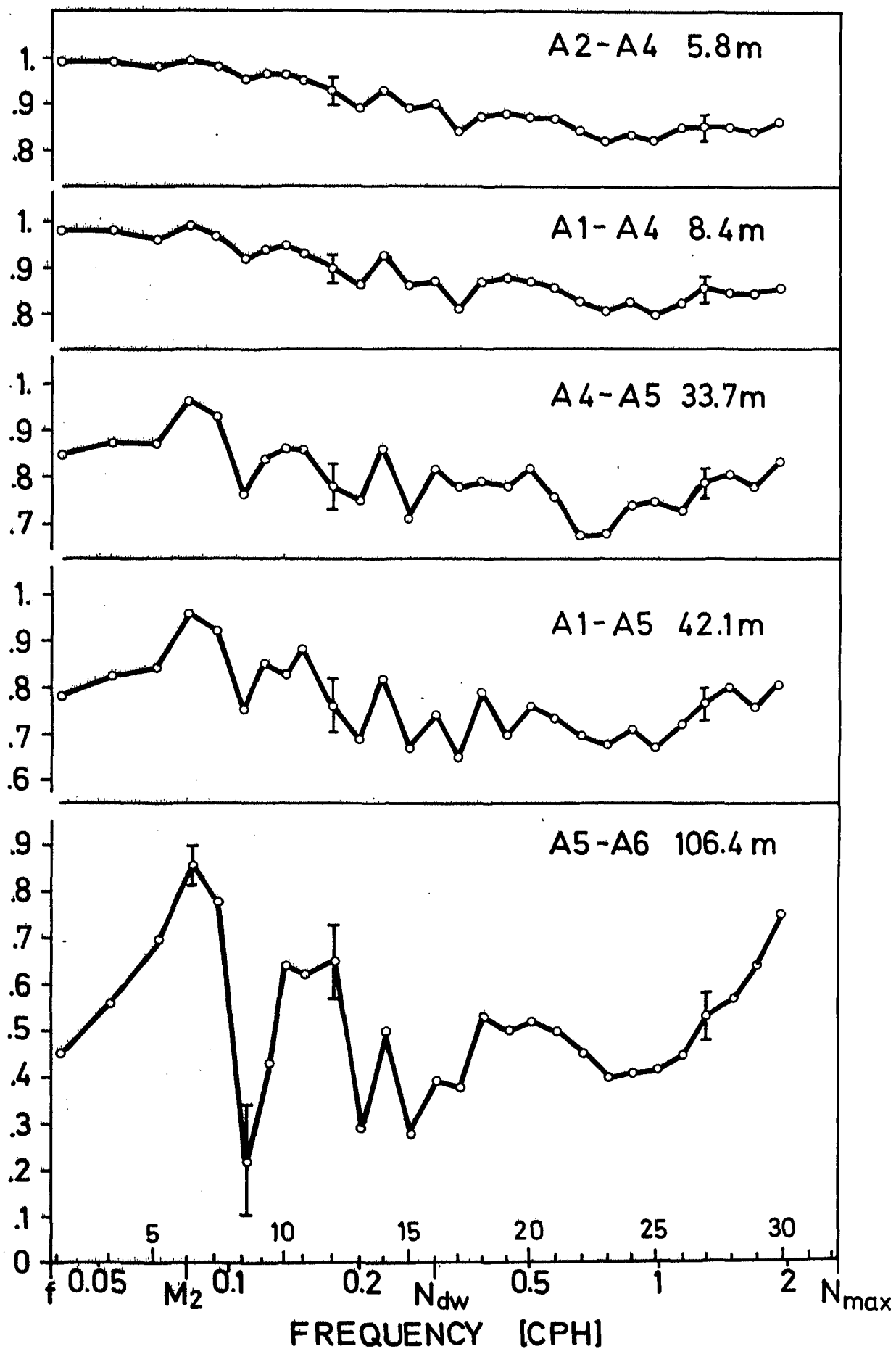


Fig. I.15

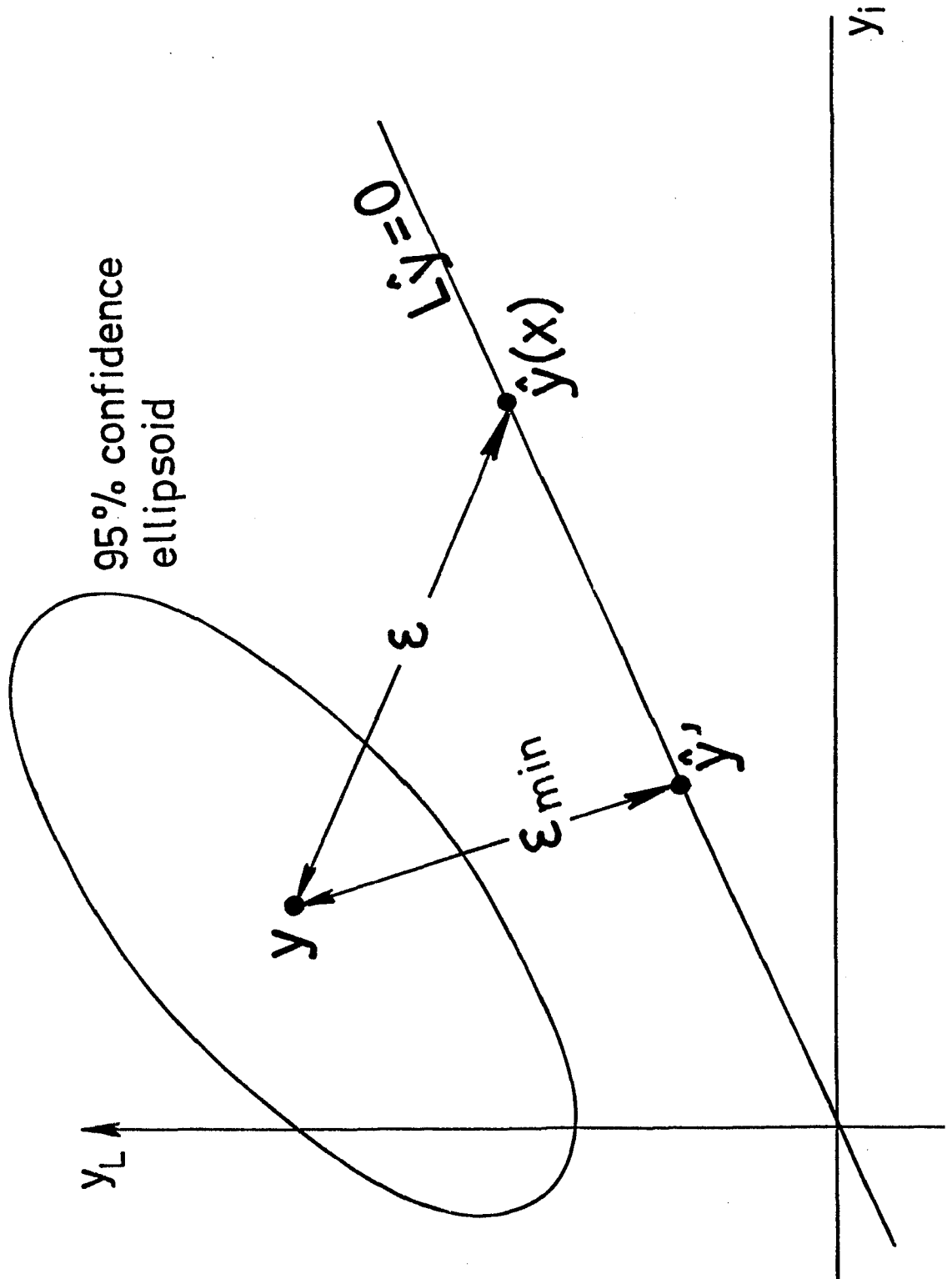


Fig. III.1

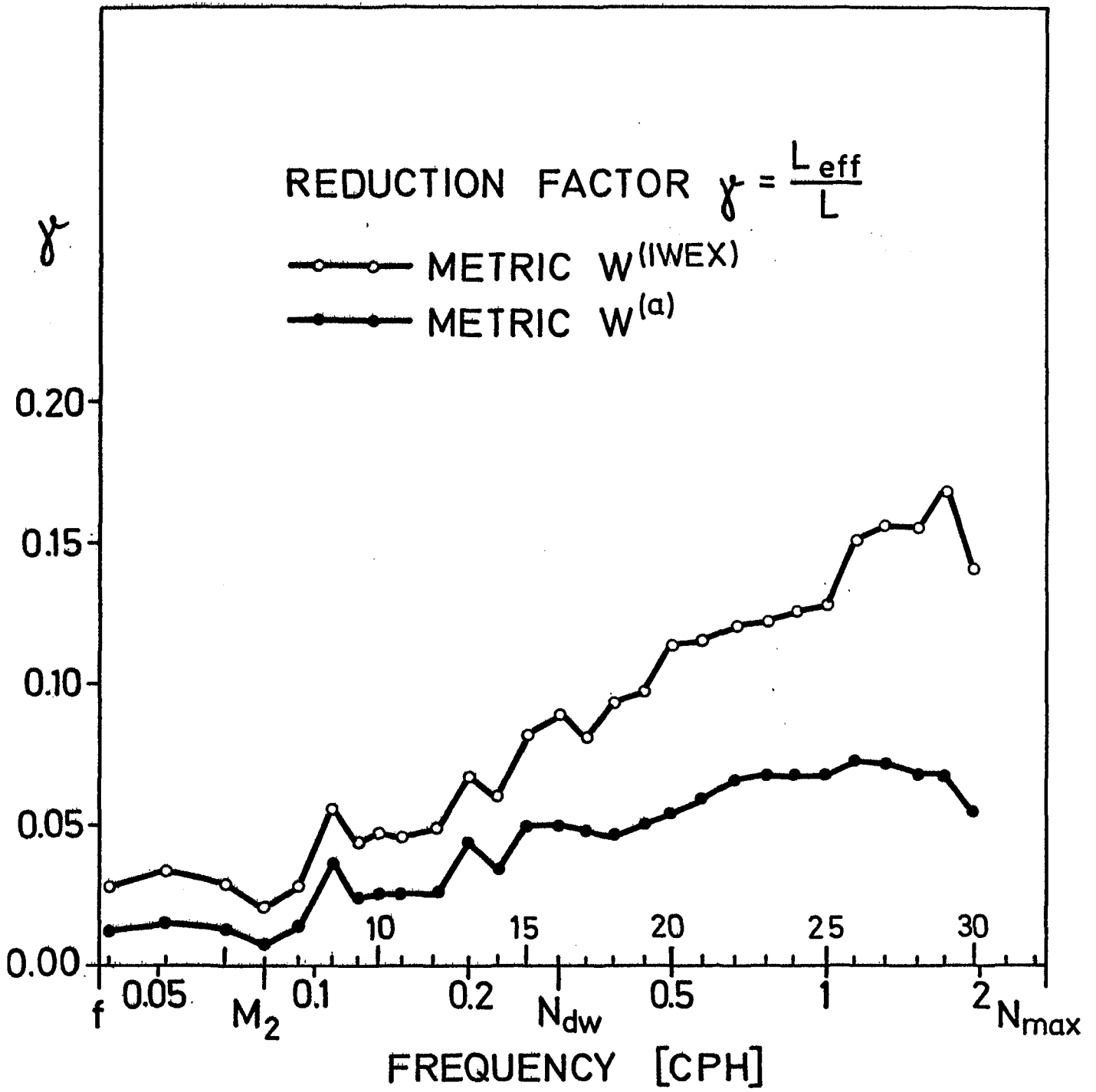


Fig. III.2

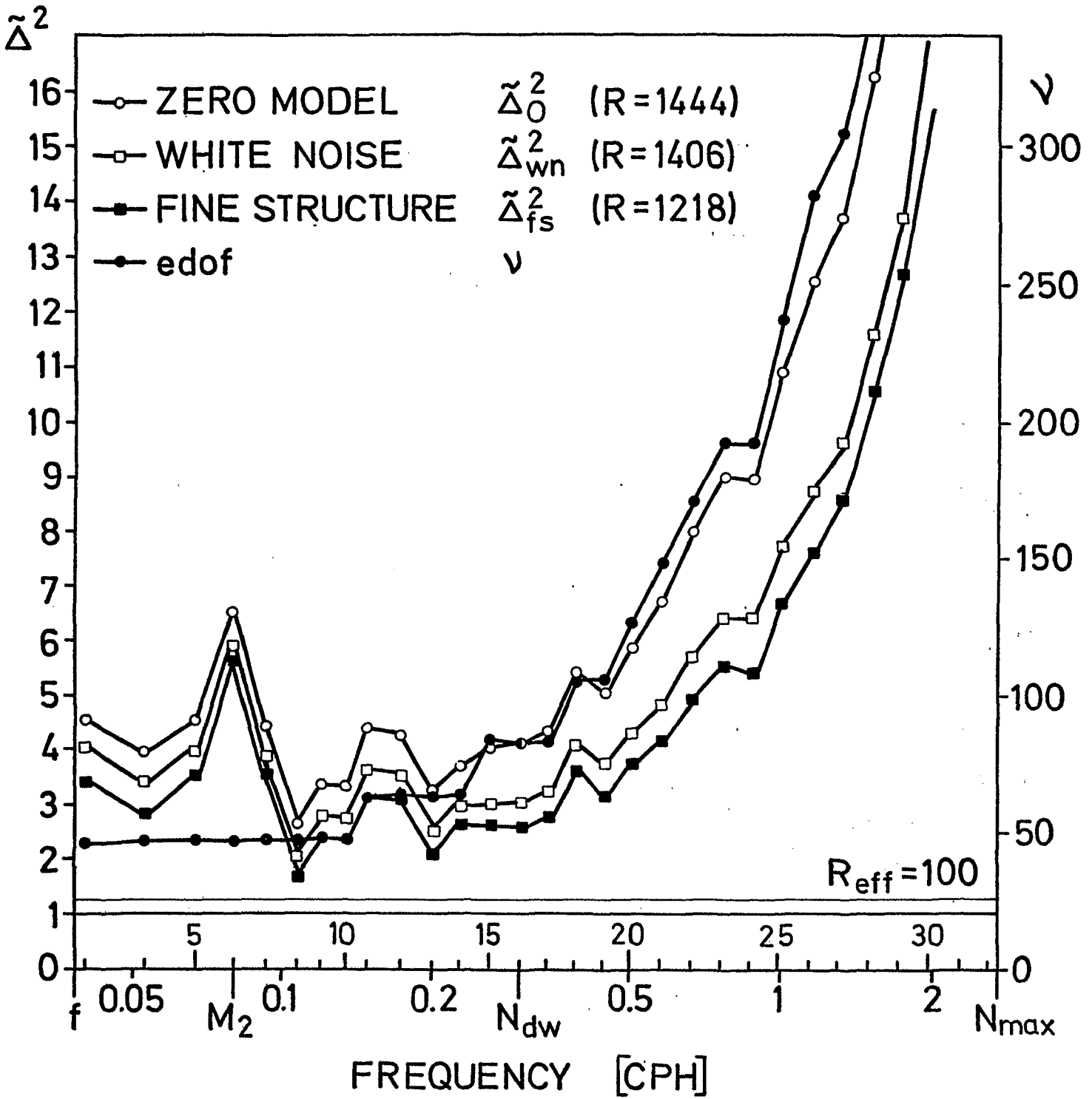


Fig. IV.1

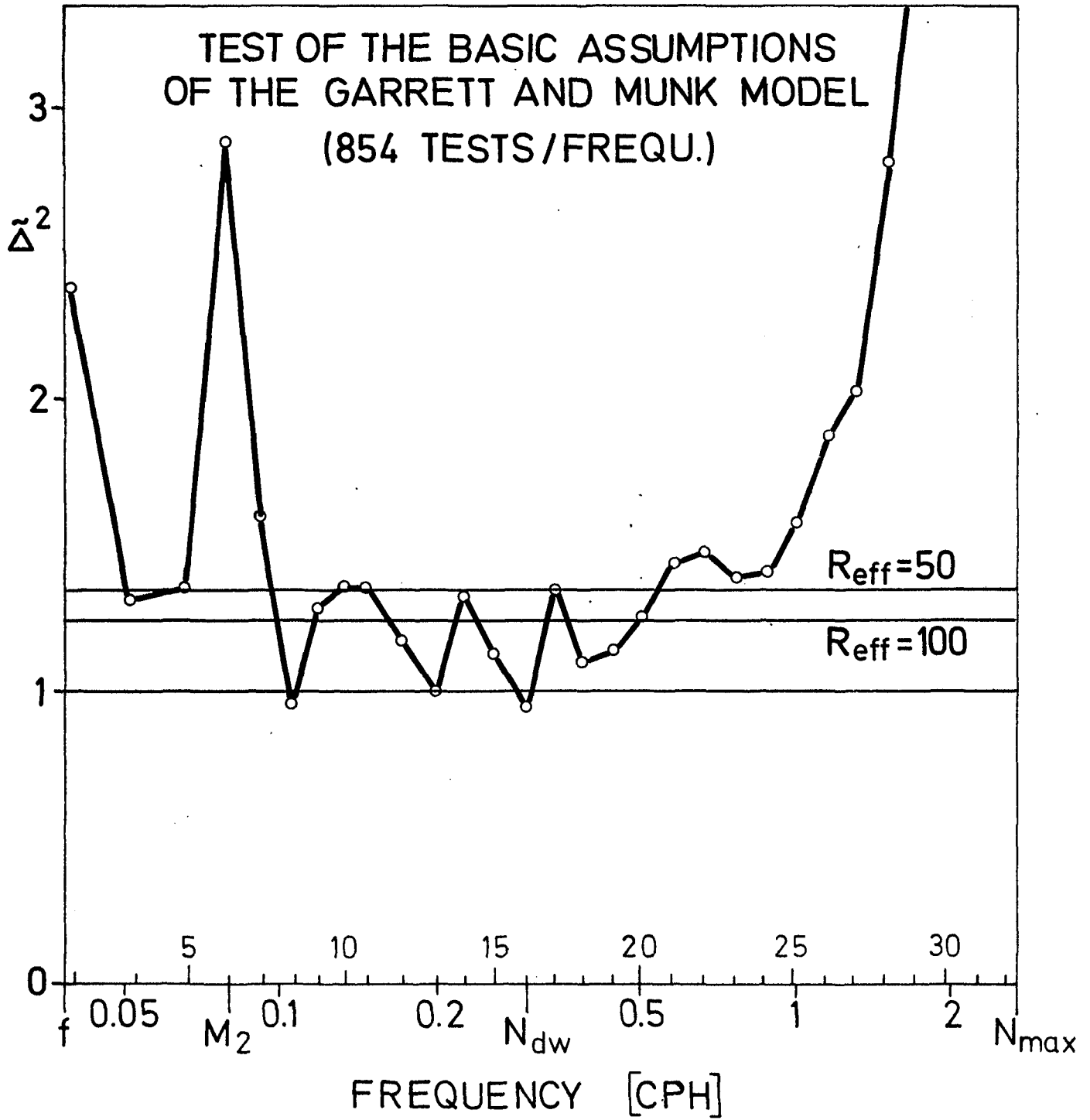


Fig. IV.2

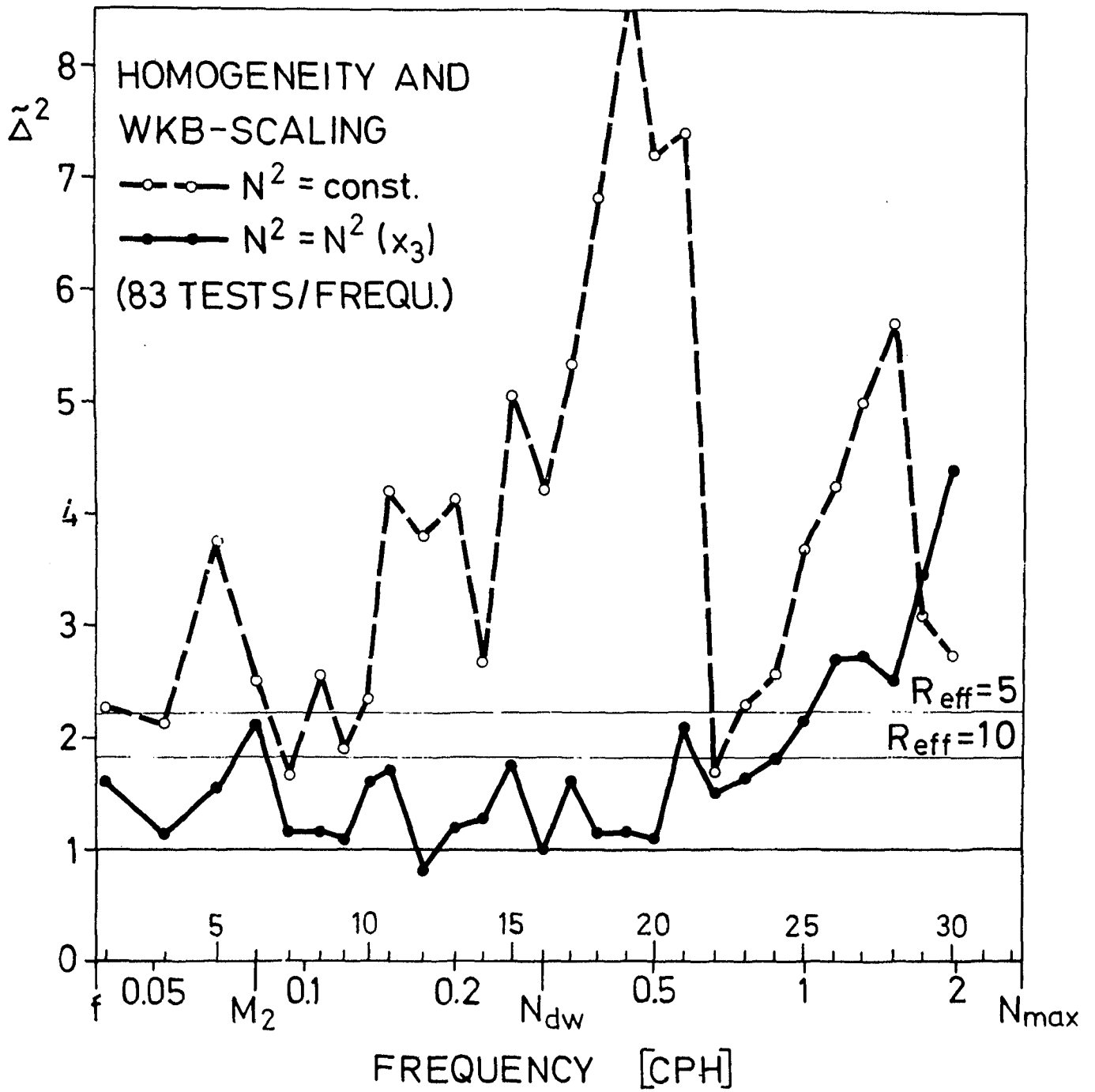


Fig. IV.3

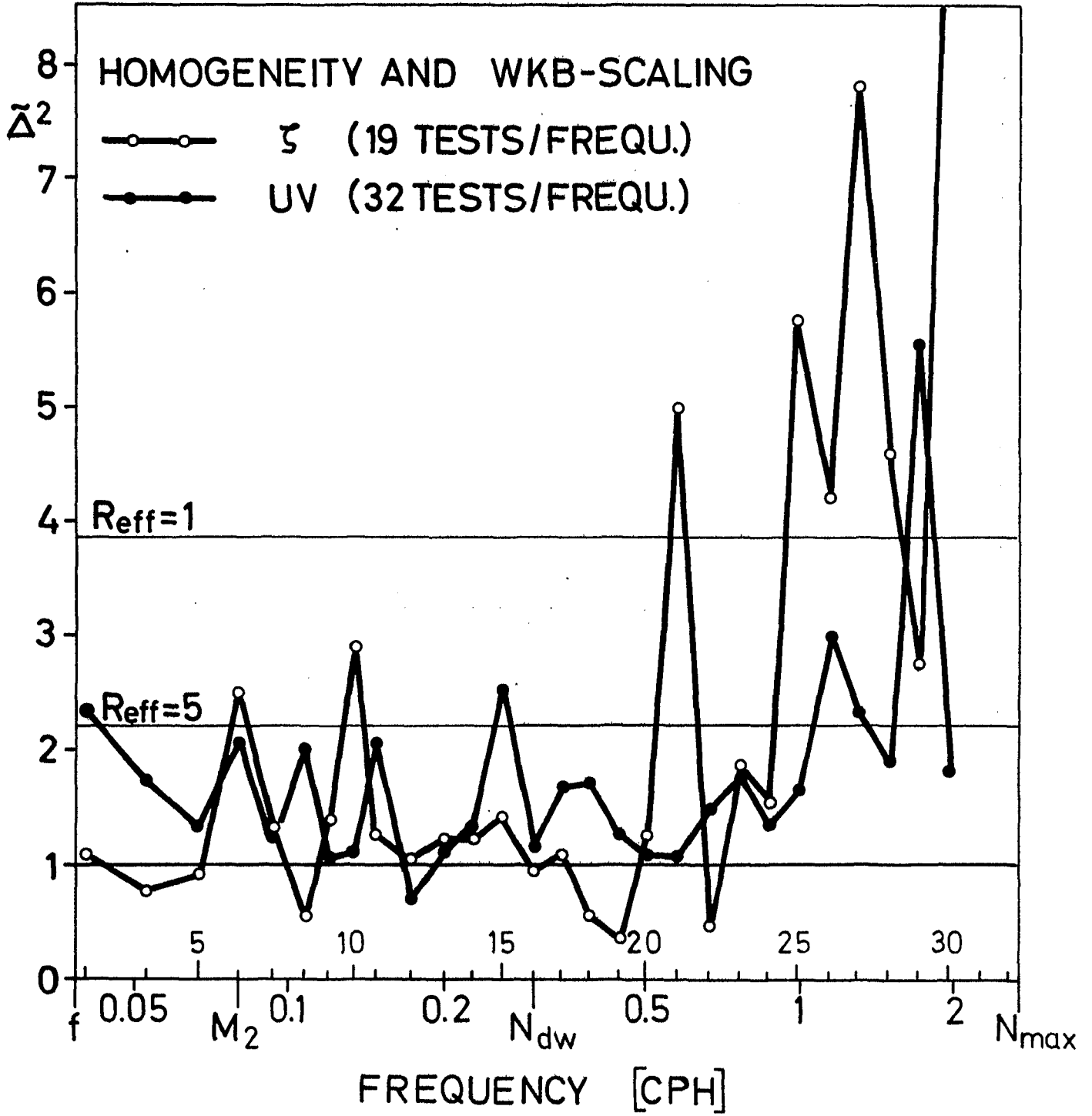


Fig. IV.4



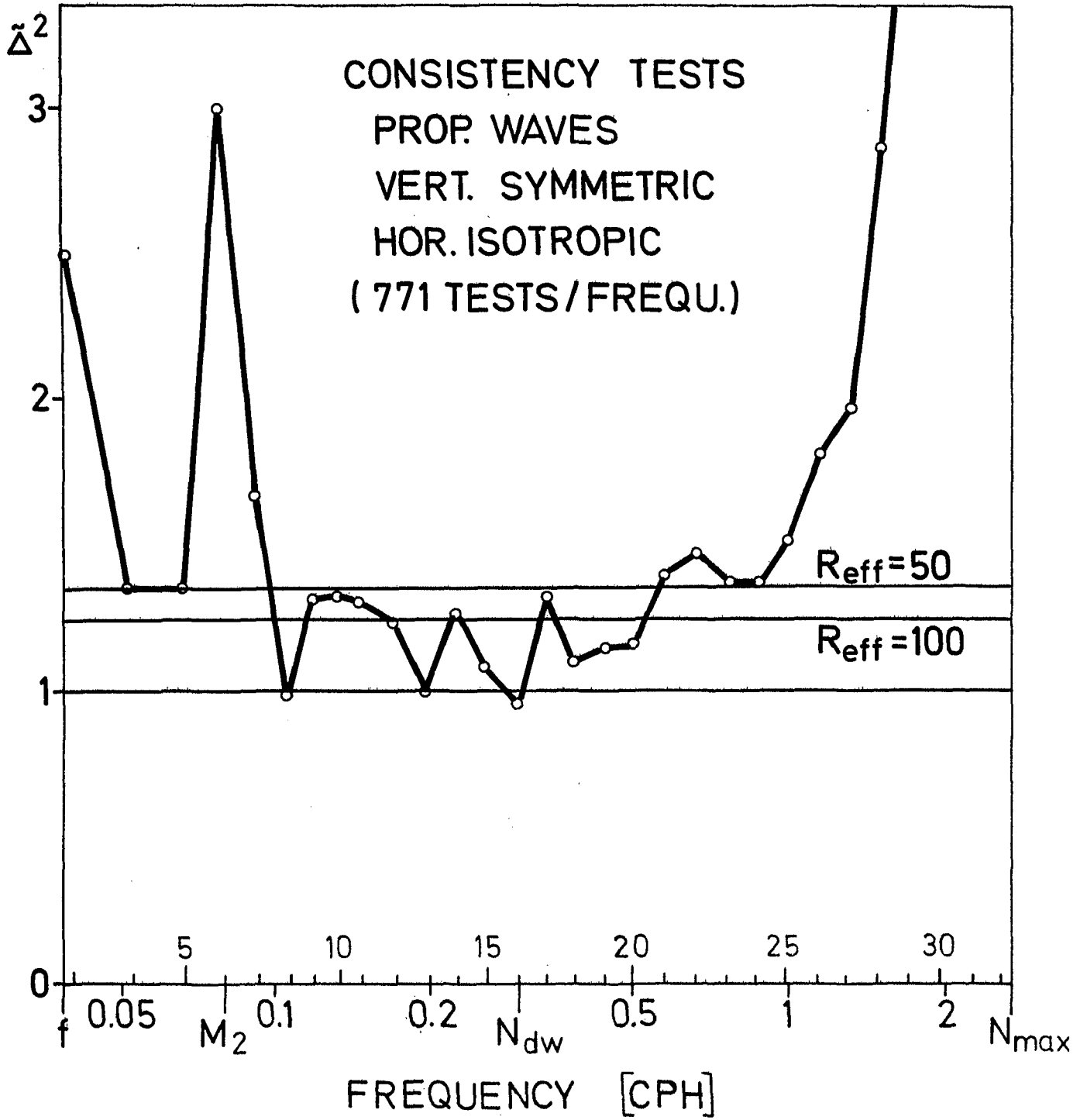


Fig. IV.5

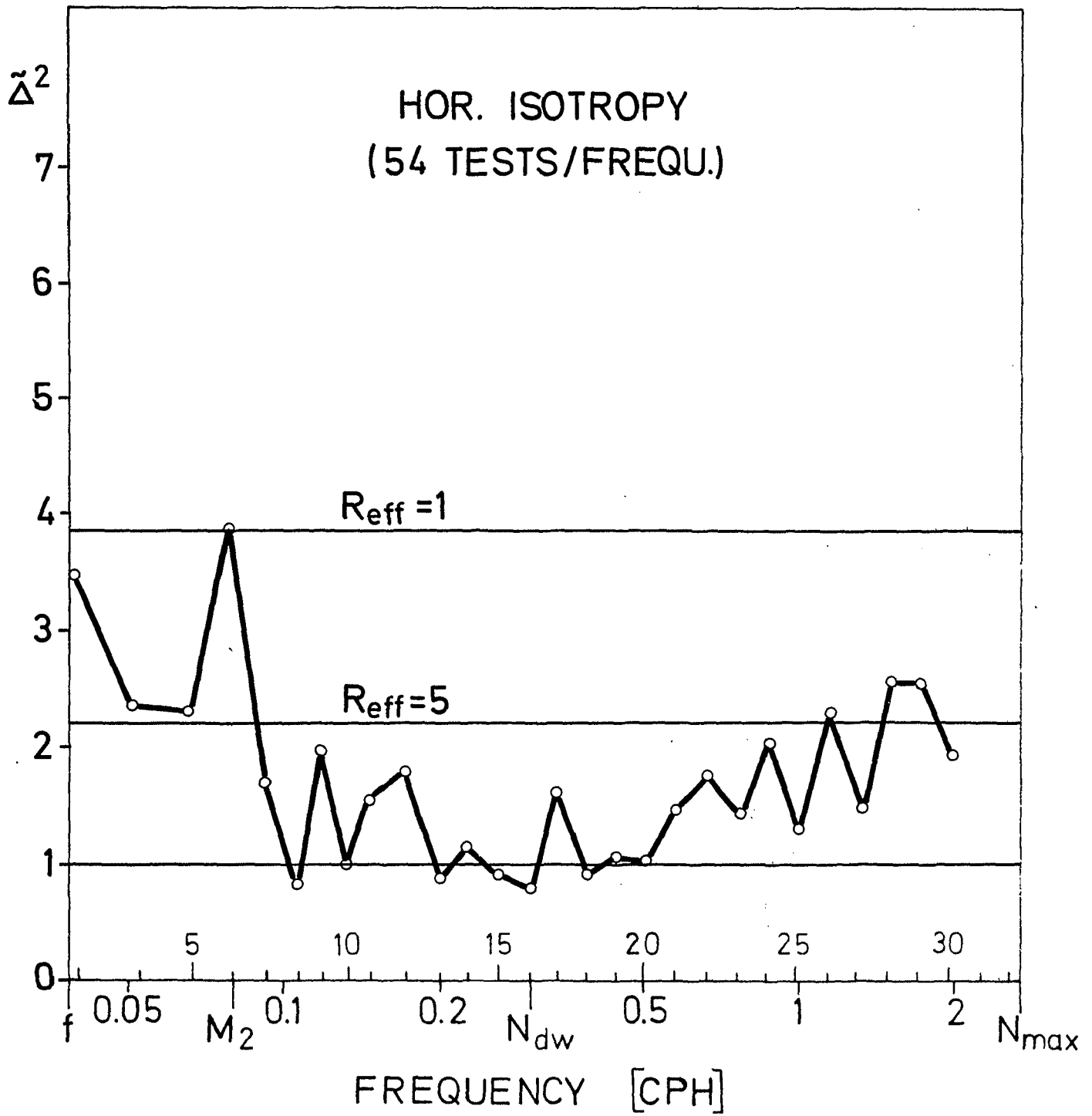


Fig. IV.6

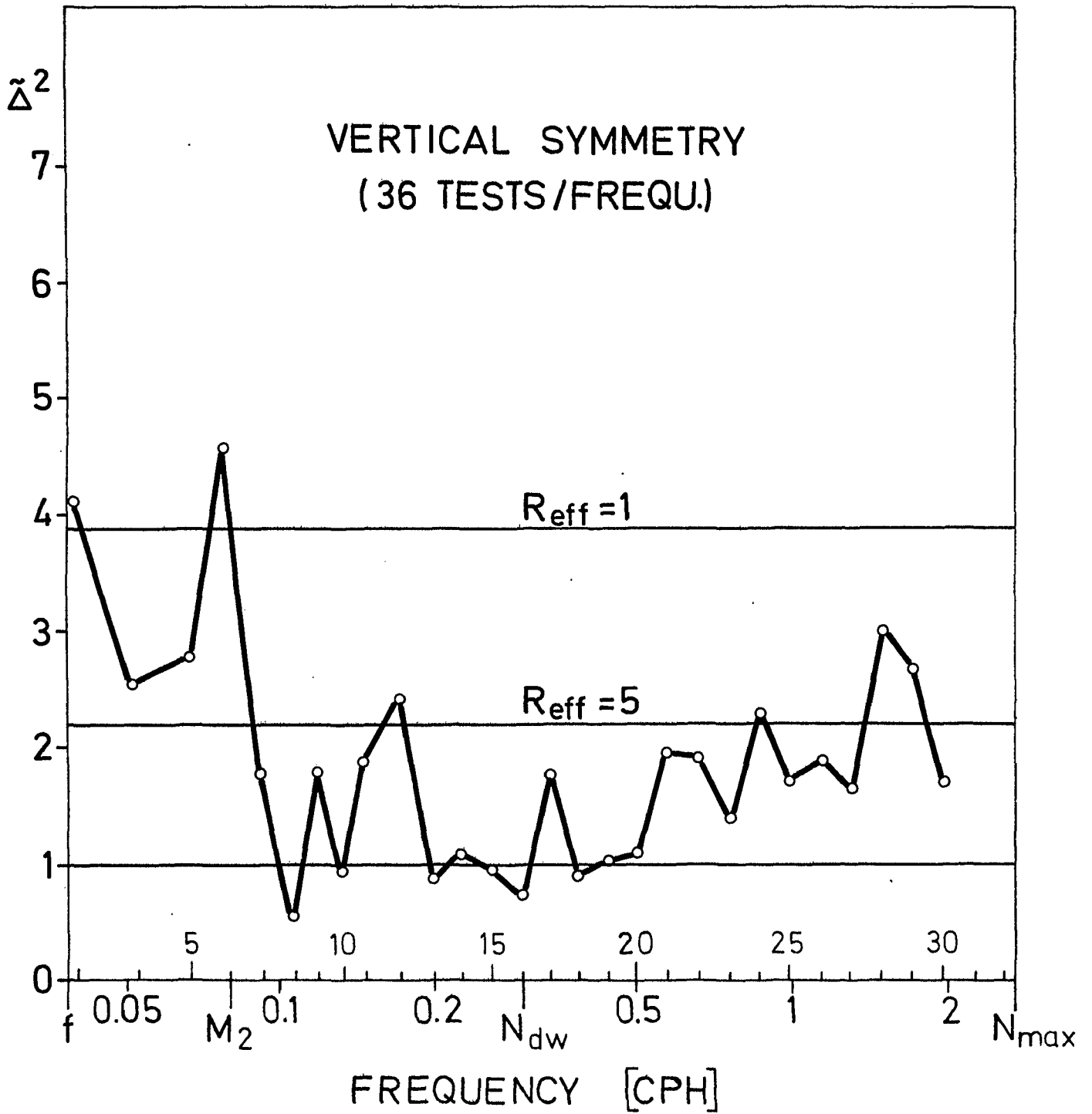


Fig. IV.7

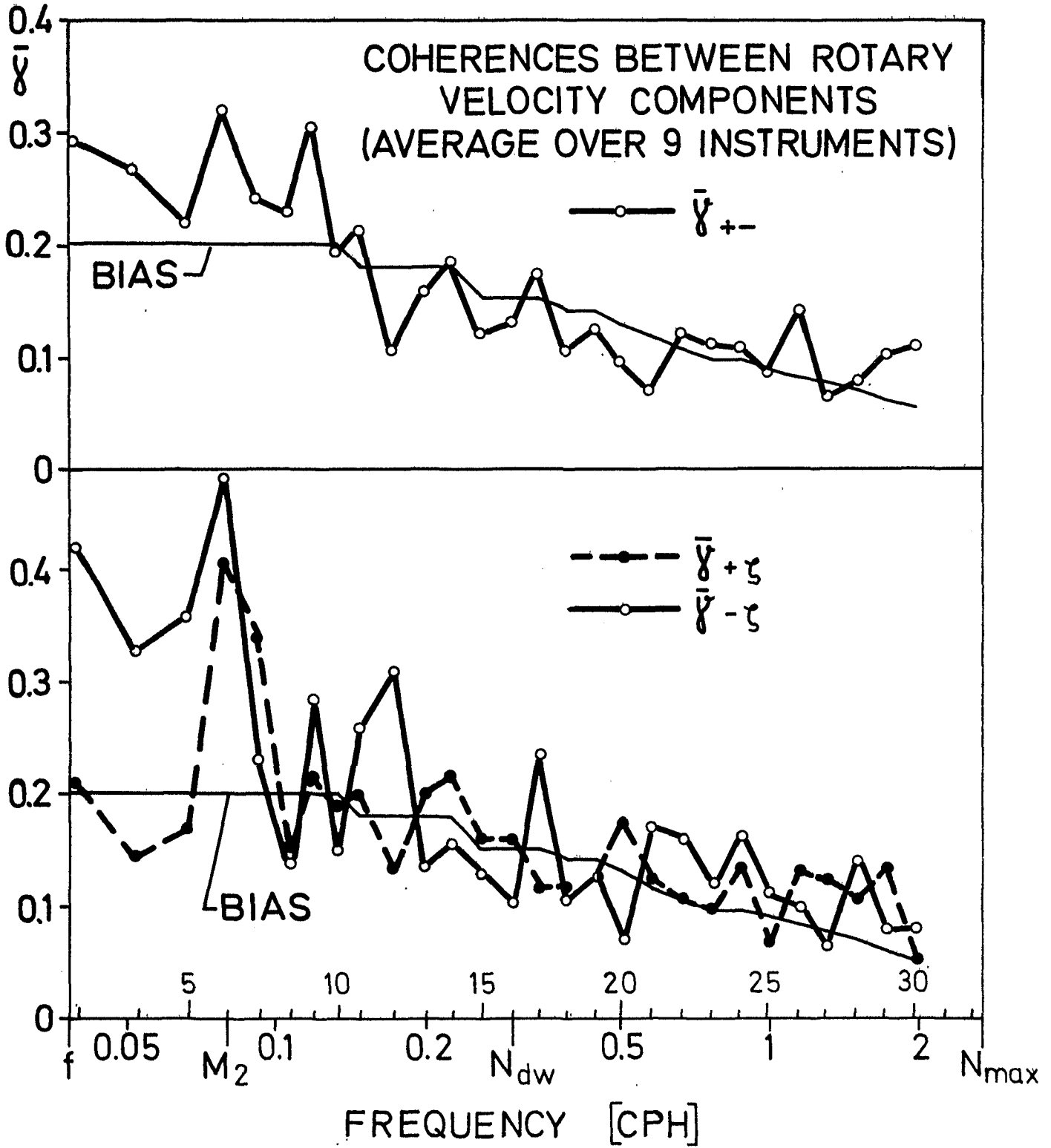


Fig. IV.8

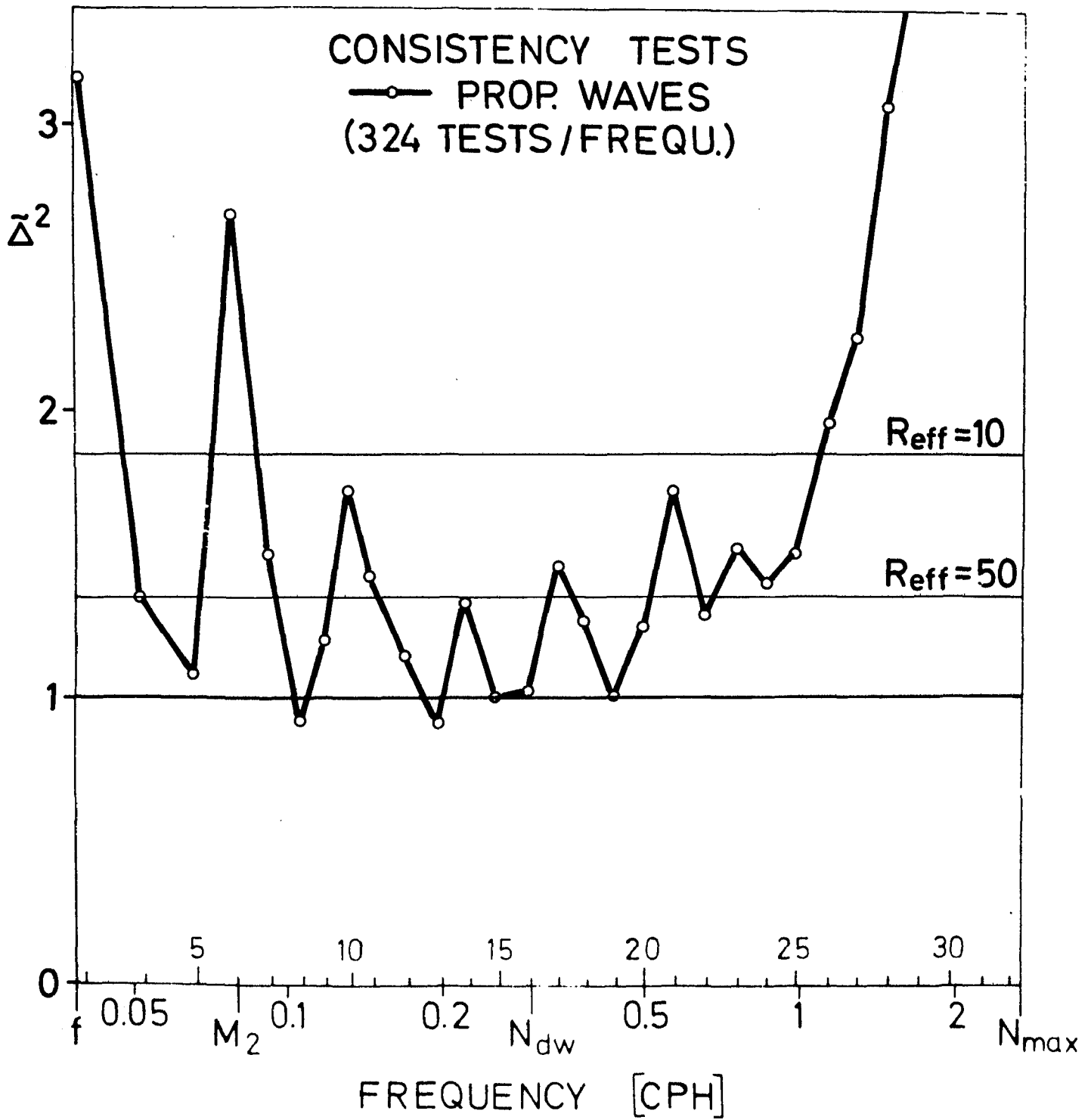


Fig. IV.9

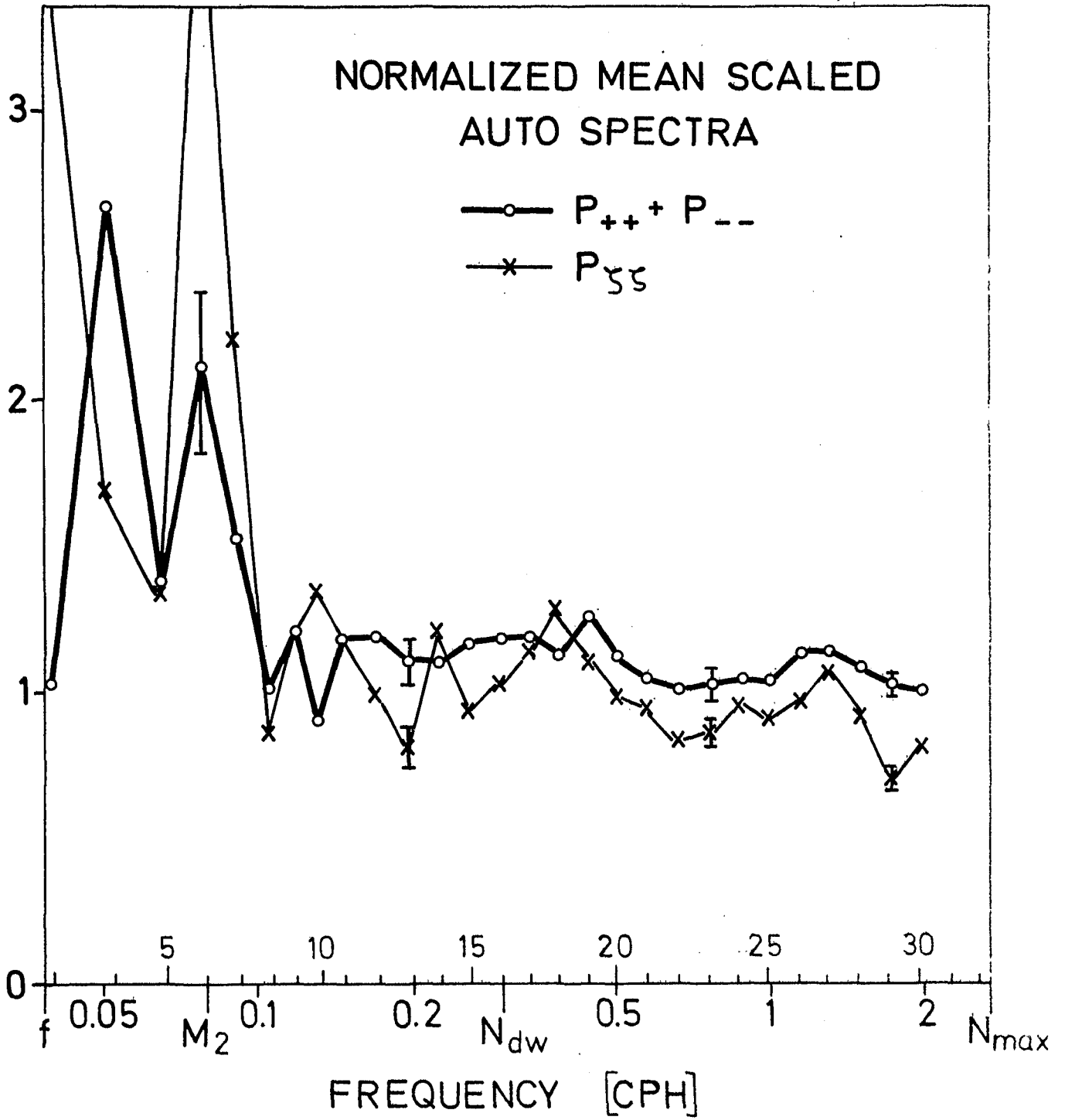


Fig. IV.10

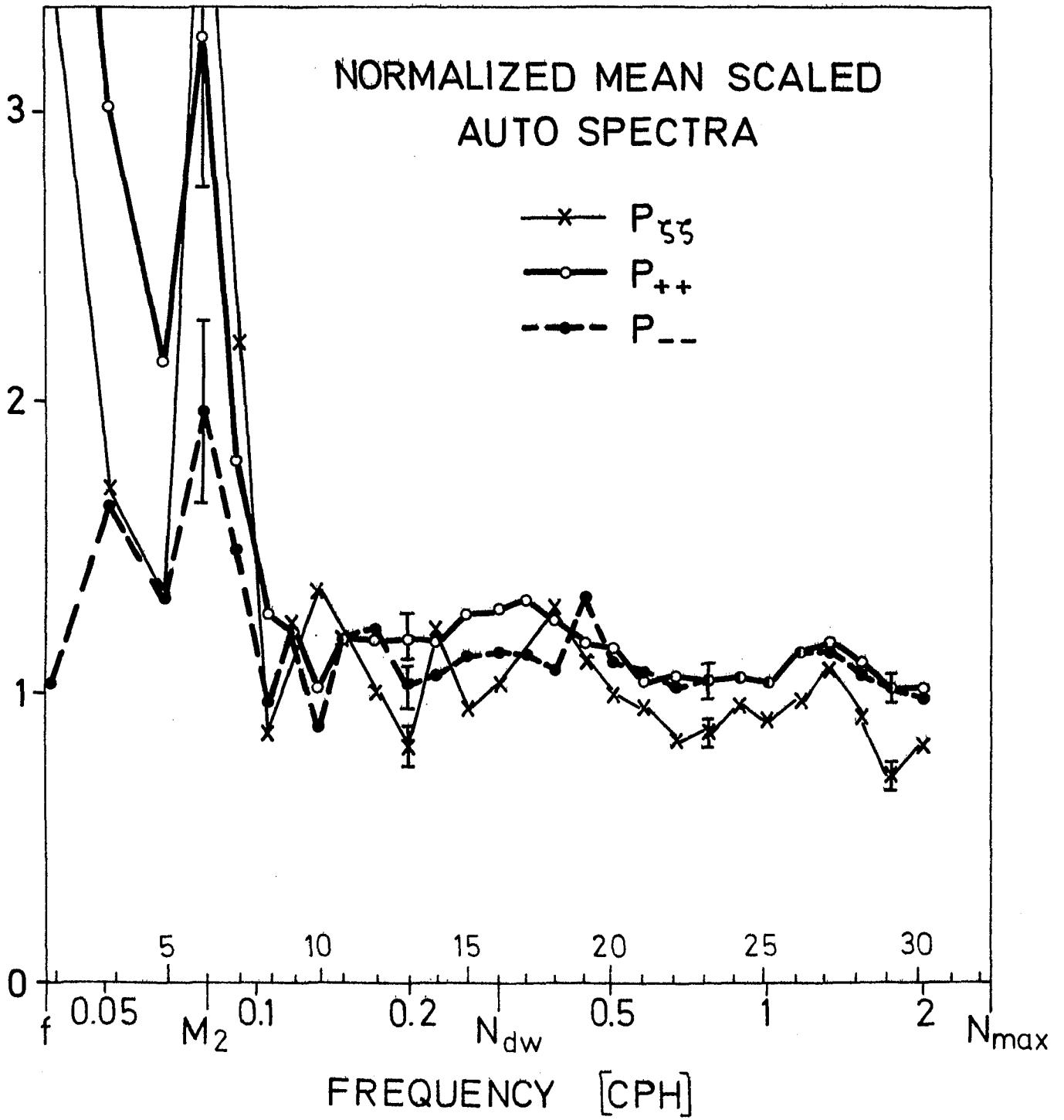


Fig. IV.11

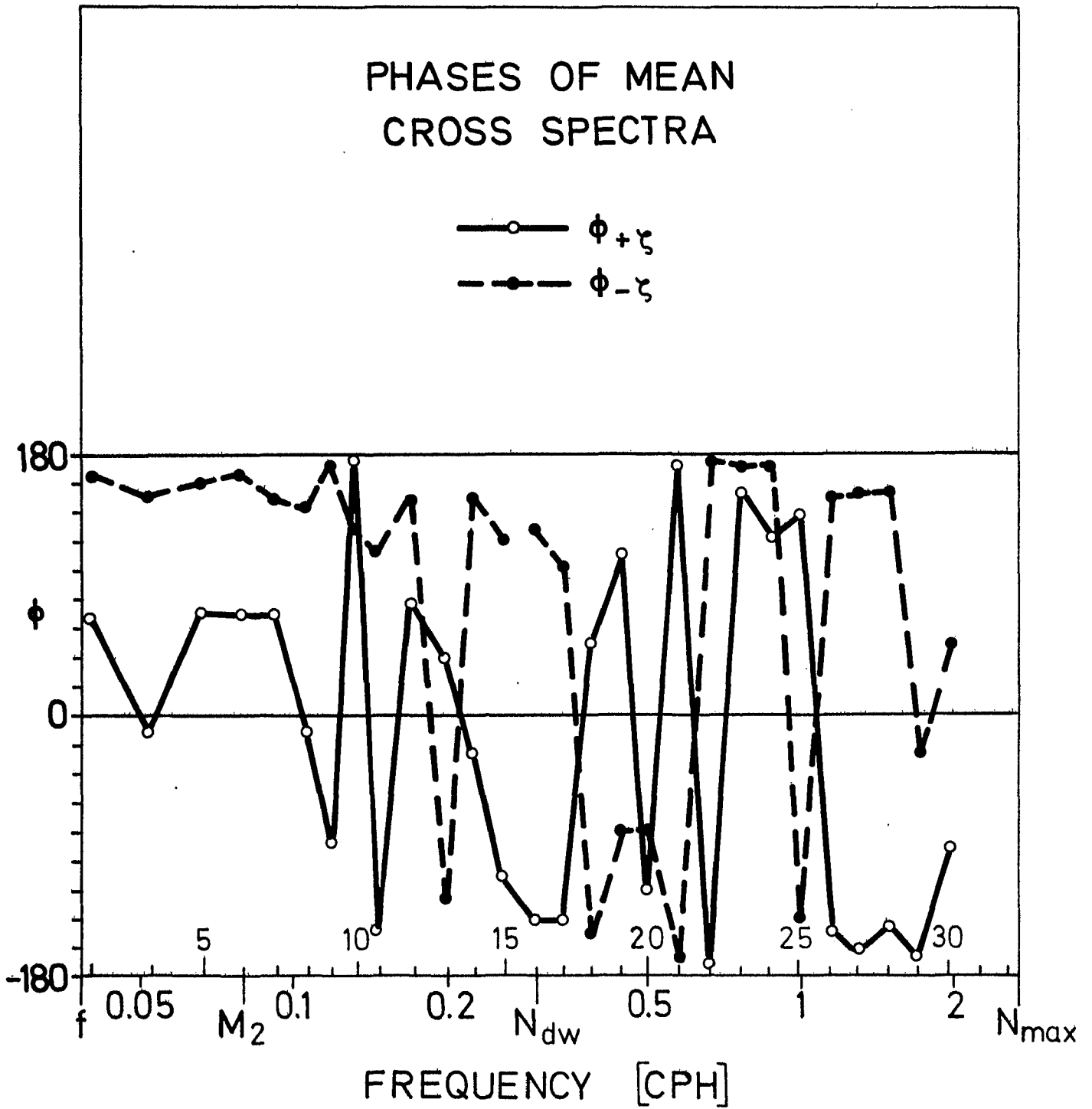


Fig. IV.12



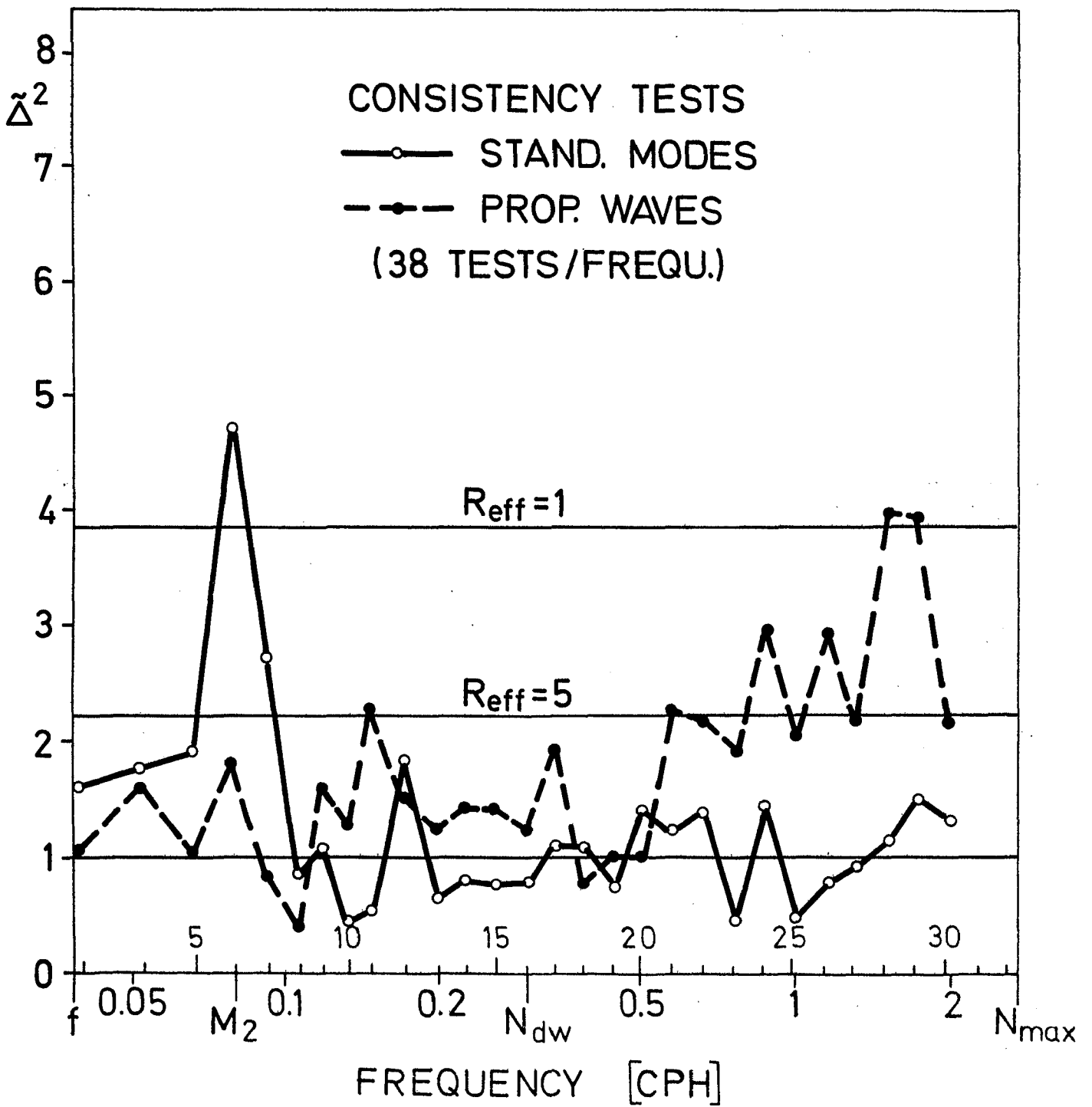


Fig. IV.13

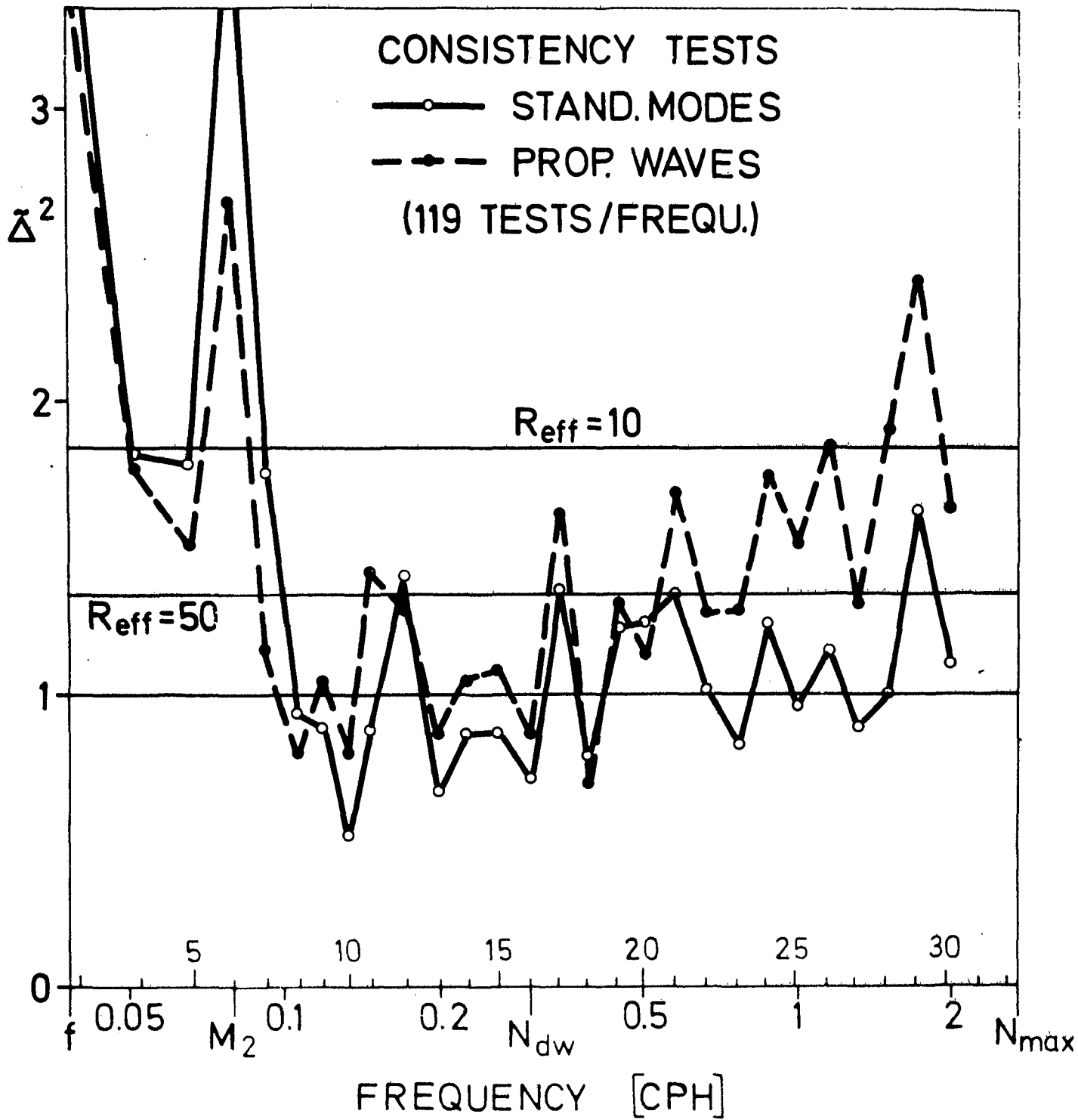


Fig. IV.14

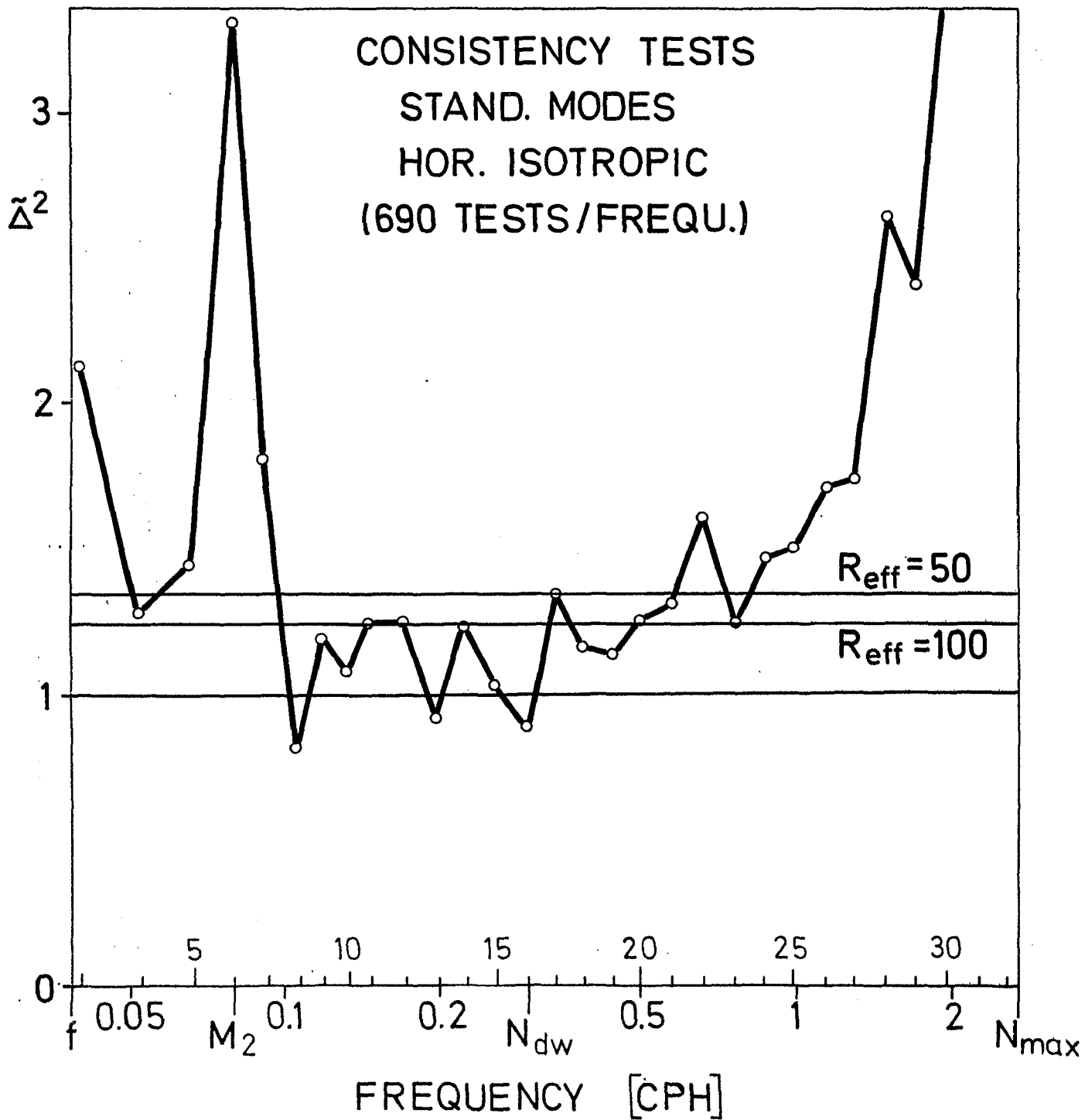


Fig. IV.15

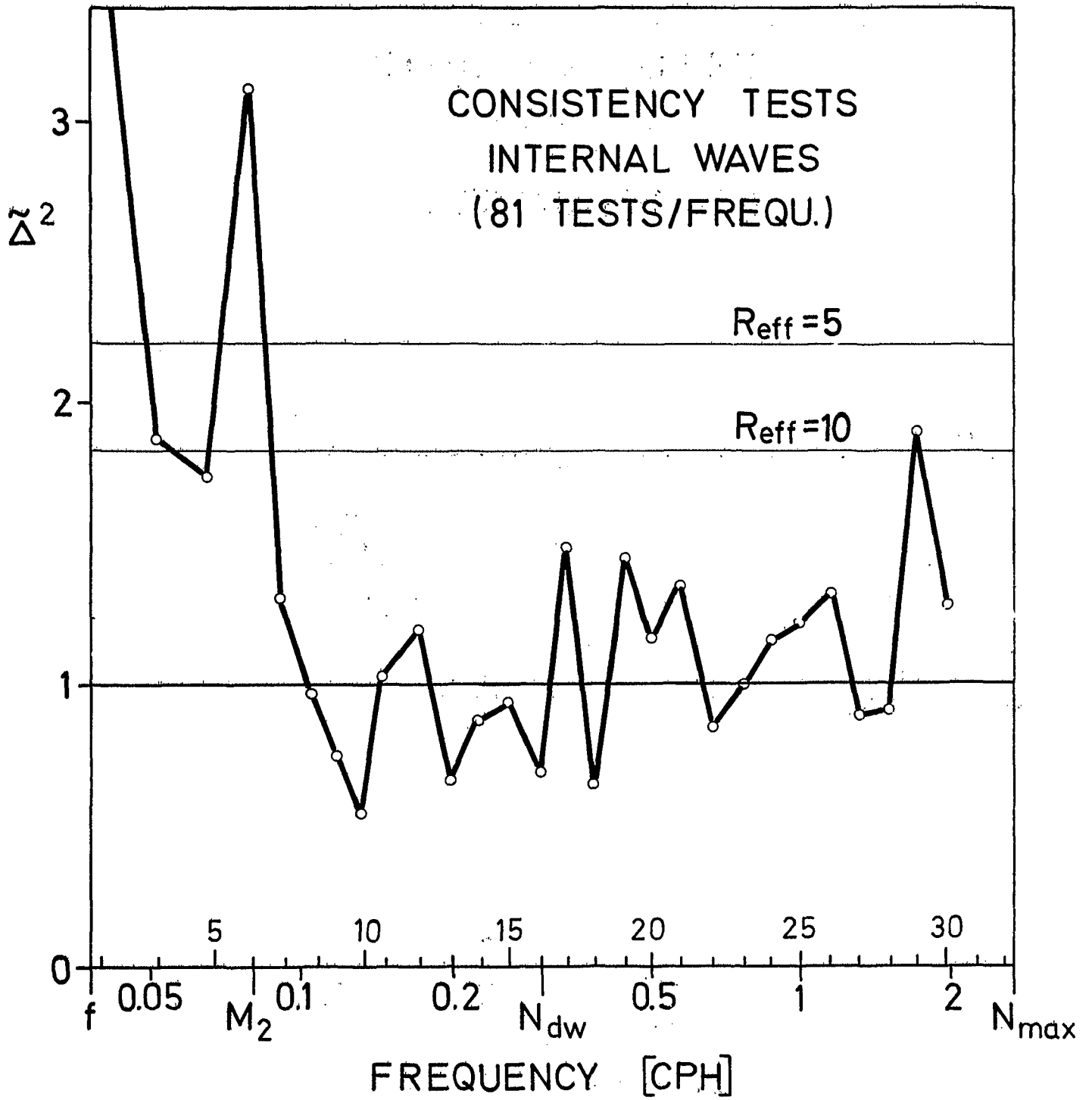


Fig. IV.16

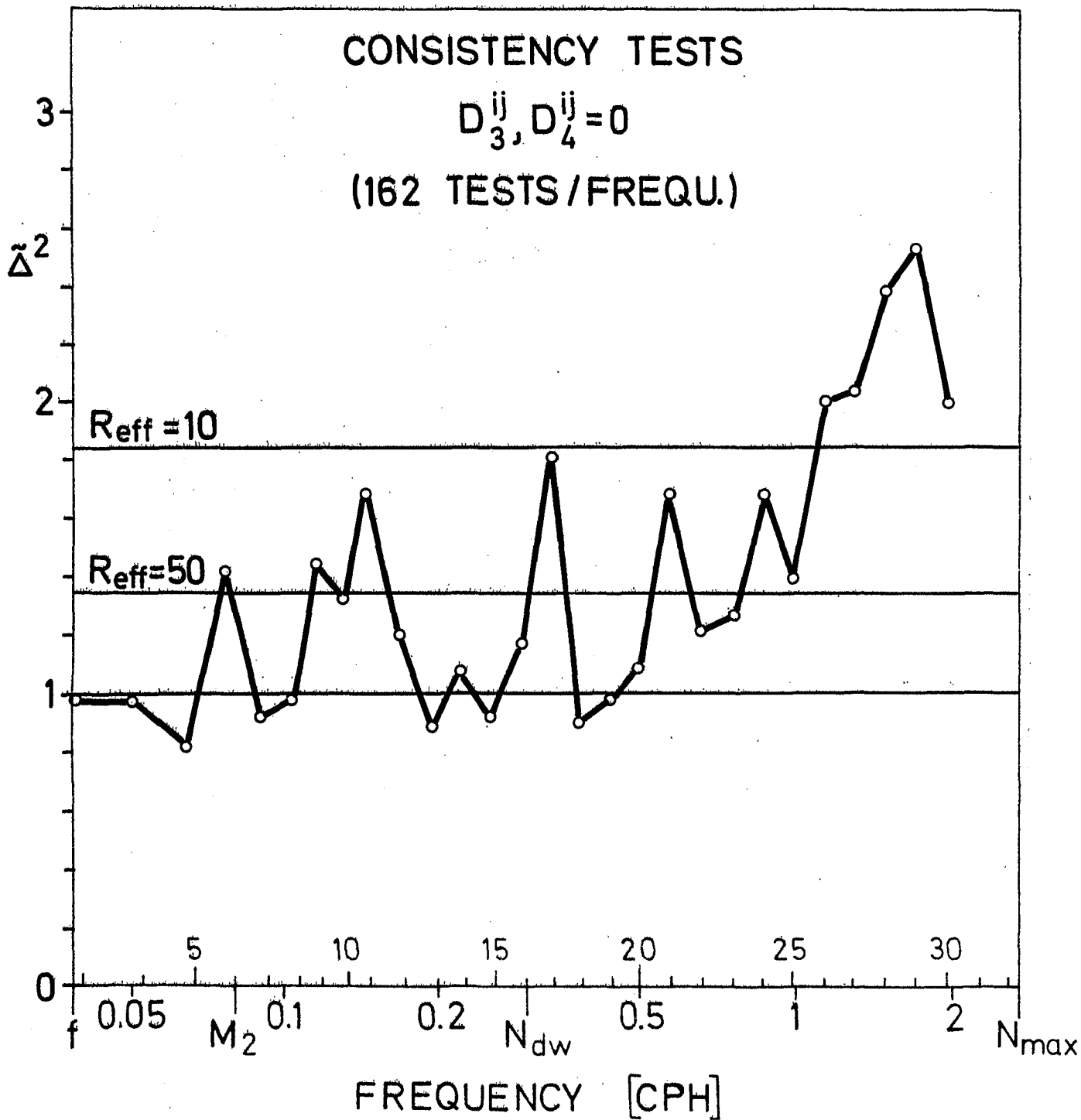


Fig. IV.17

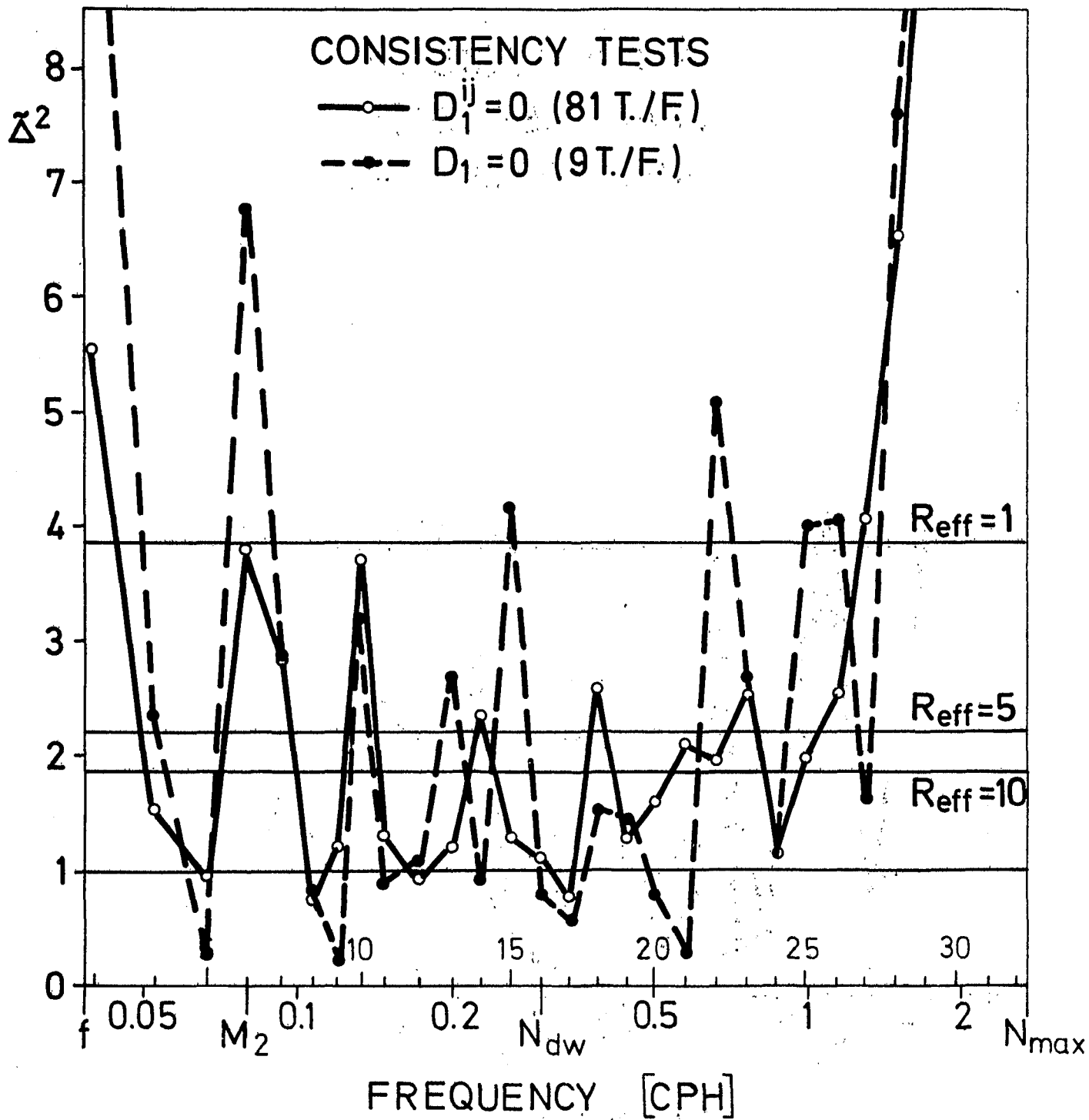


Fig. IV.18

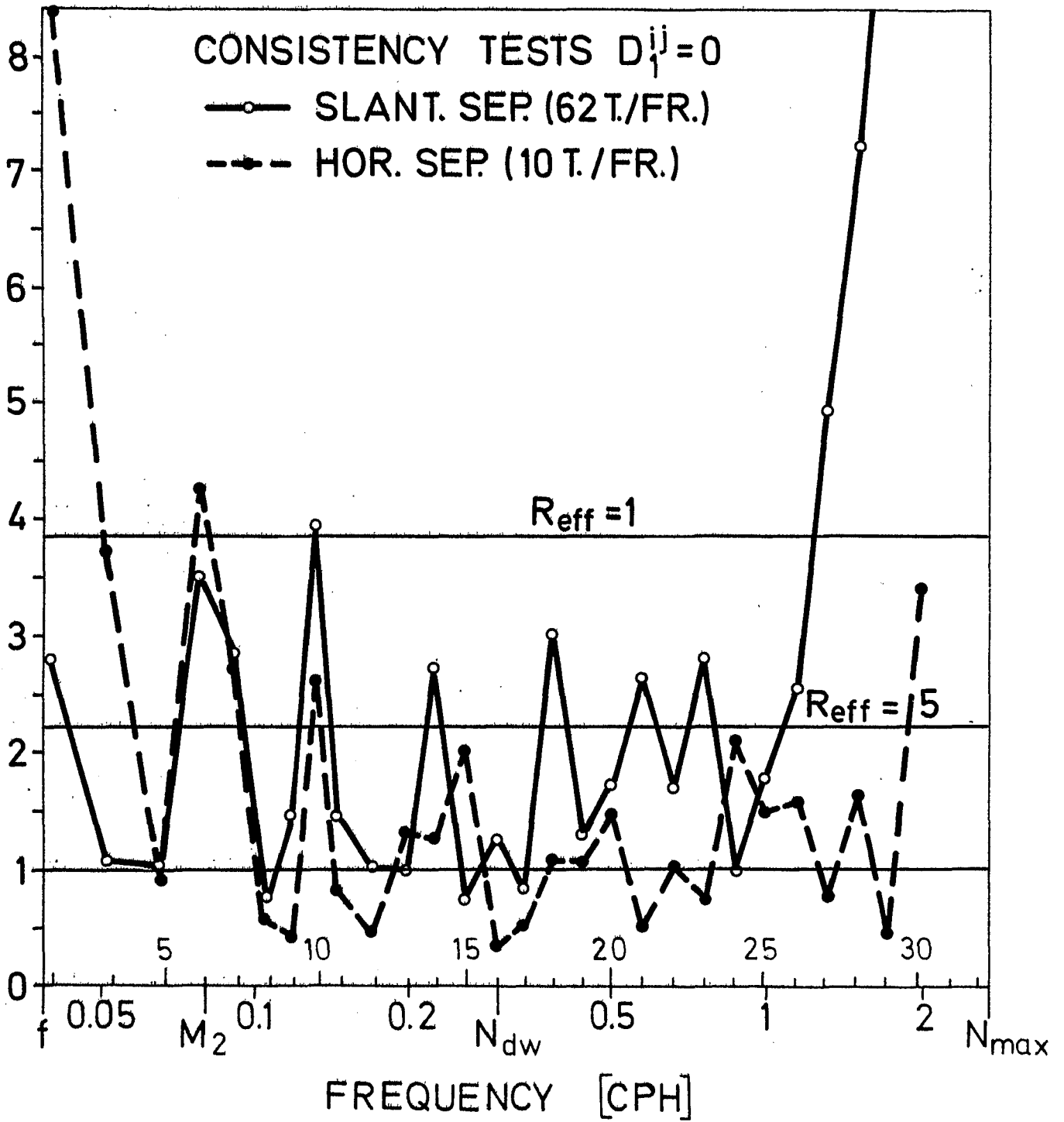


Fig. IV.19

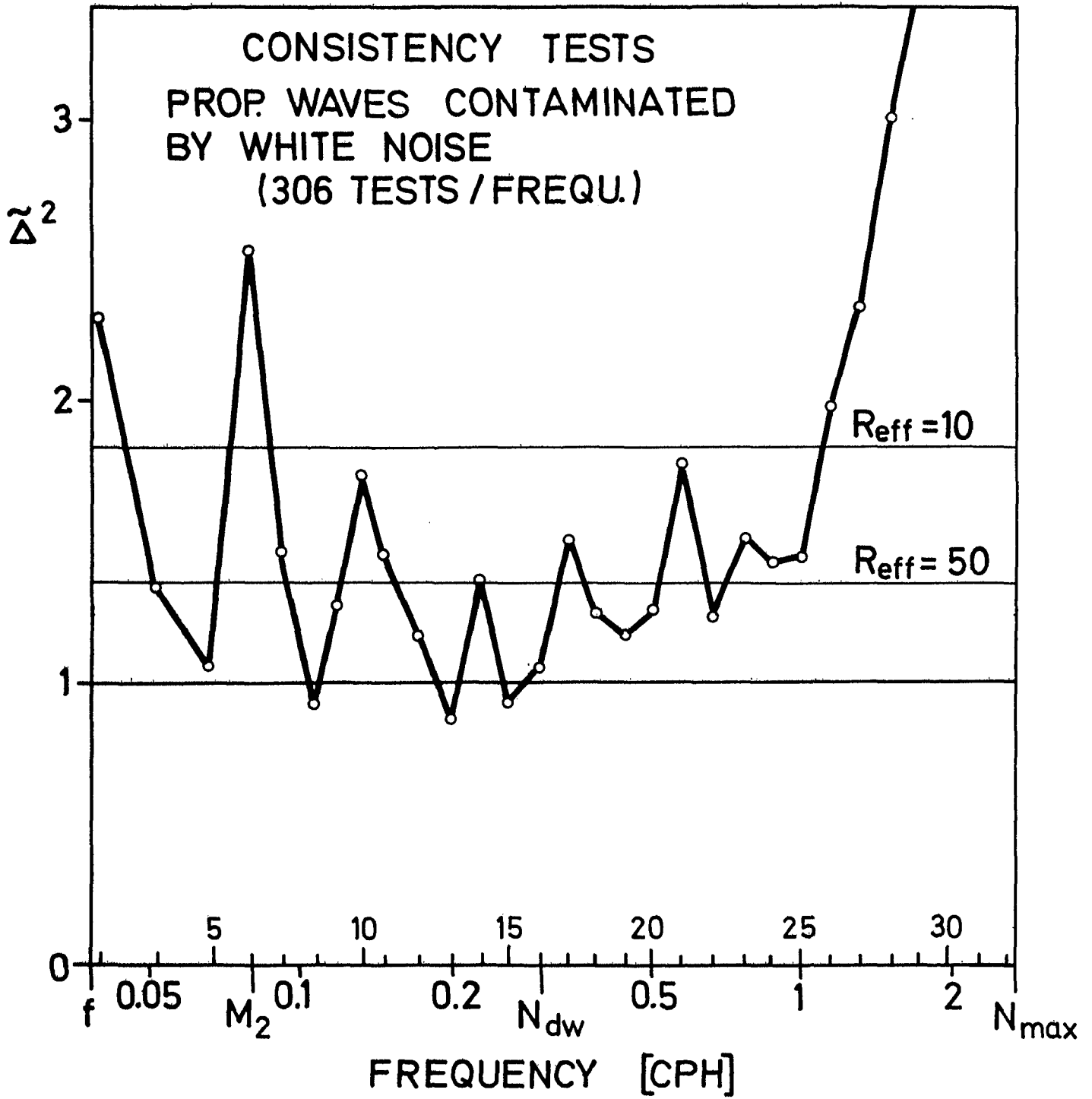


Fig. IV.20



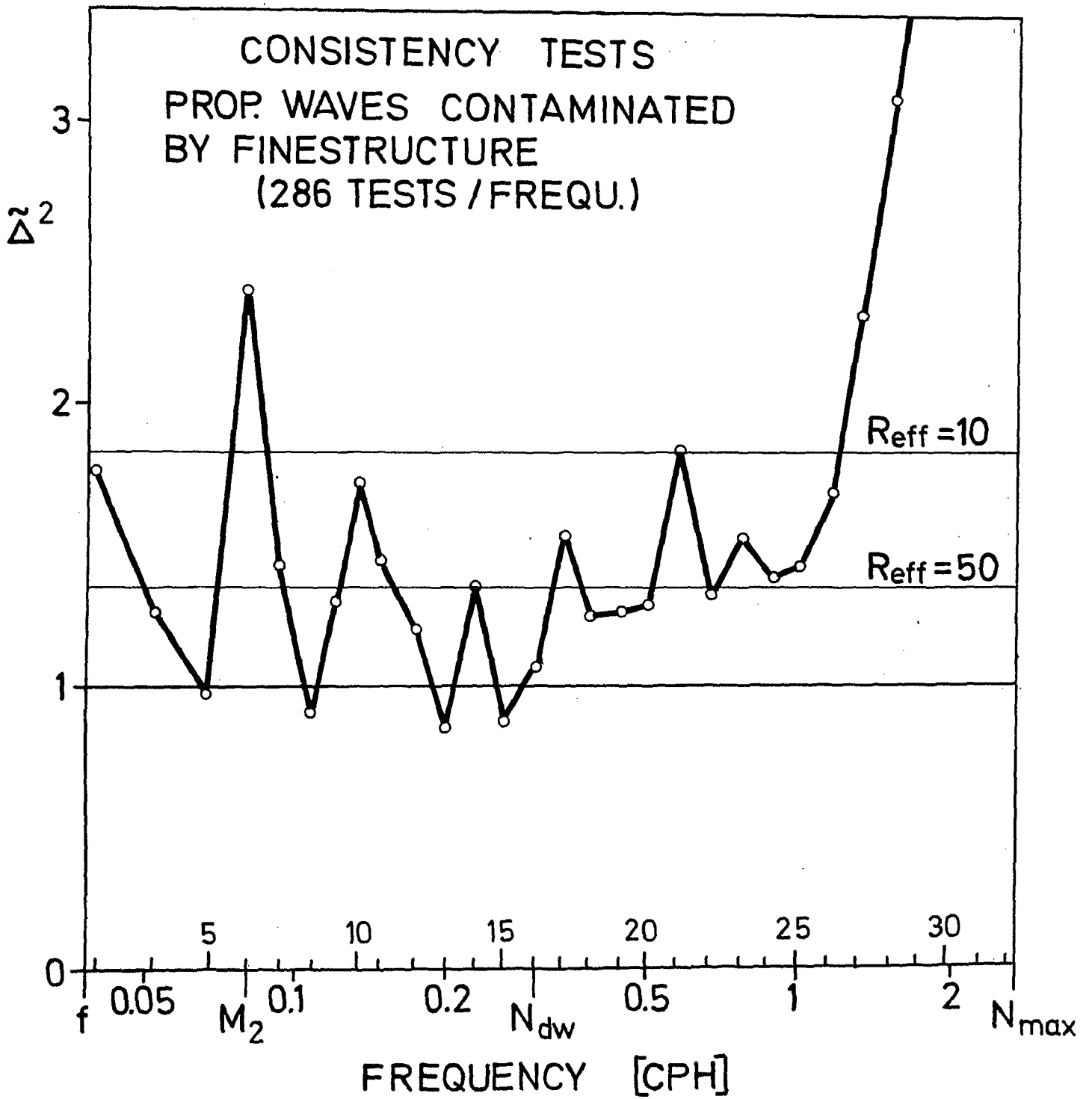


Fig. IV.21

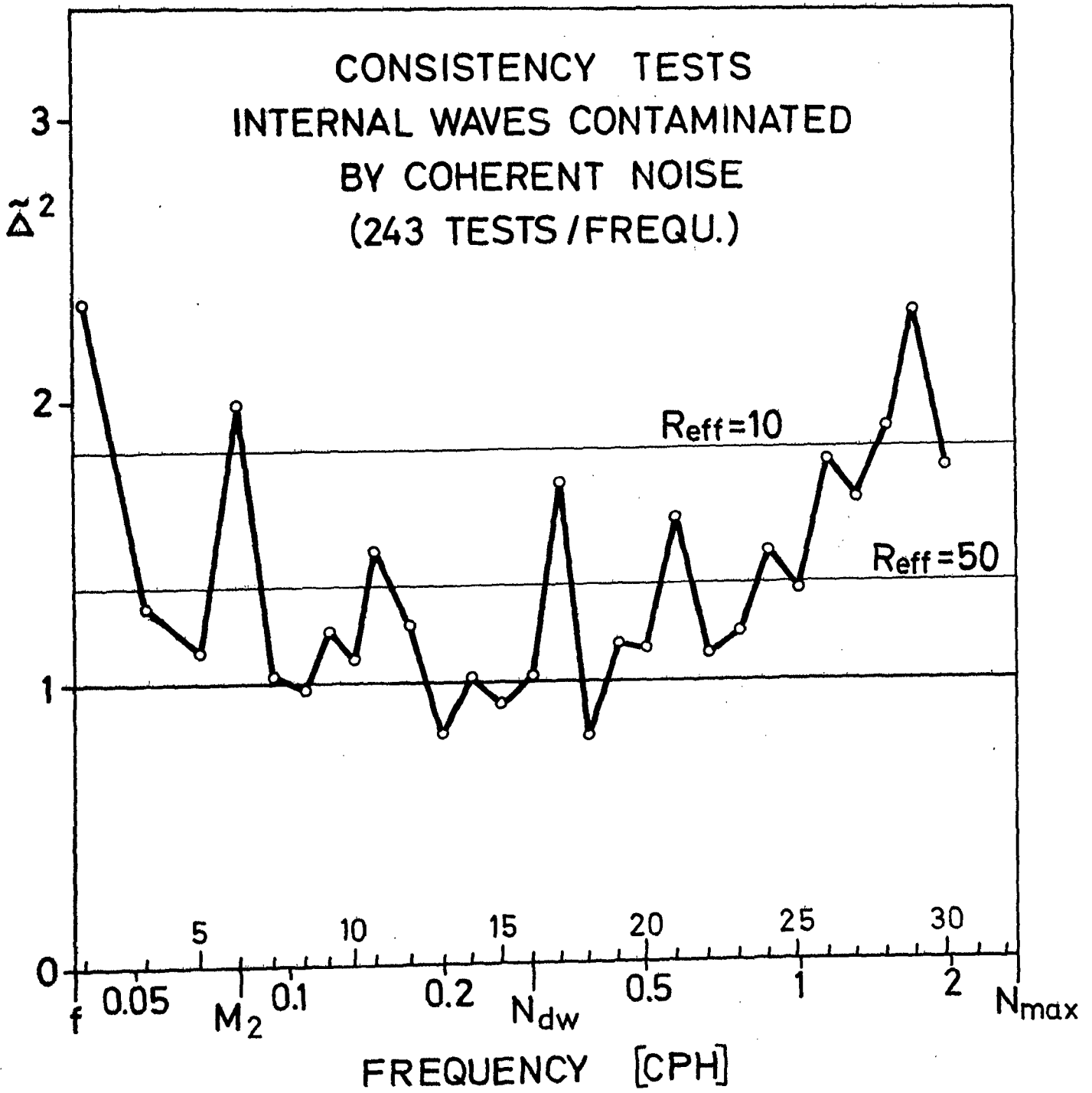


Fig. IV.22

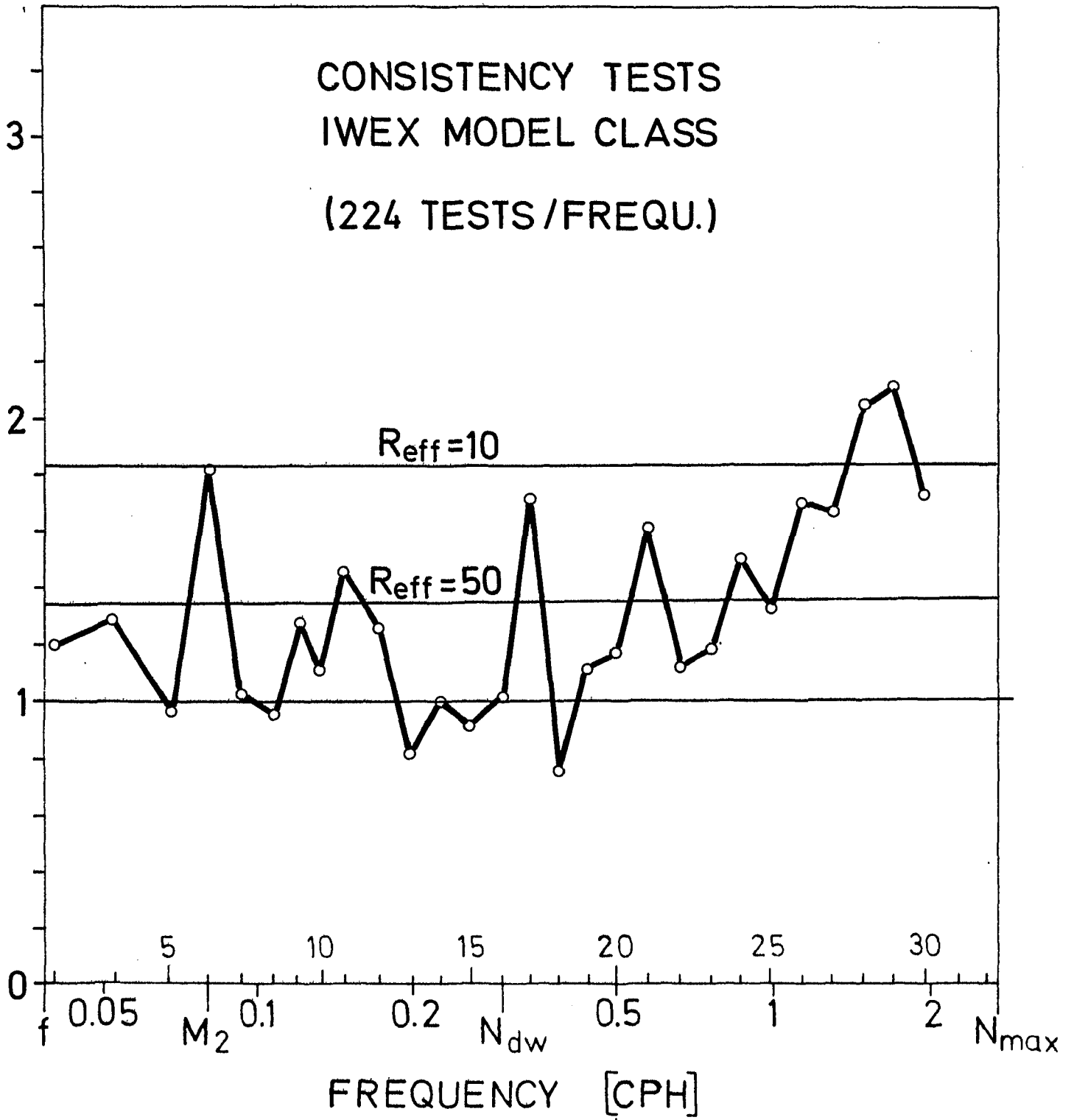


Fig. IV.23

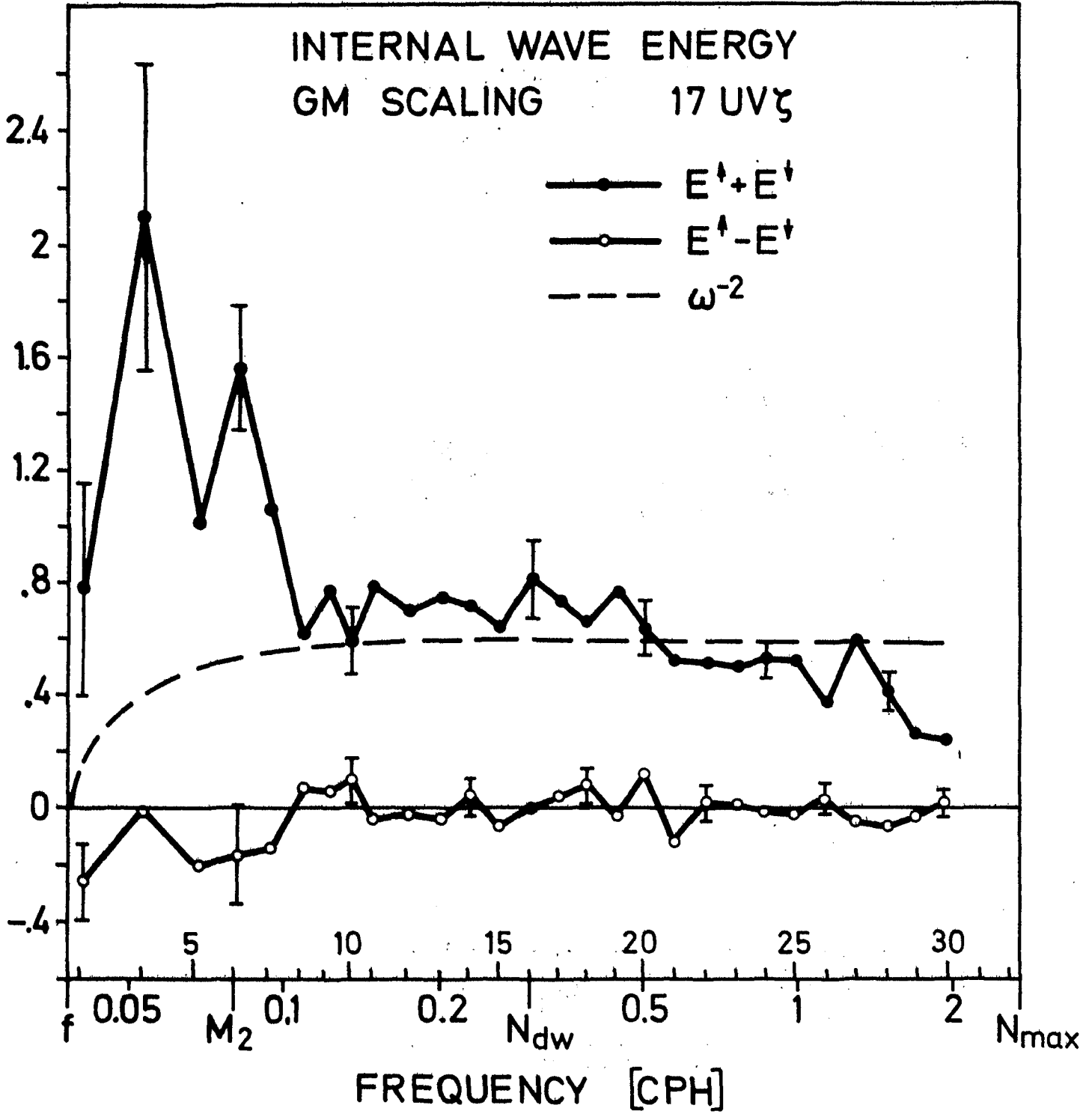


Fig. V.1

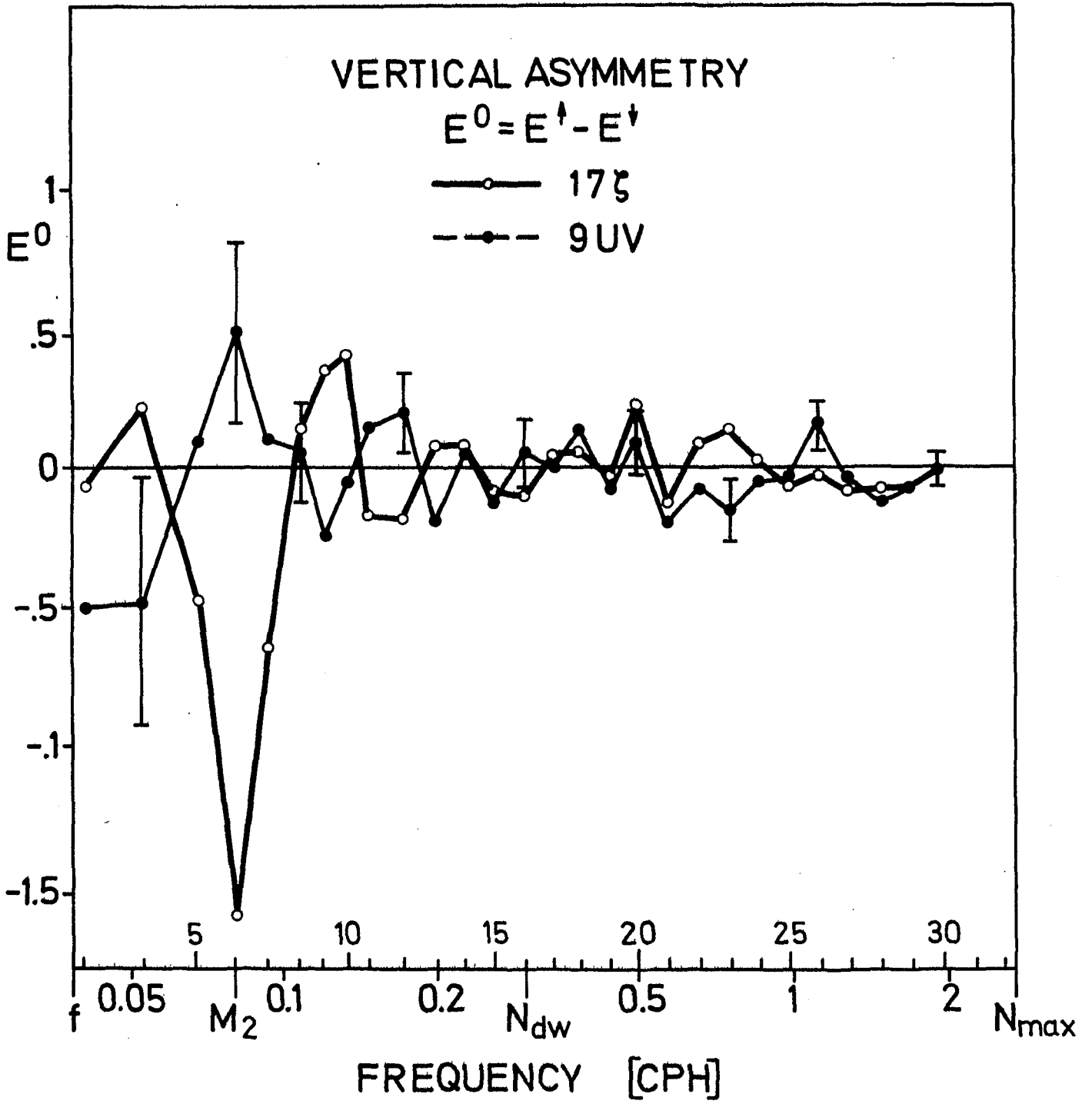


Fig. V.2

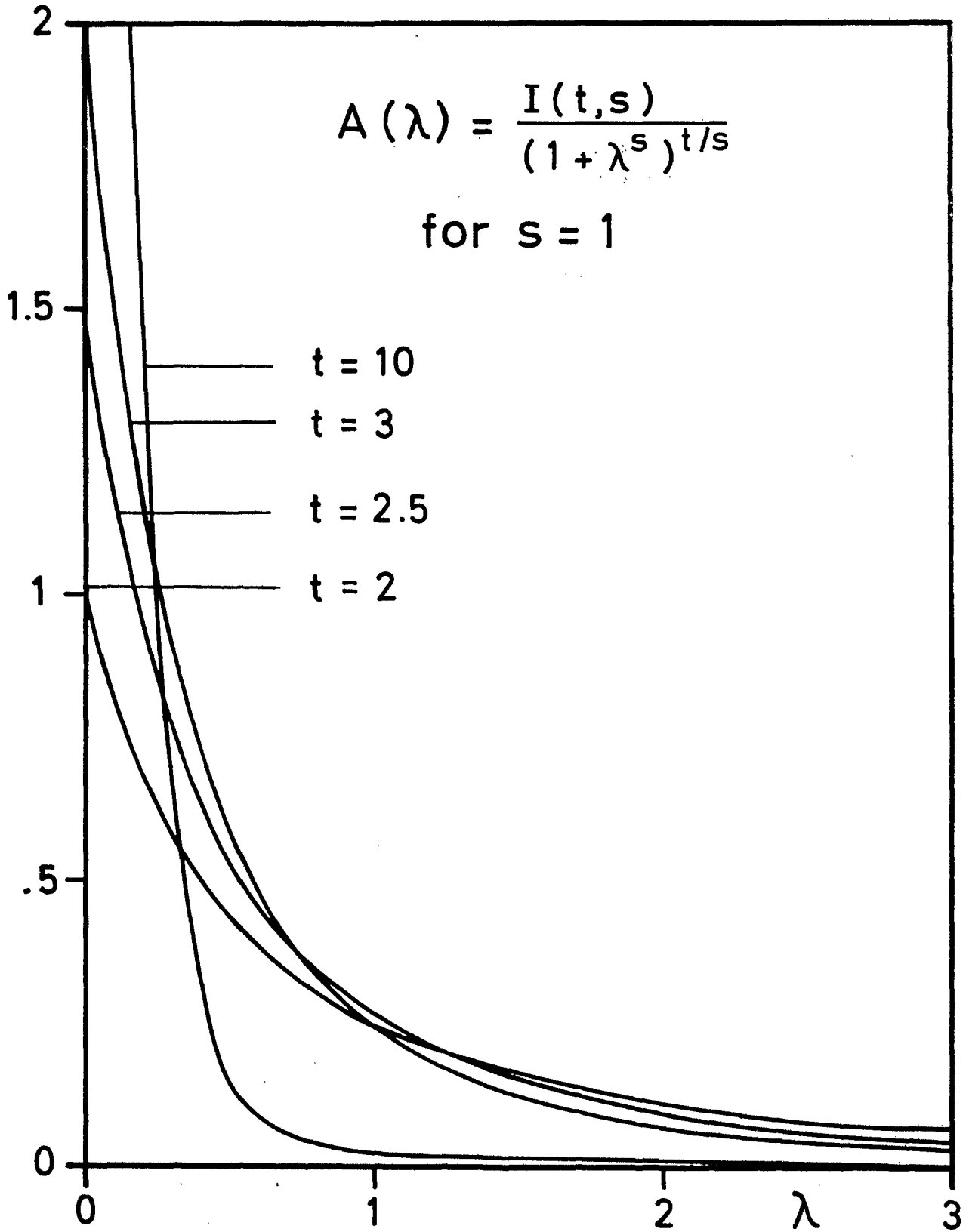


Fig. V.3a

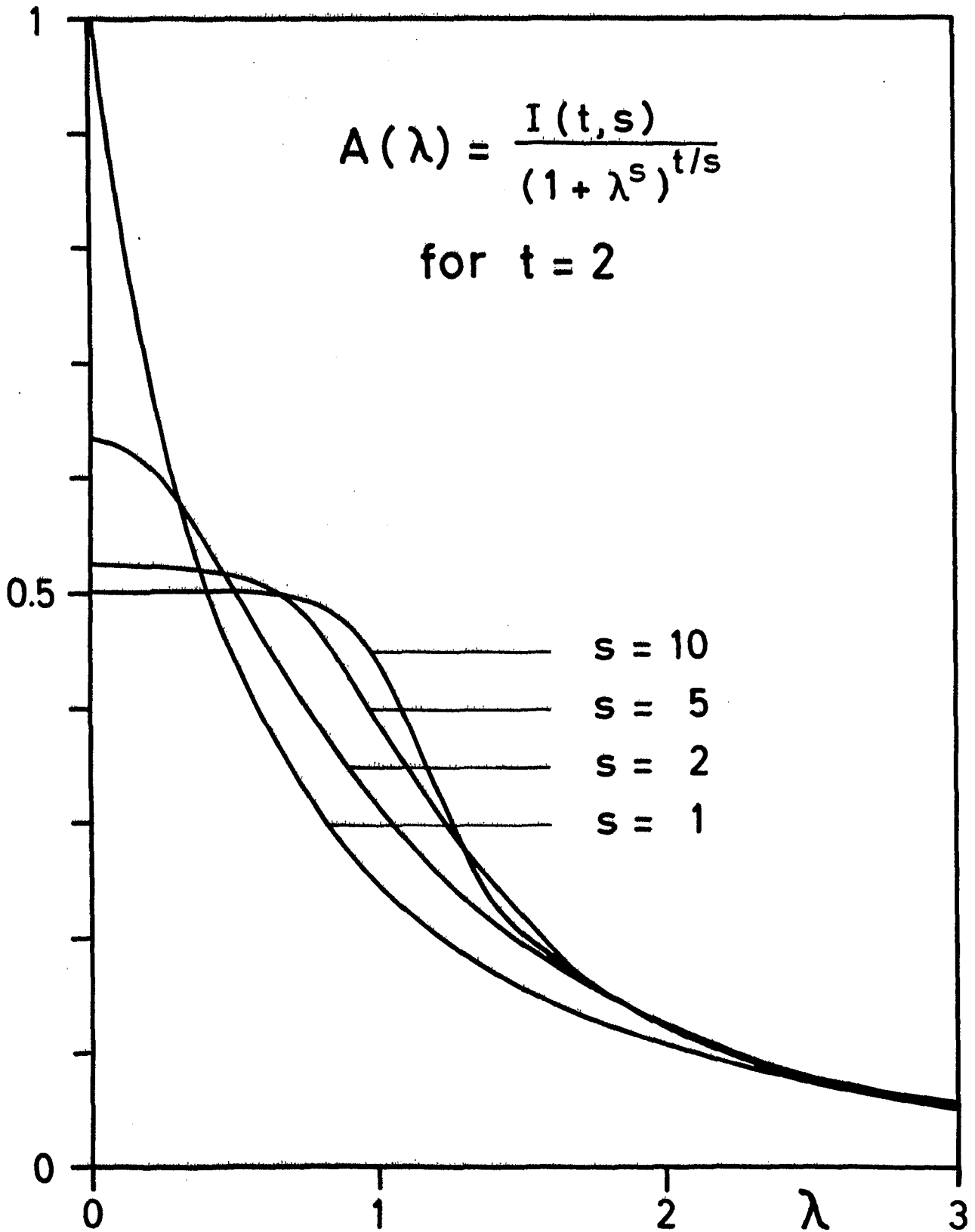


Fig. V.3b

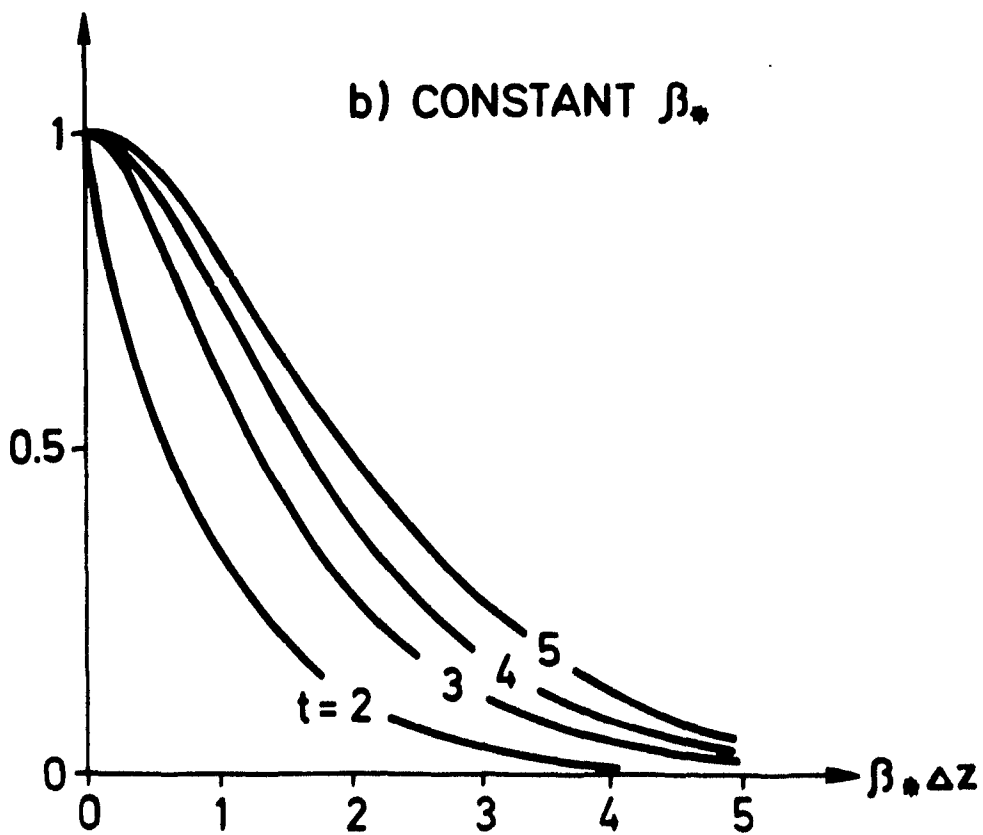
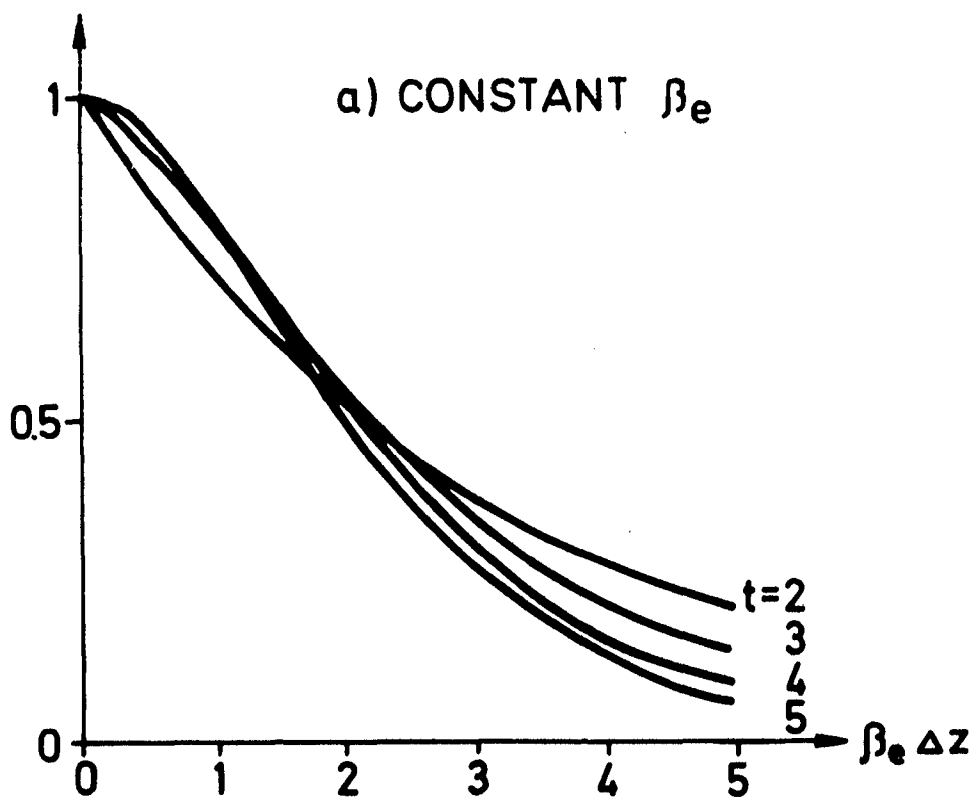


Fig. V.4



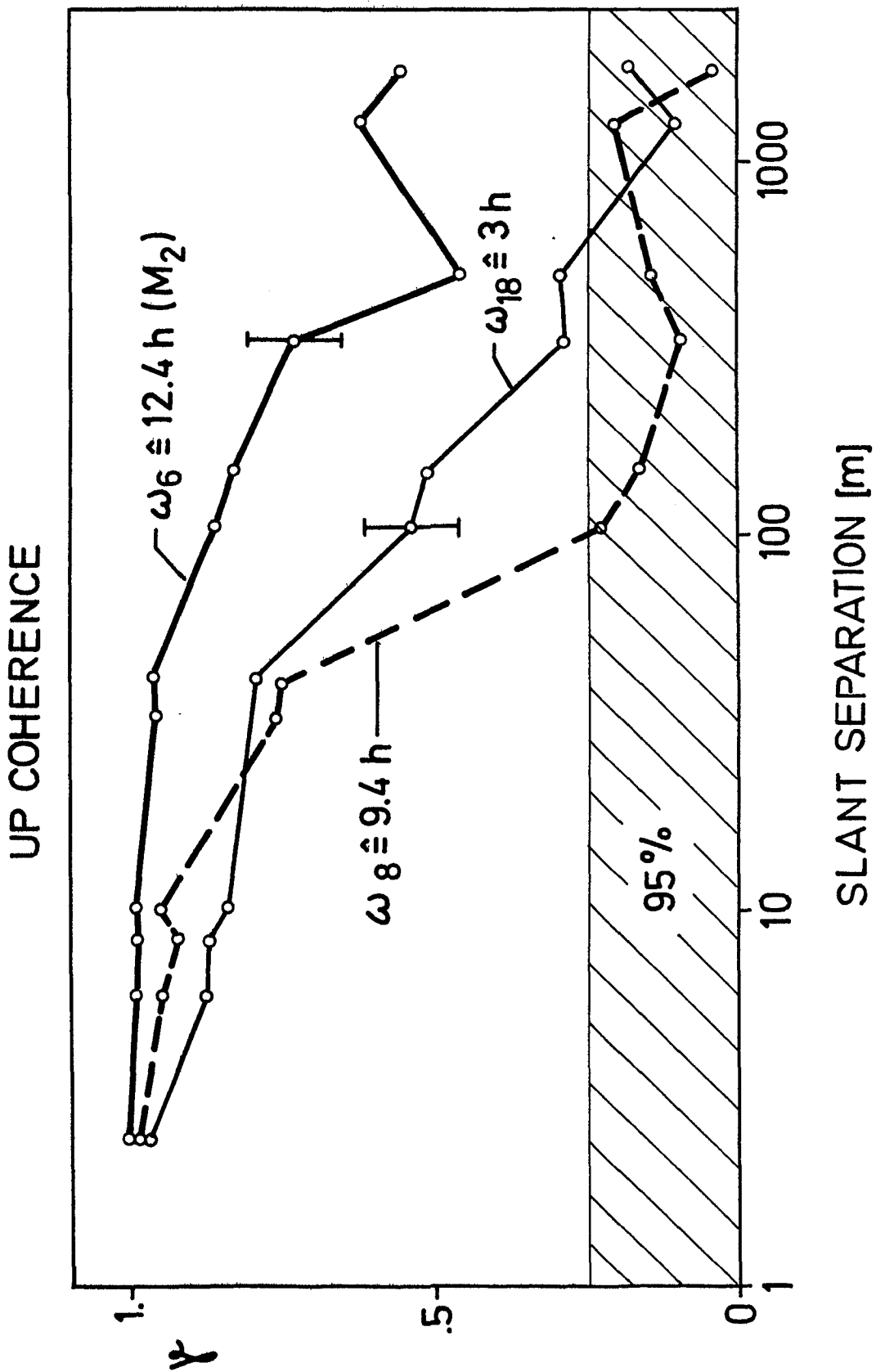


Fig. V.5

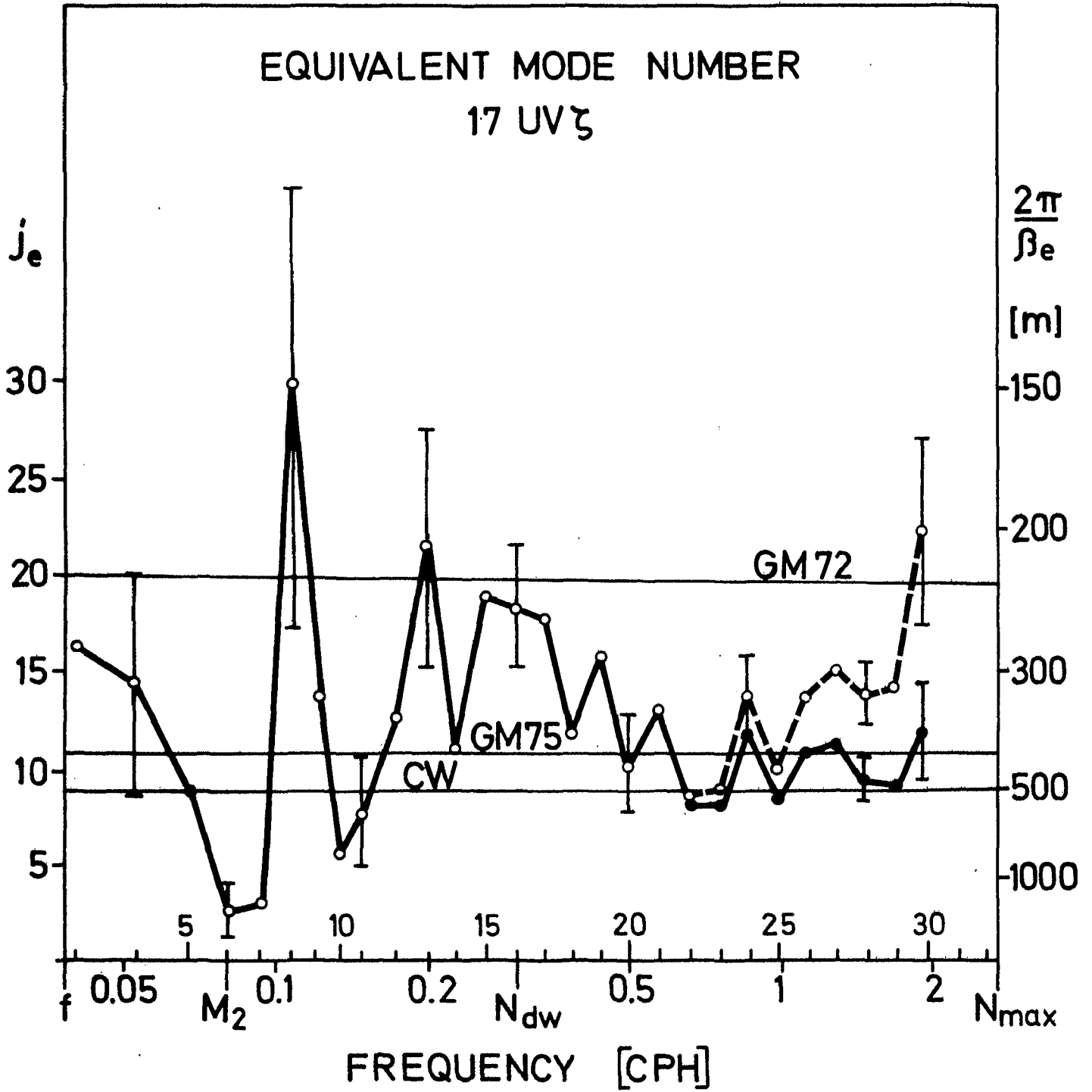


Fig. V.6

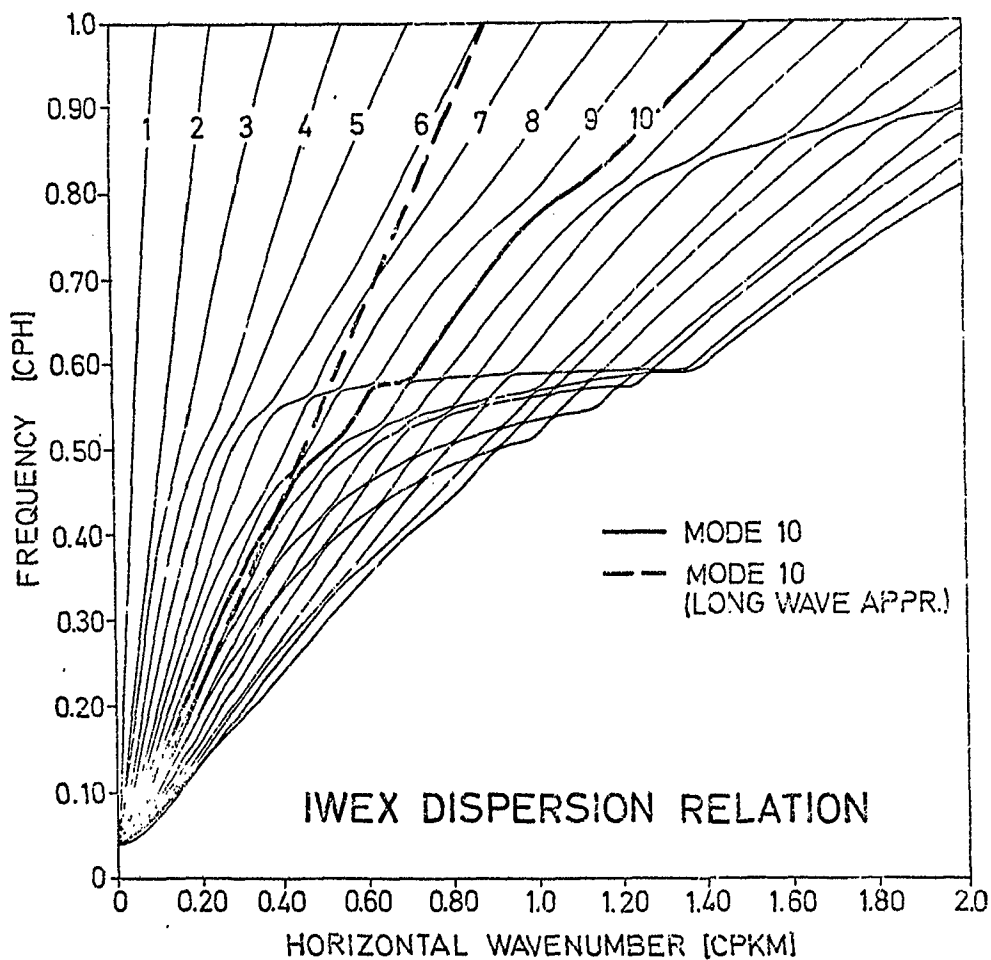
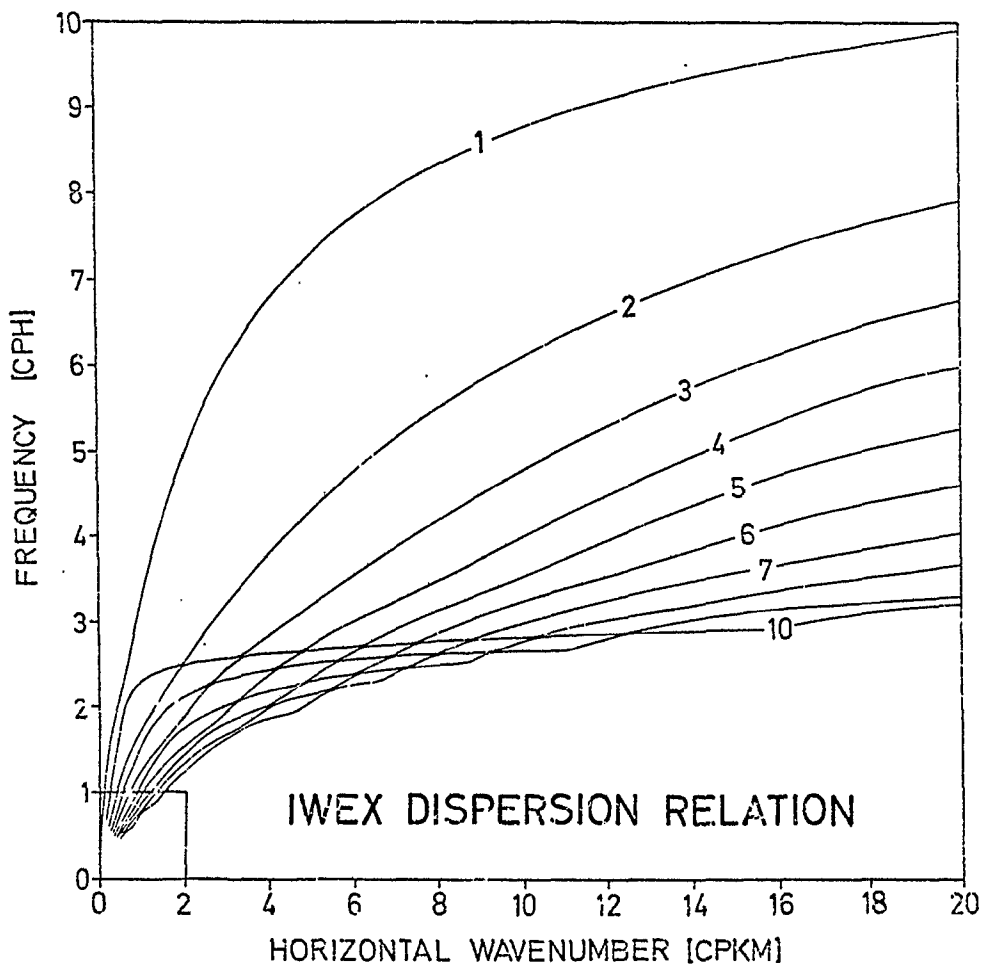


Fig. V.7

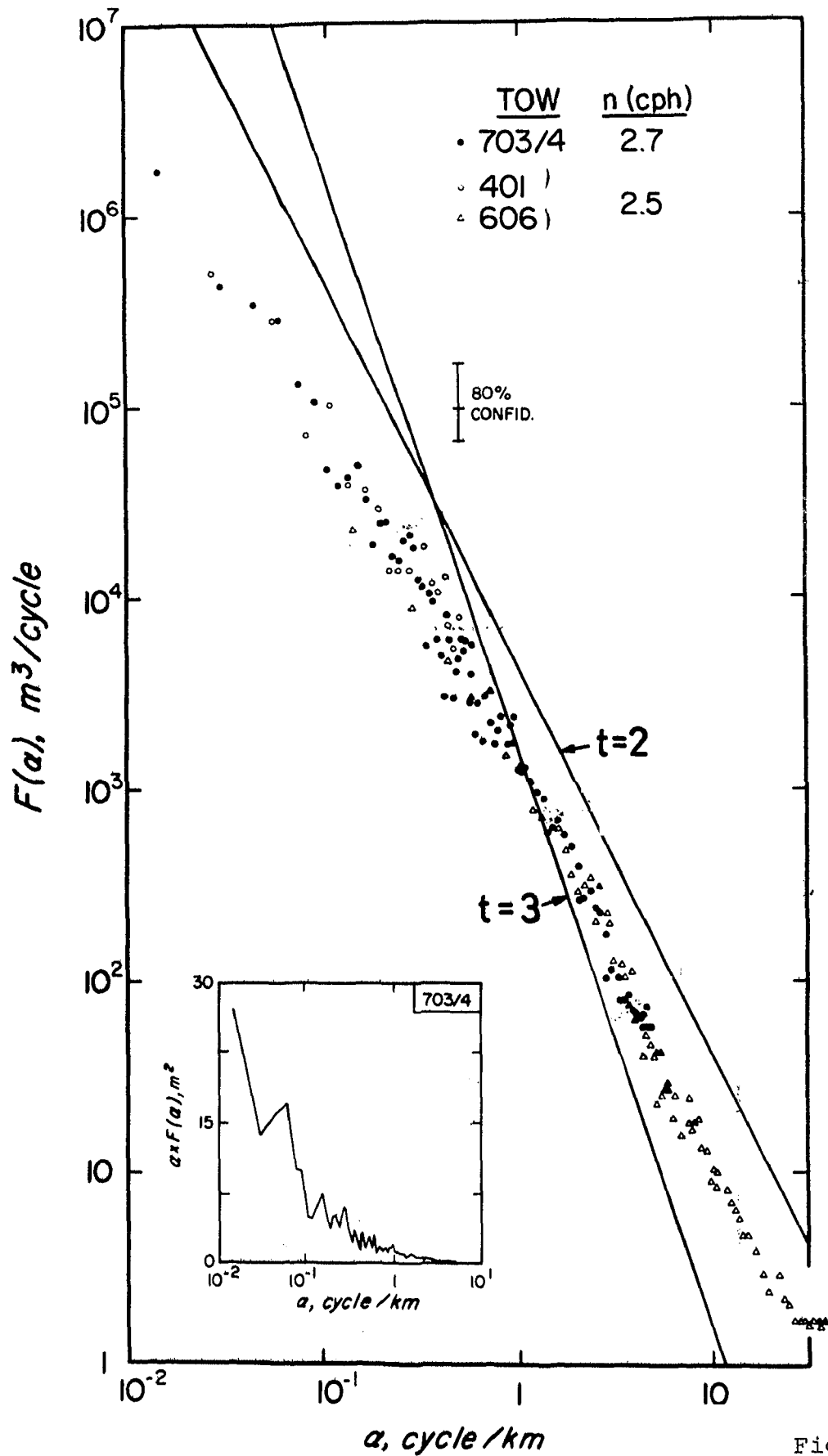


Fig. V.8

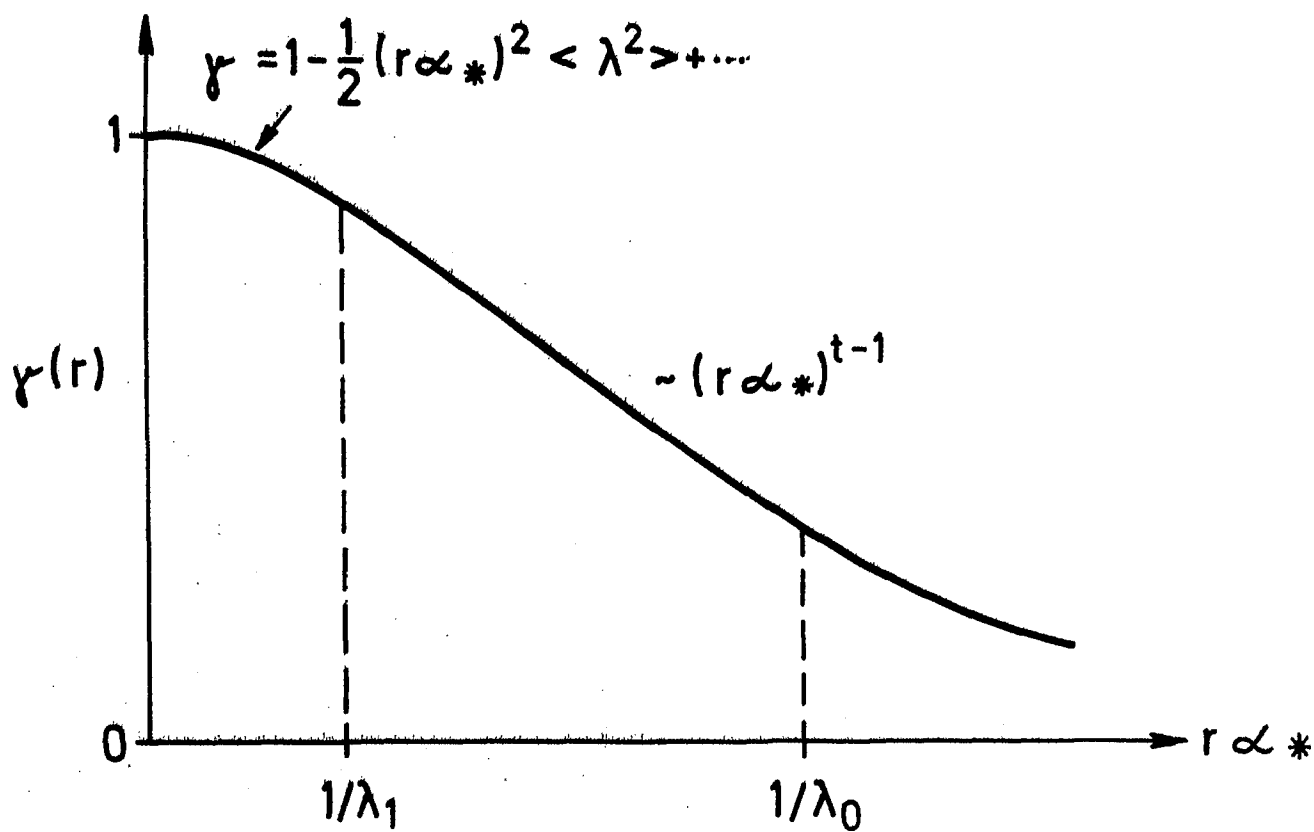
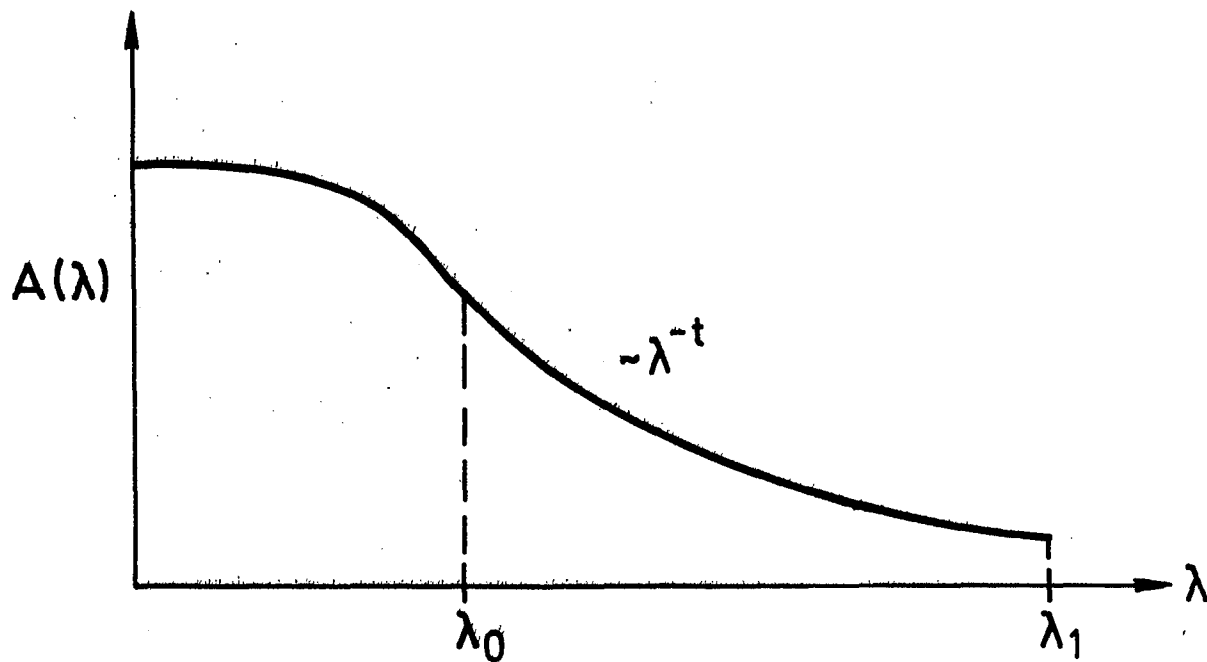


Fig. V.9

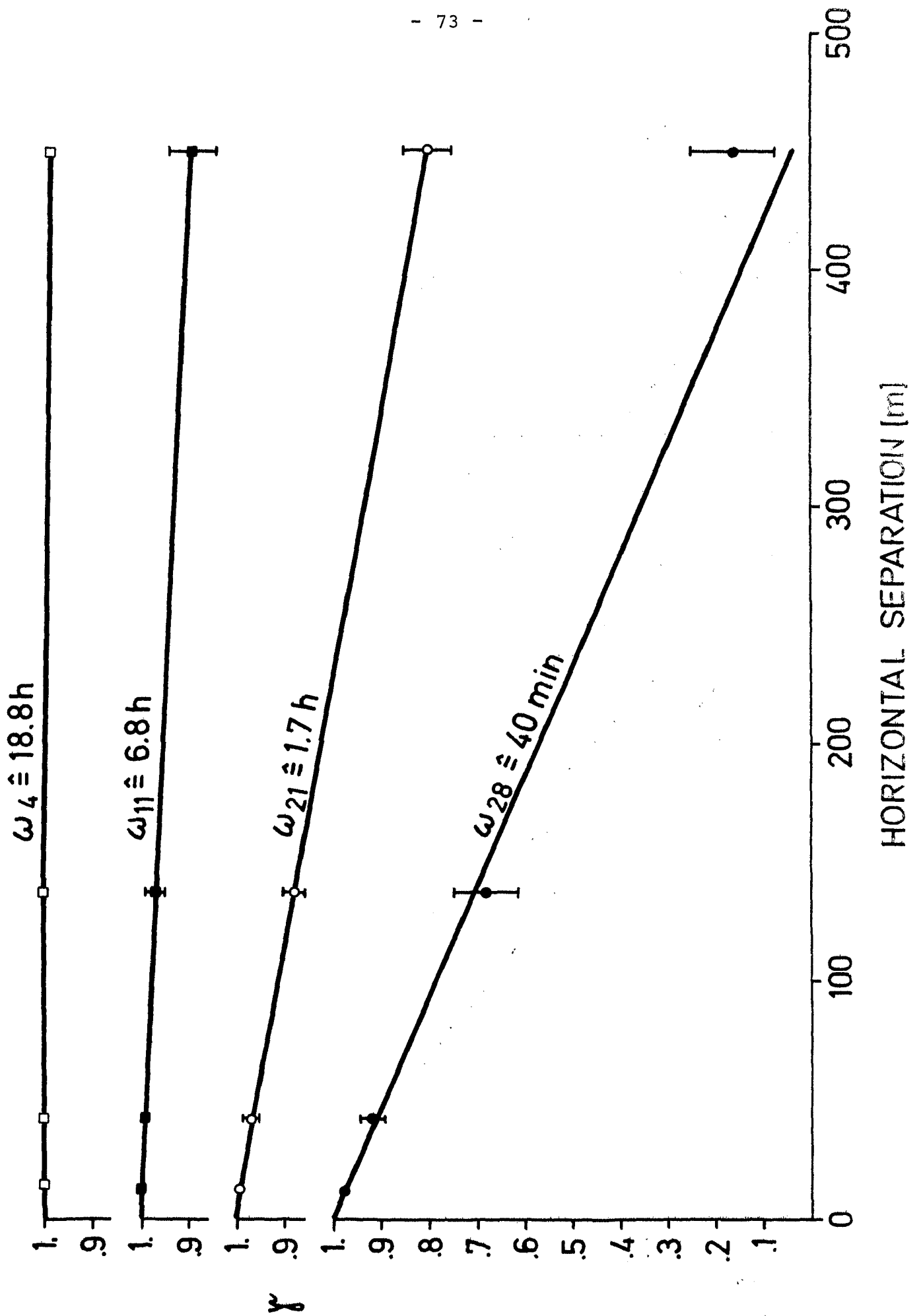


Fig. V.10

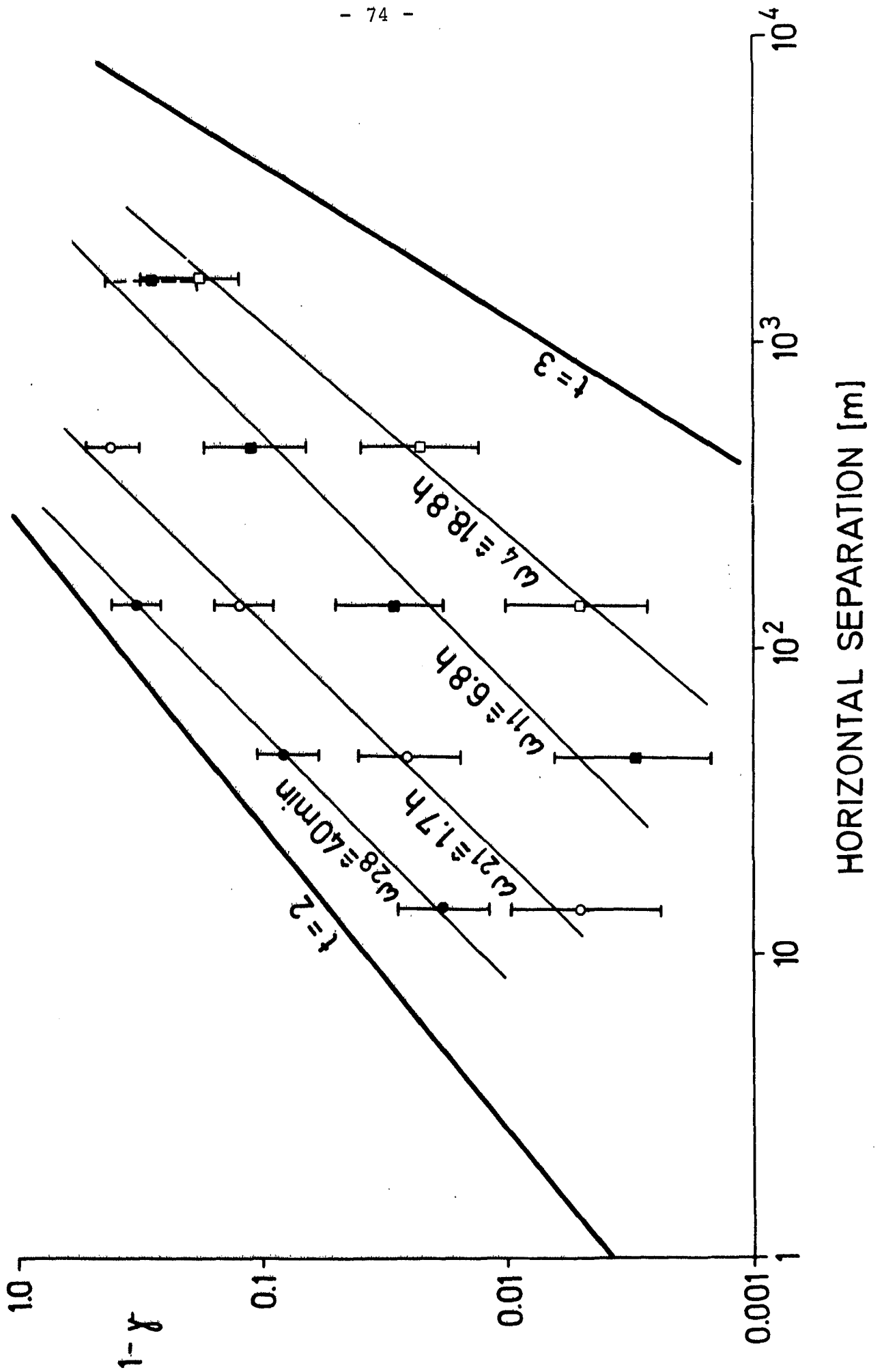


Fig. V.11

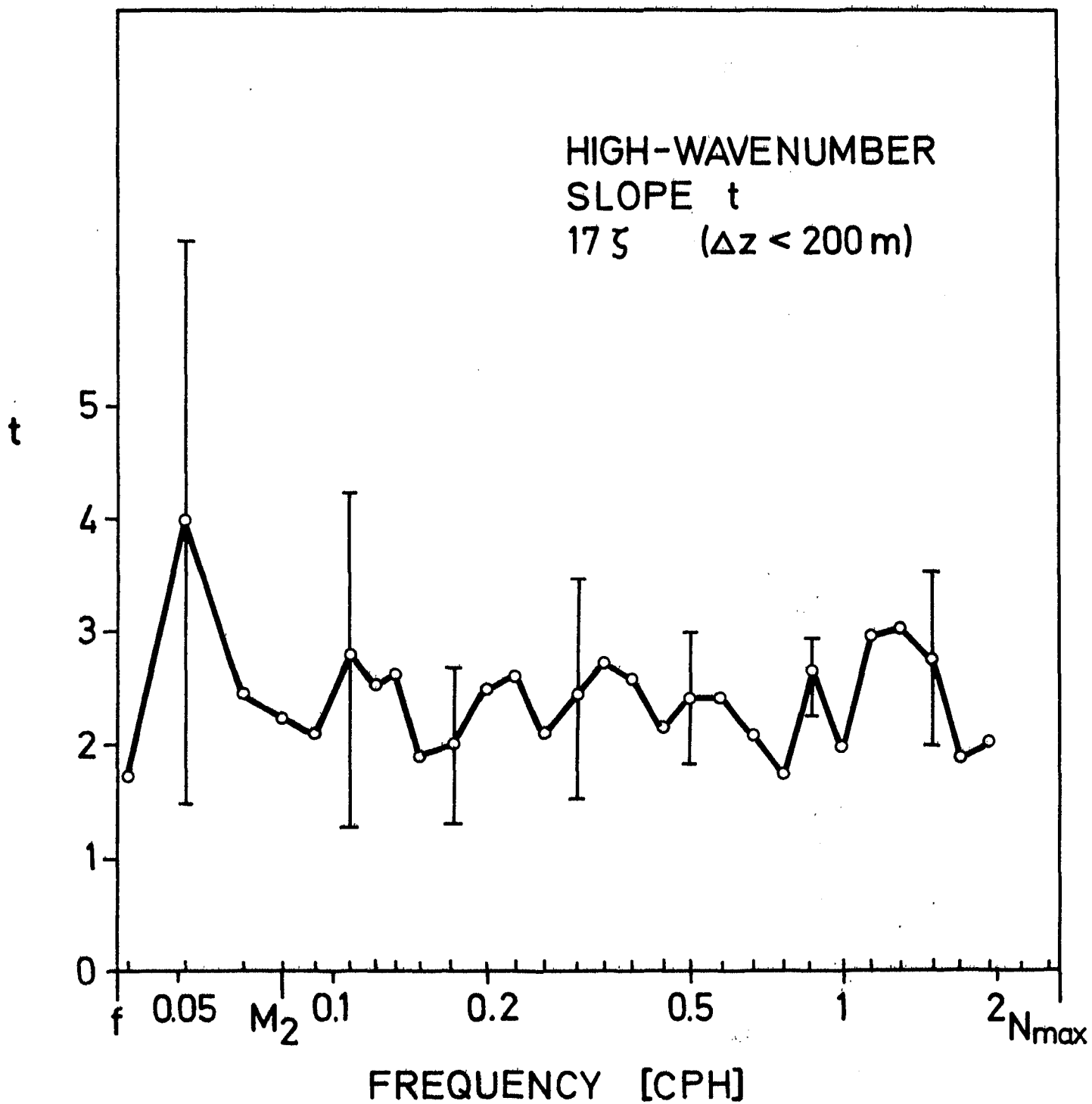


Fig. V.12



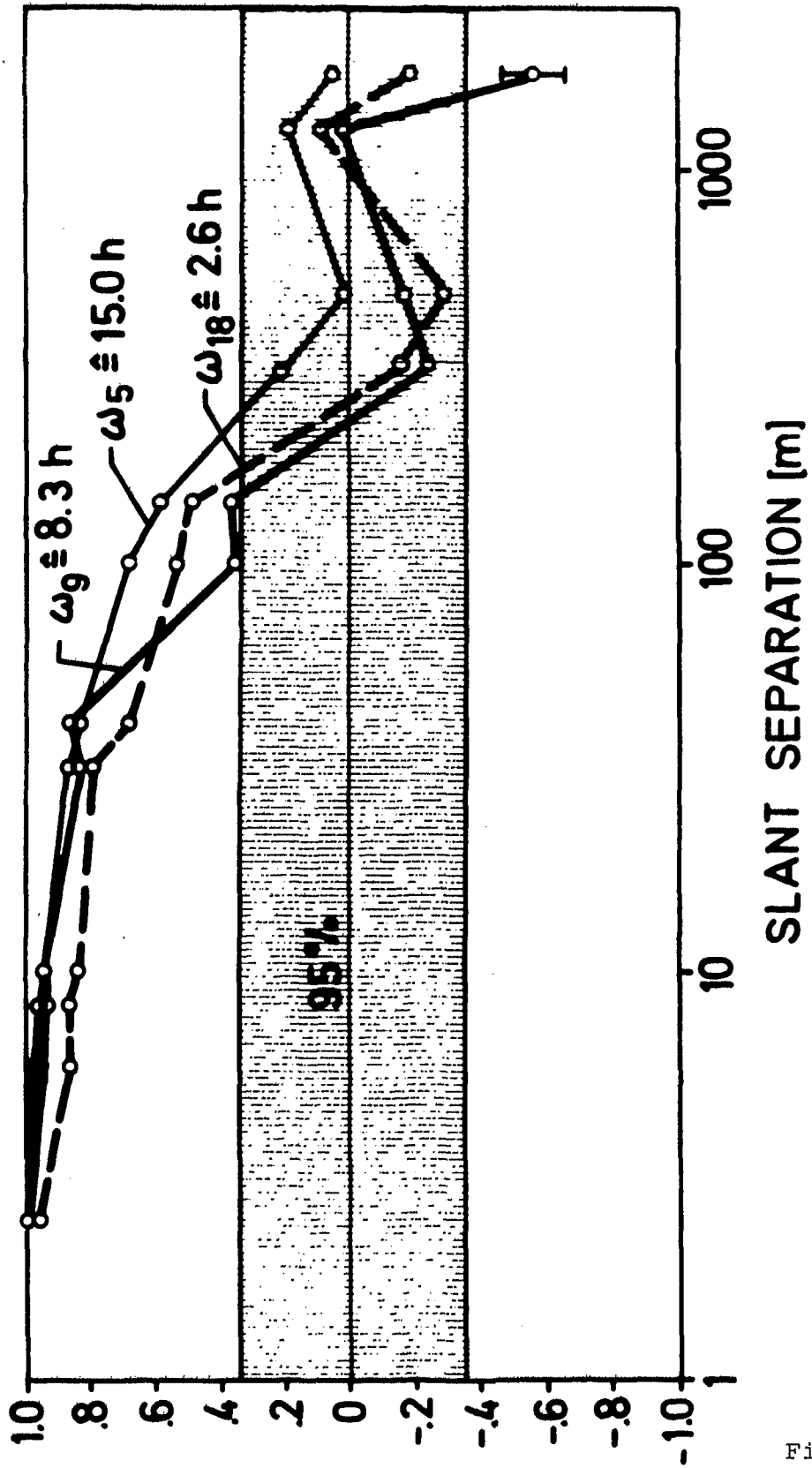


Fig. V.13

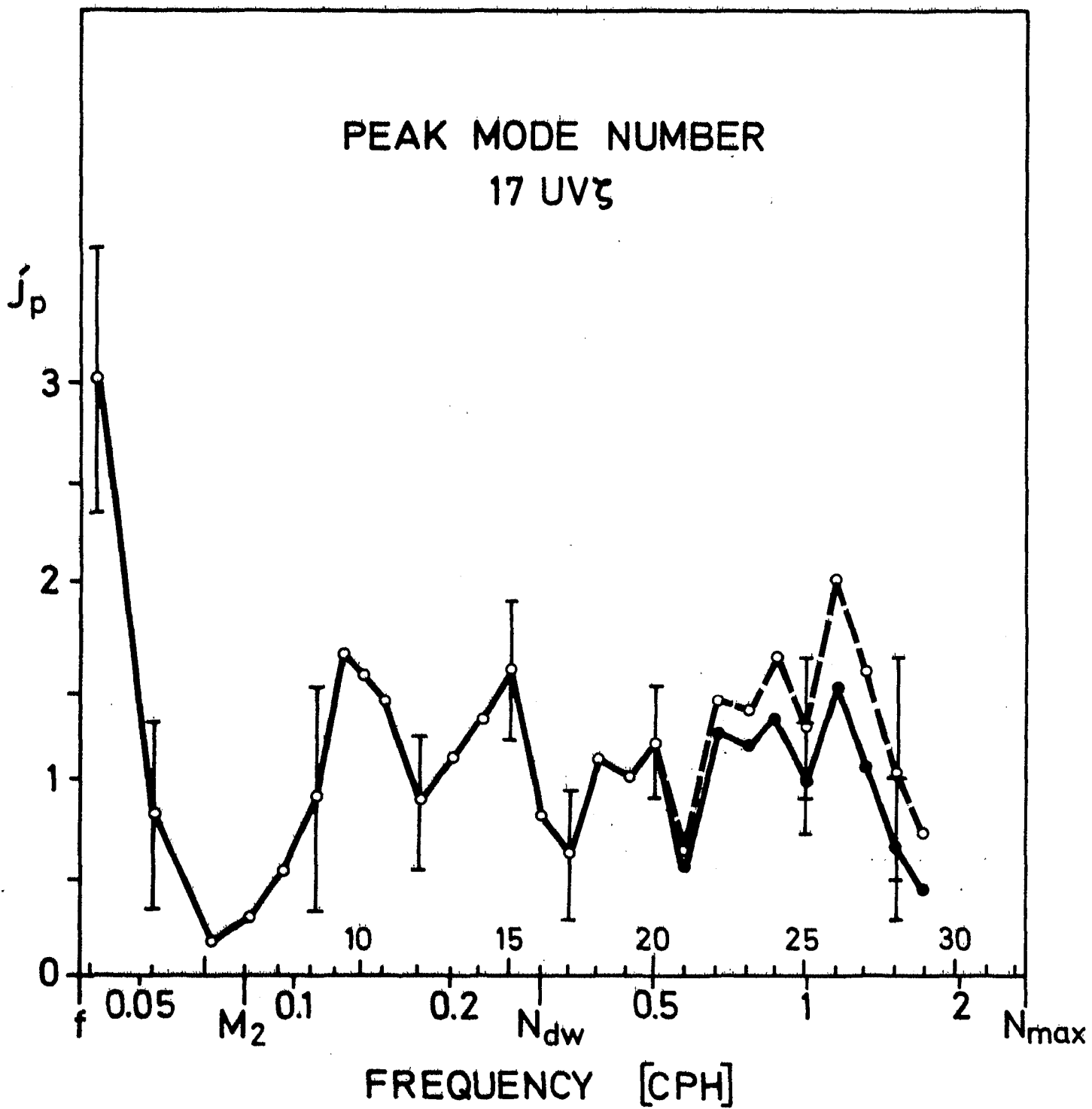


Fig. V.14

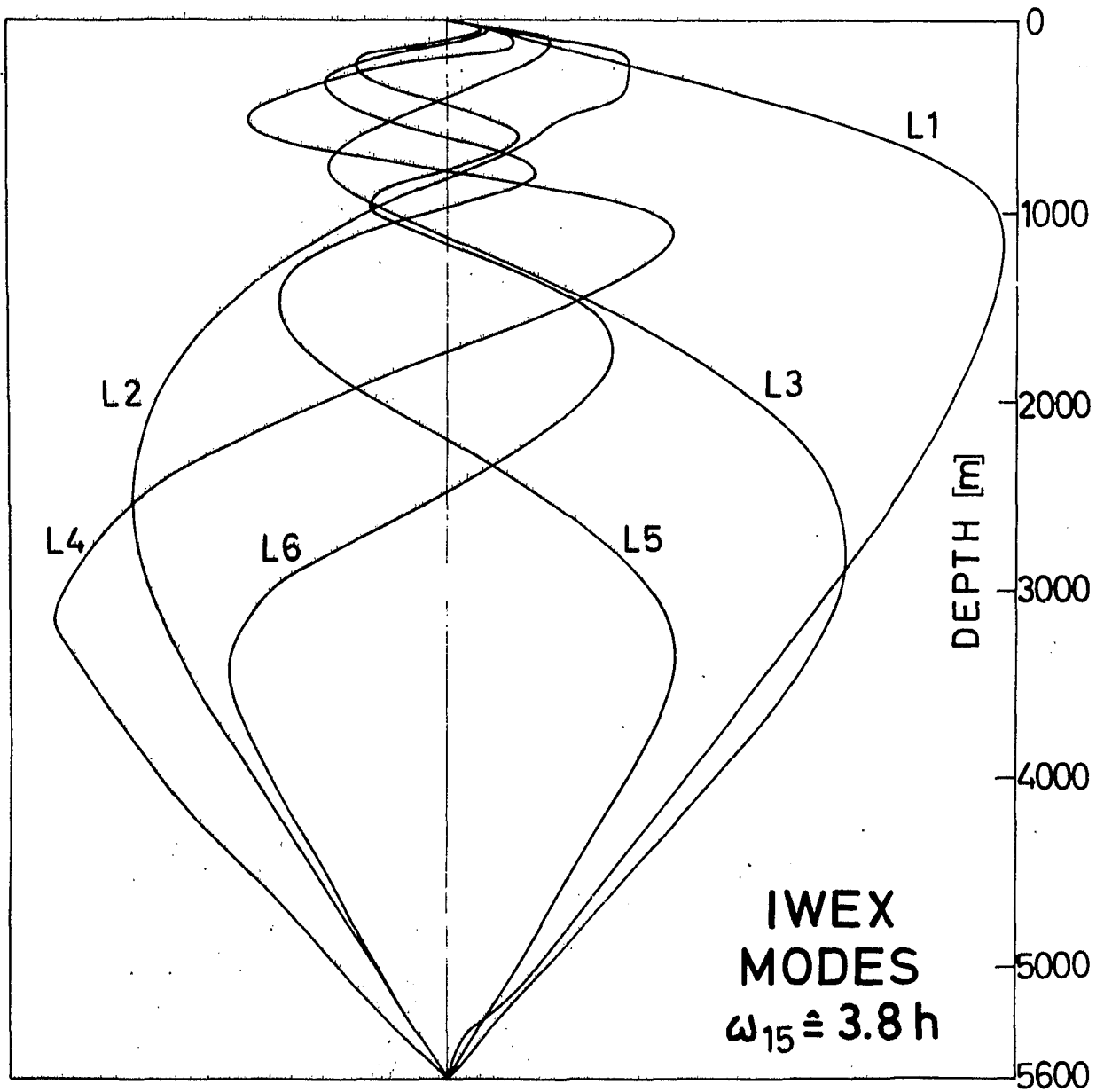


Fig. V.15

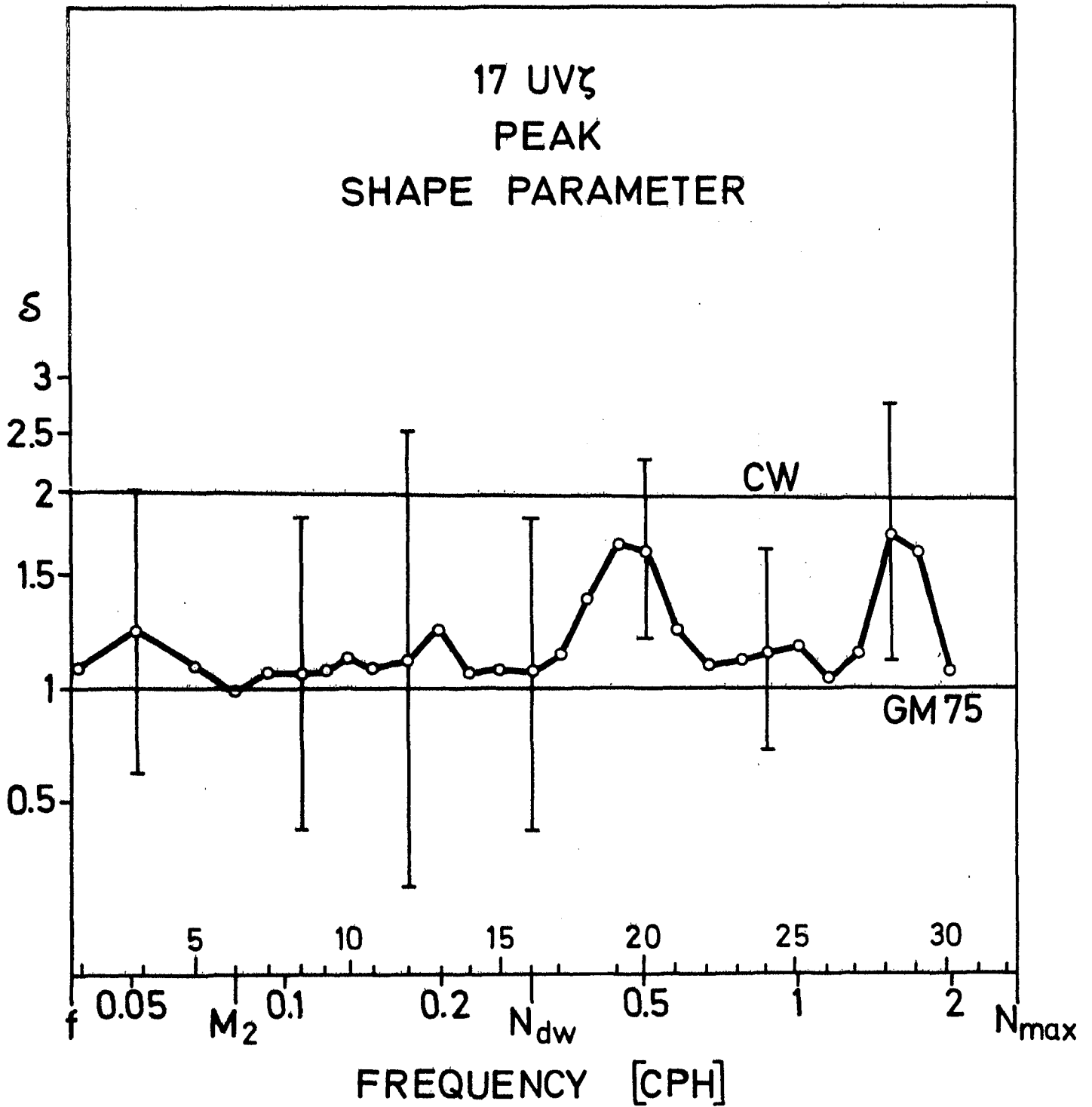


Fig. V.16

COS\*\*2P-LAW

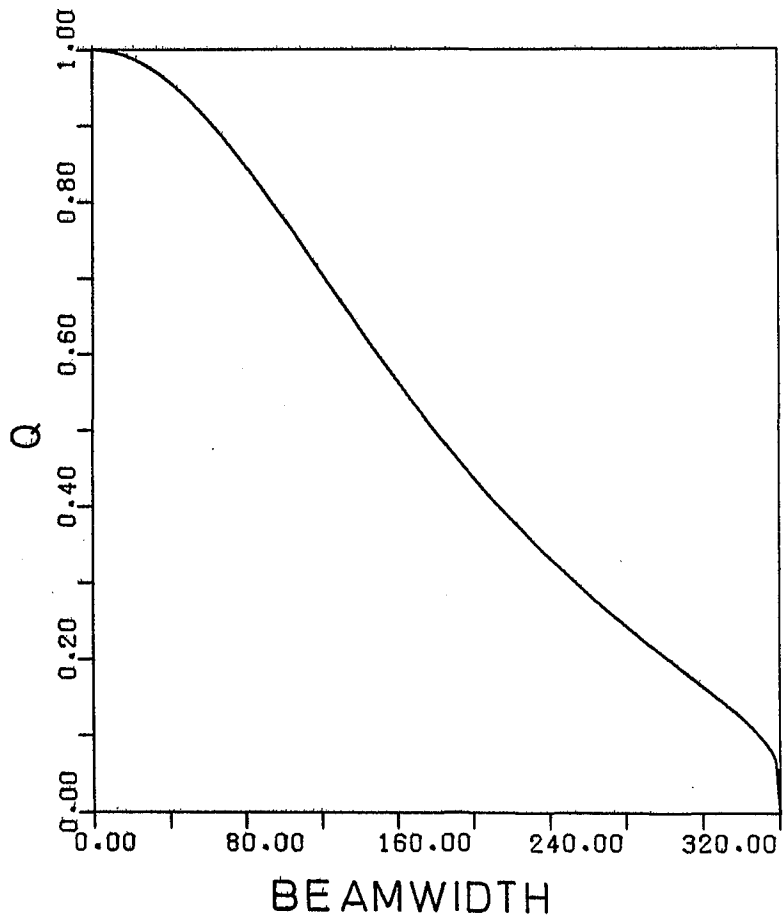


Fig. V.17

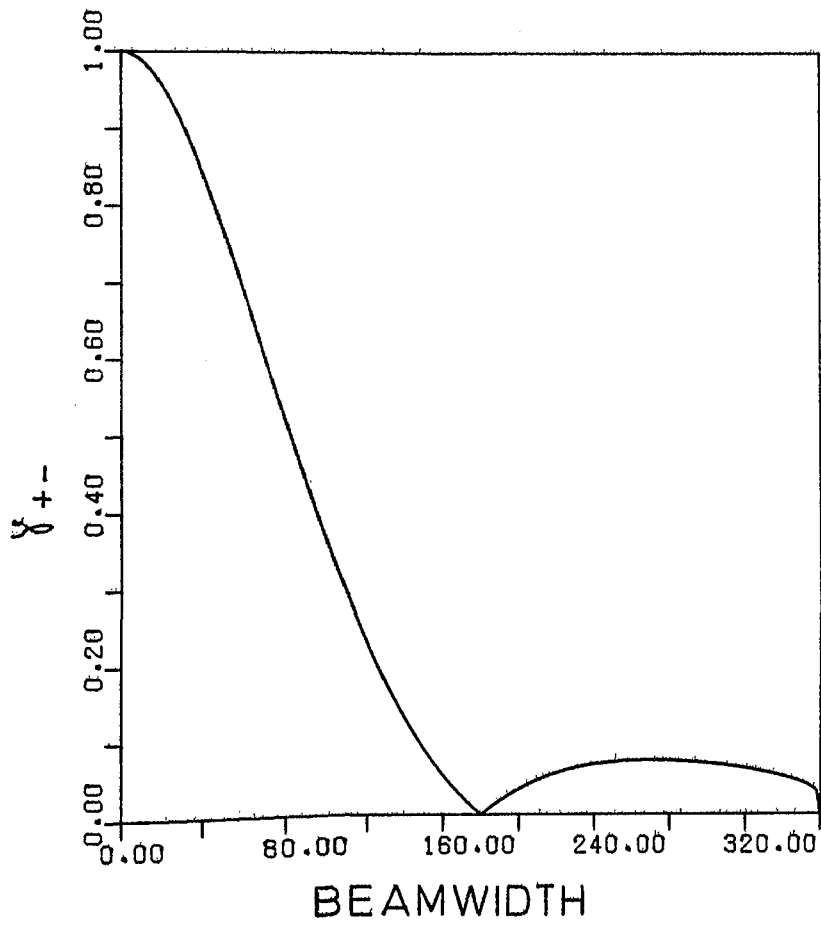


Fig. V.18

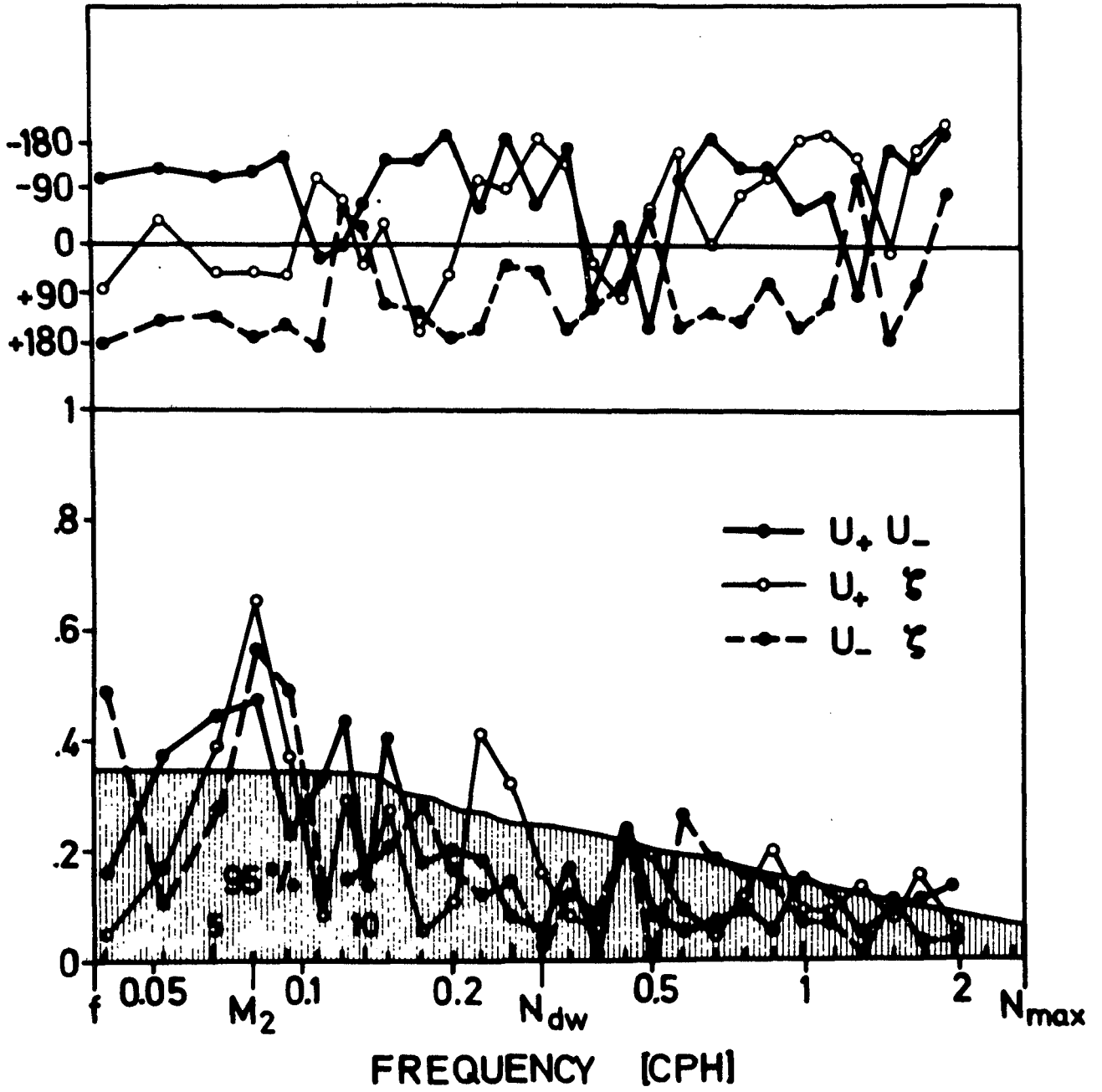


Fig. V.19

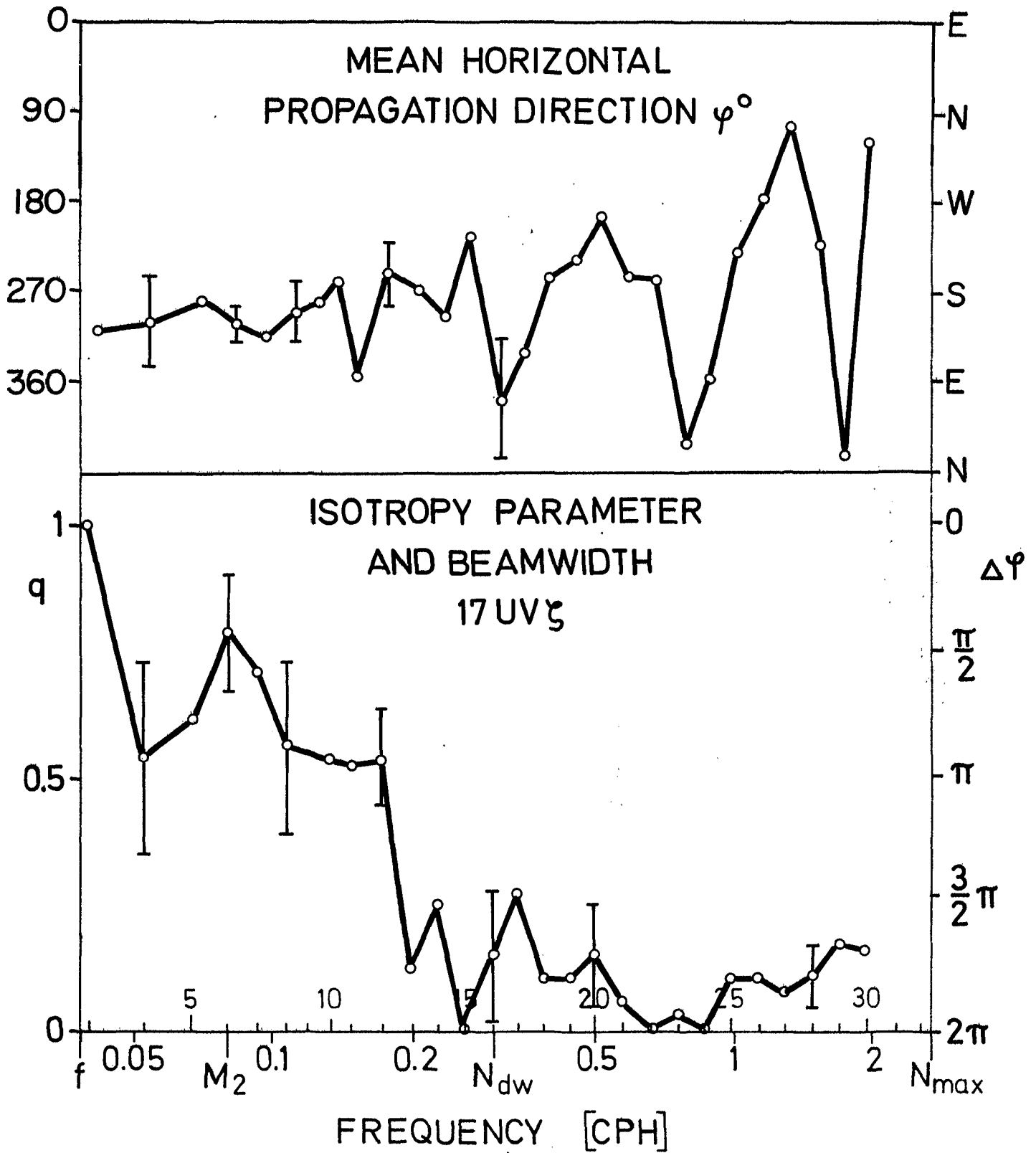


Fig. V.20



COHERENCE FREQ. 26  
1.133 CPH

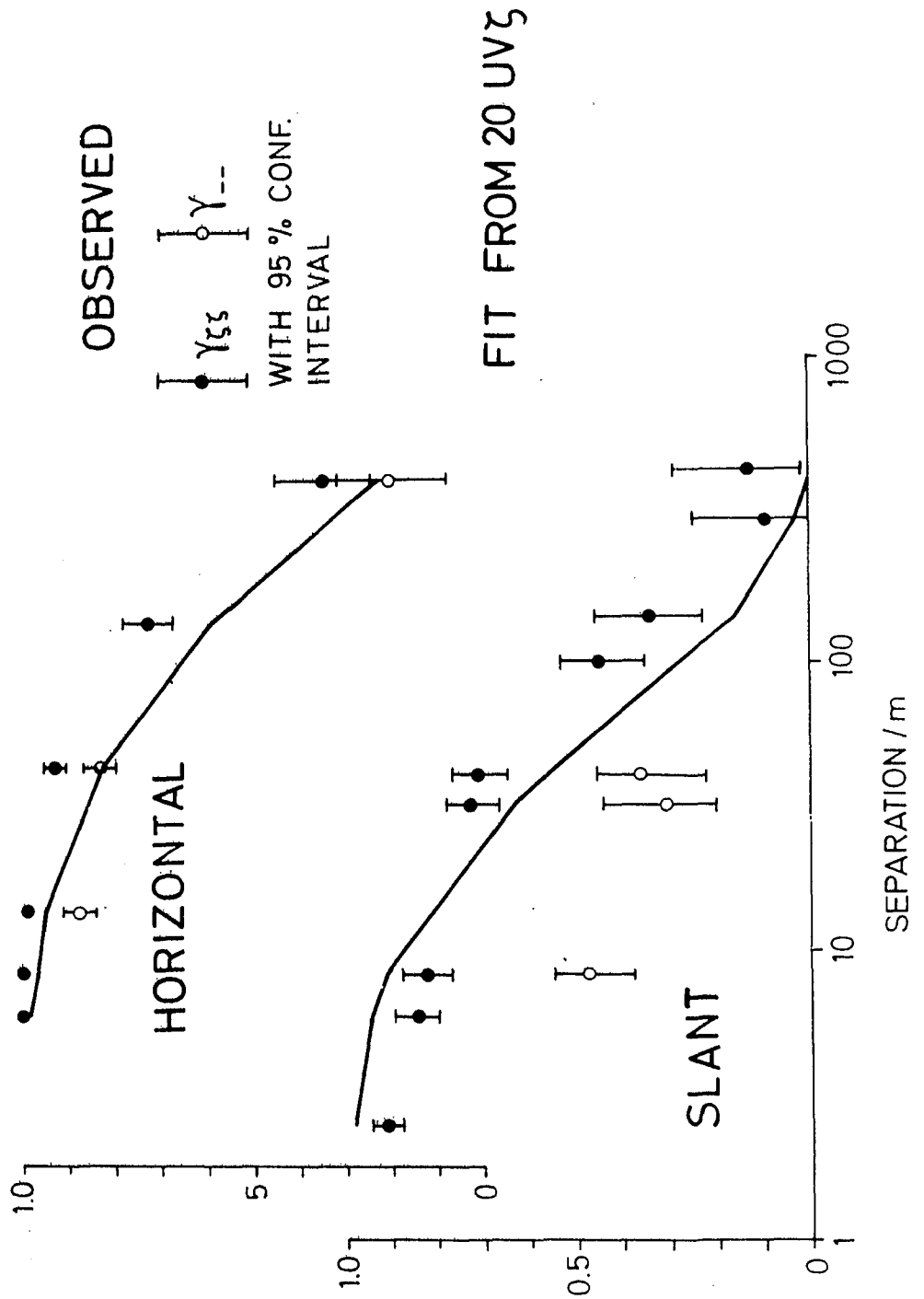


Fig. V.21

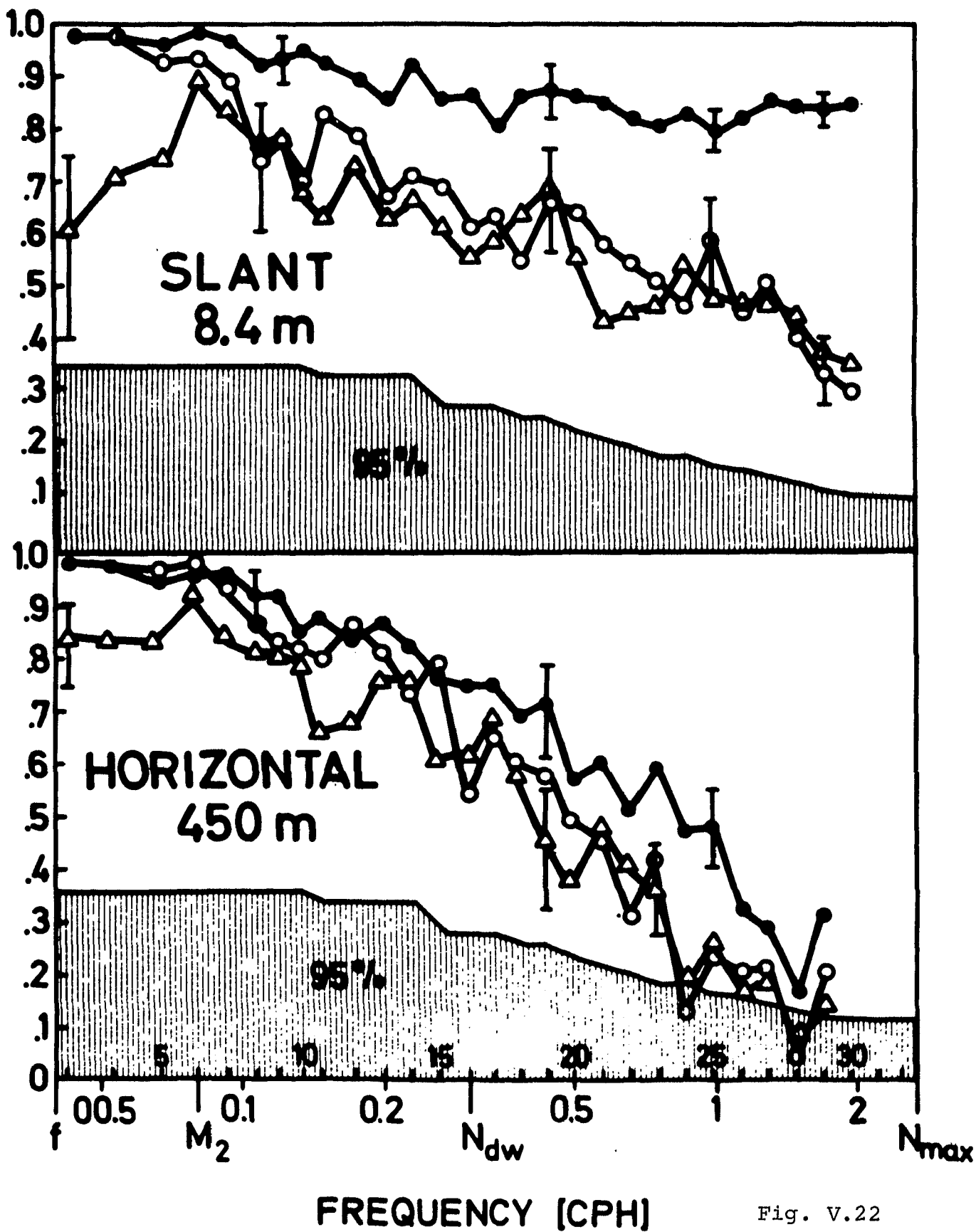


Fig. V.22

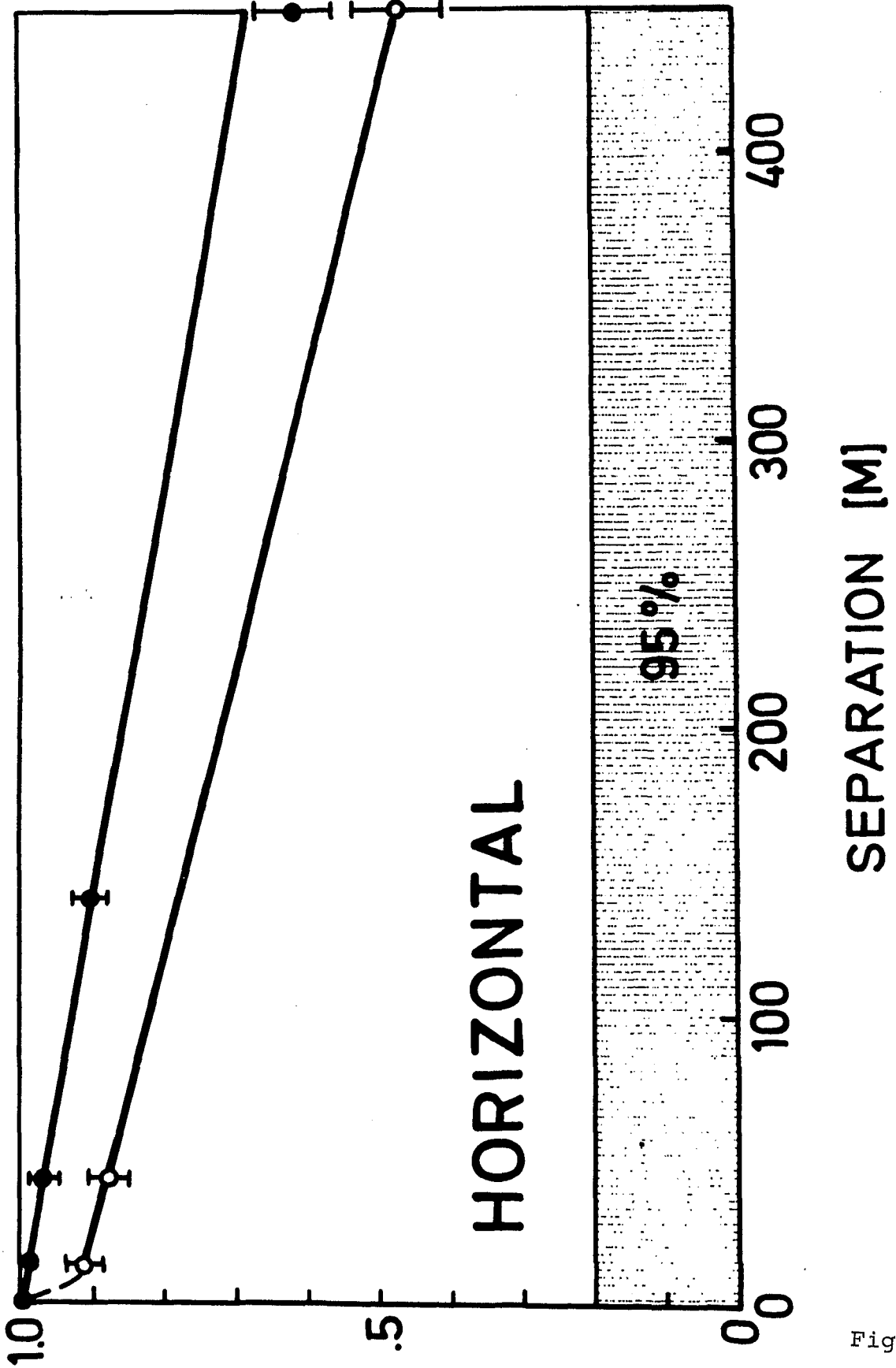


Fig. V.23

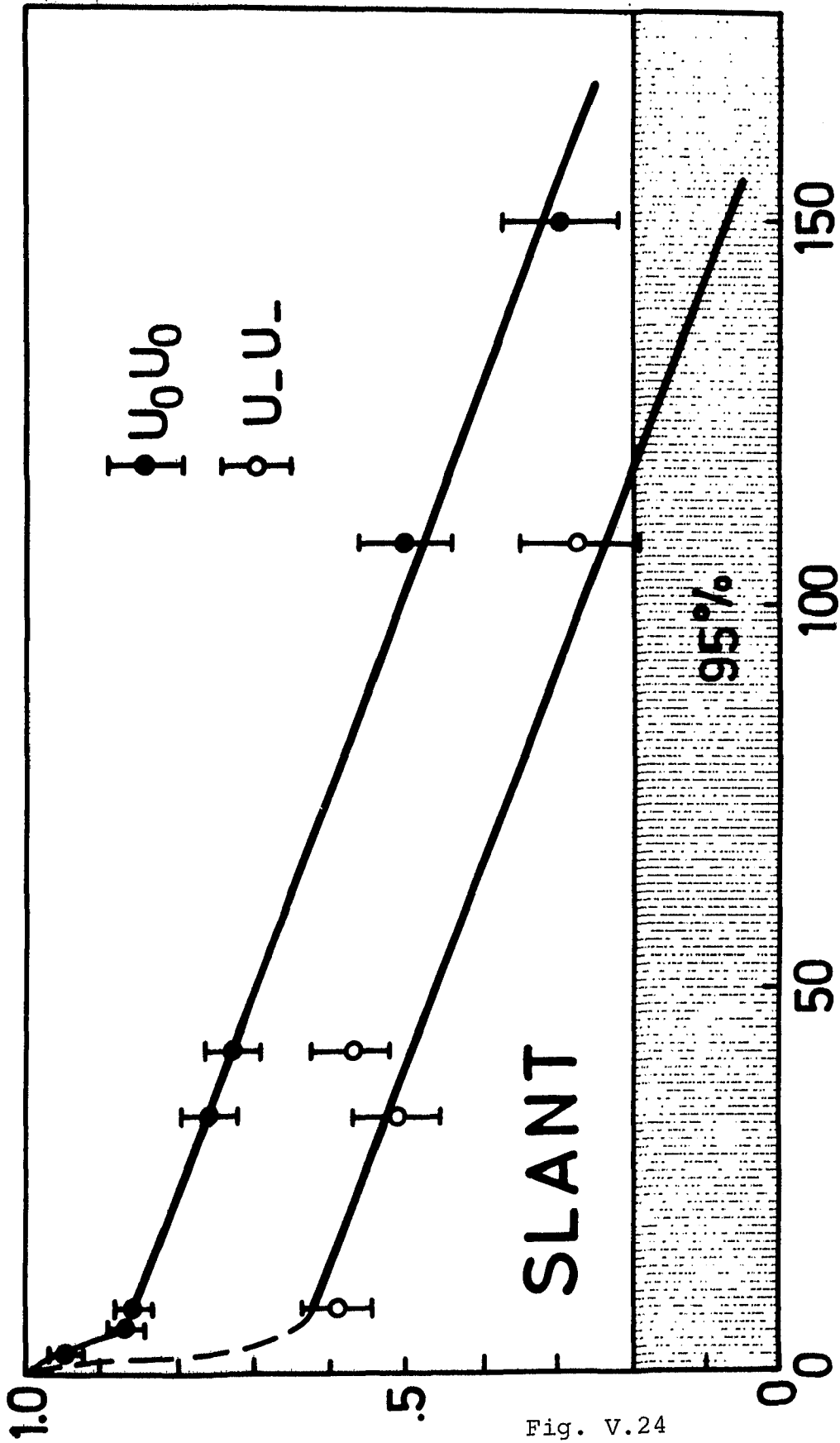


Fig. V.24

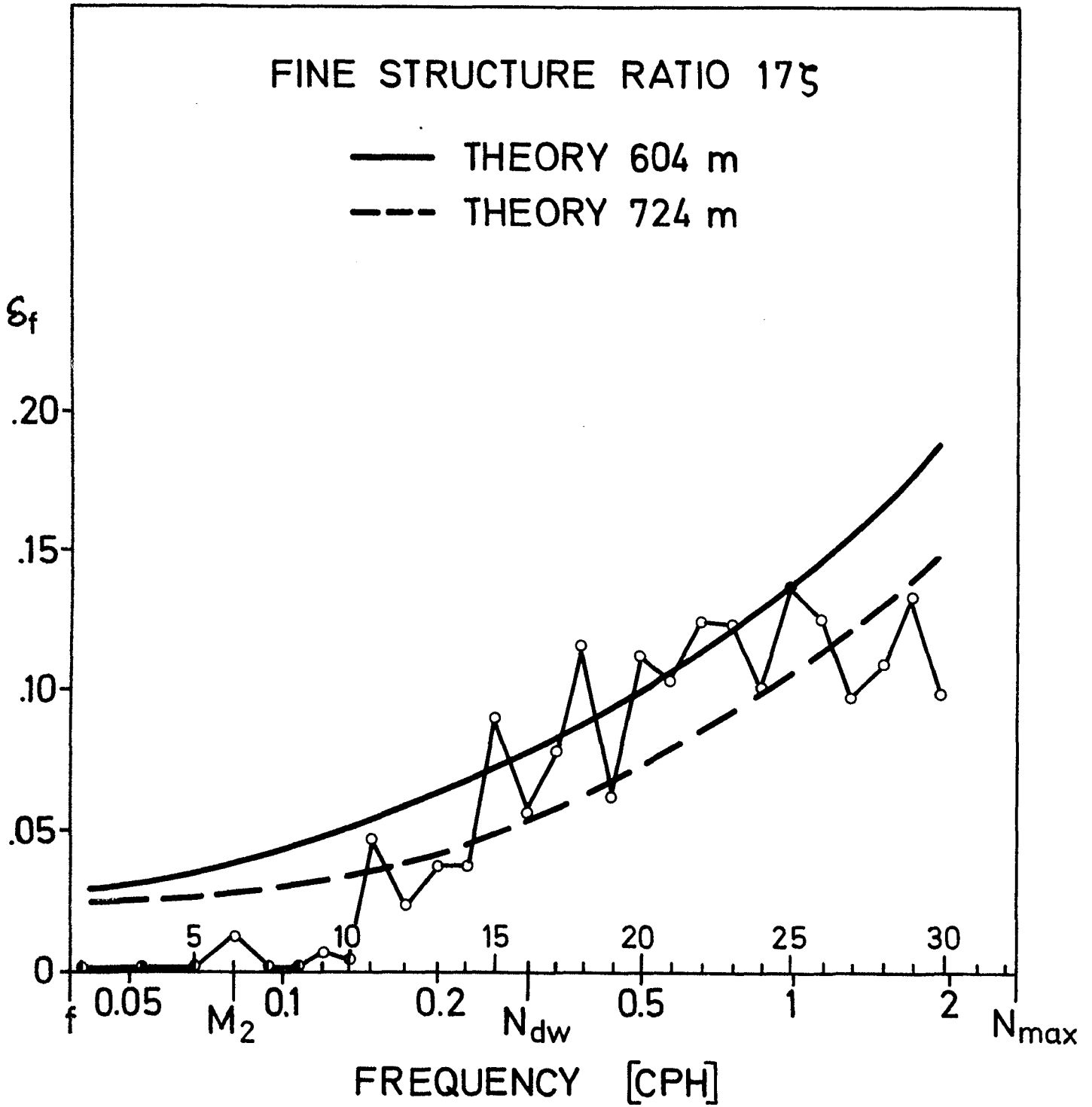


Fig. V.25

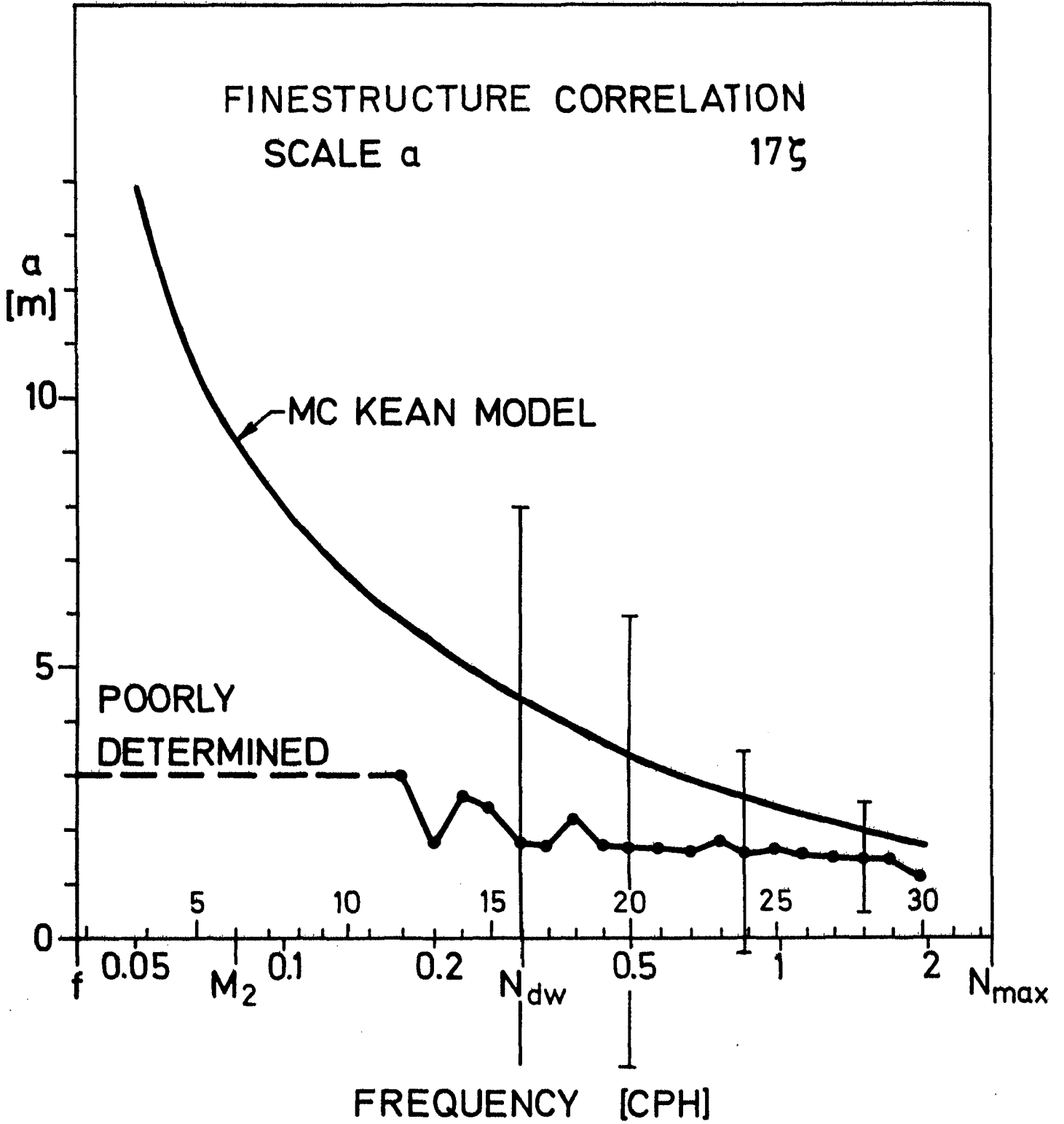


Fig. V.26

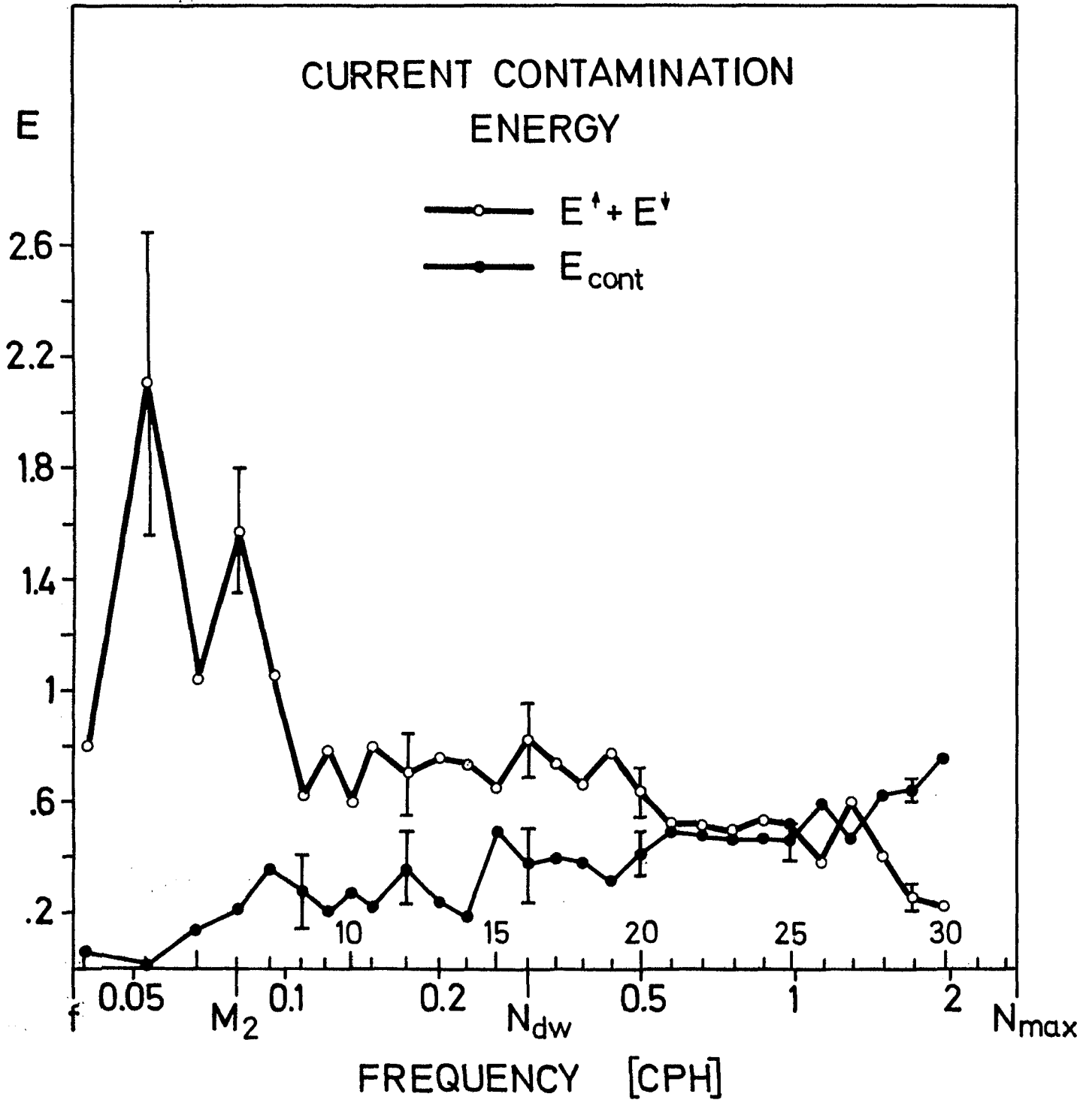


Fig. V.27

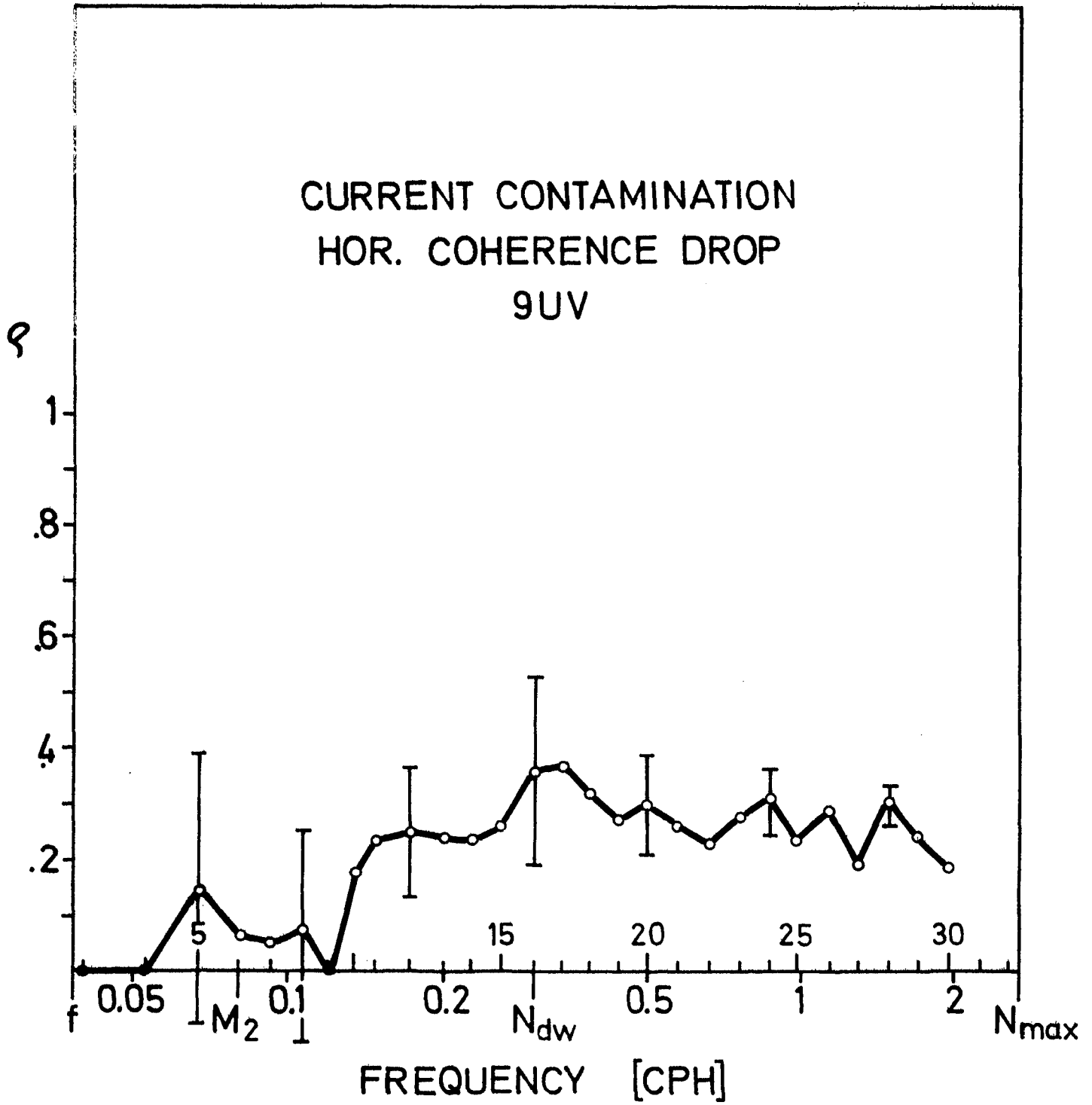


Fig. V.28



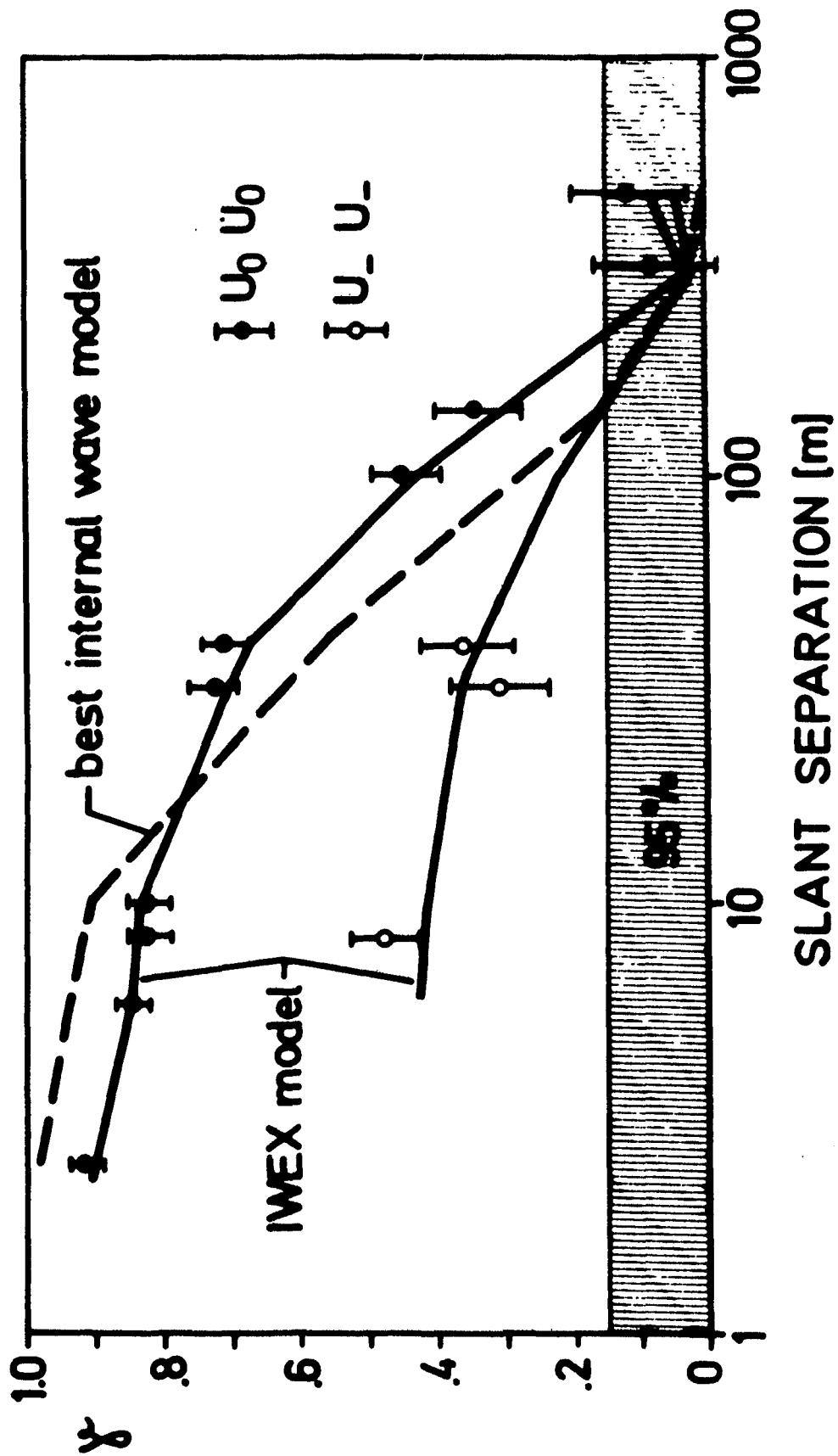


Fig. V.29

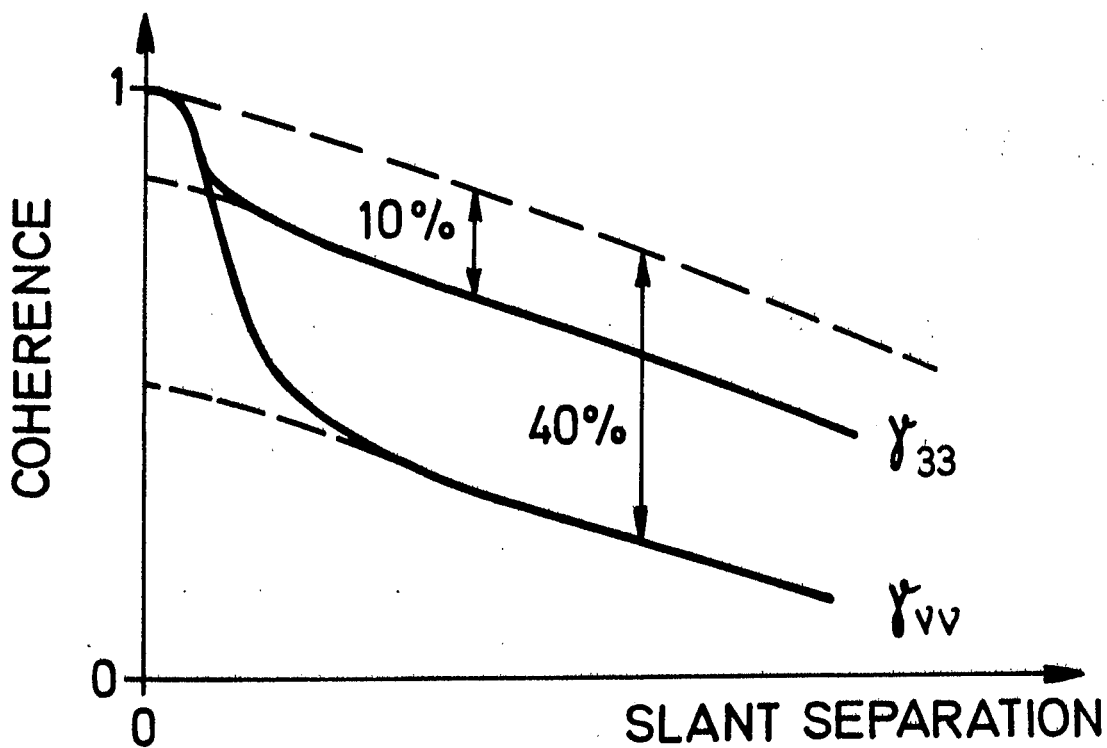
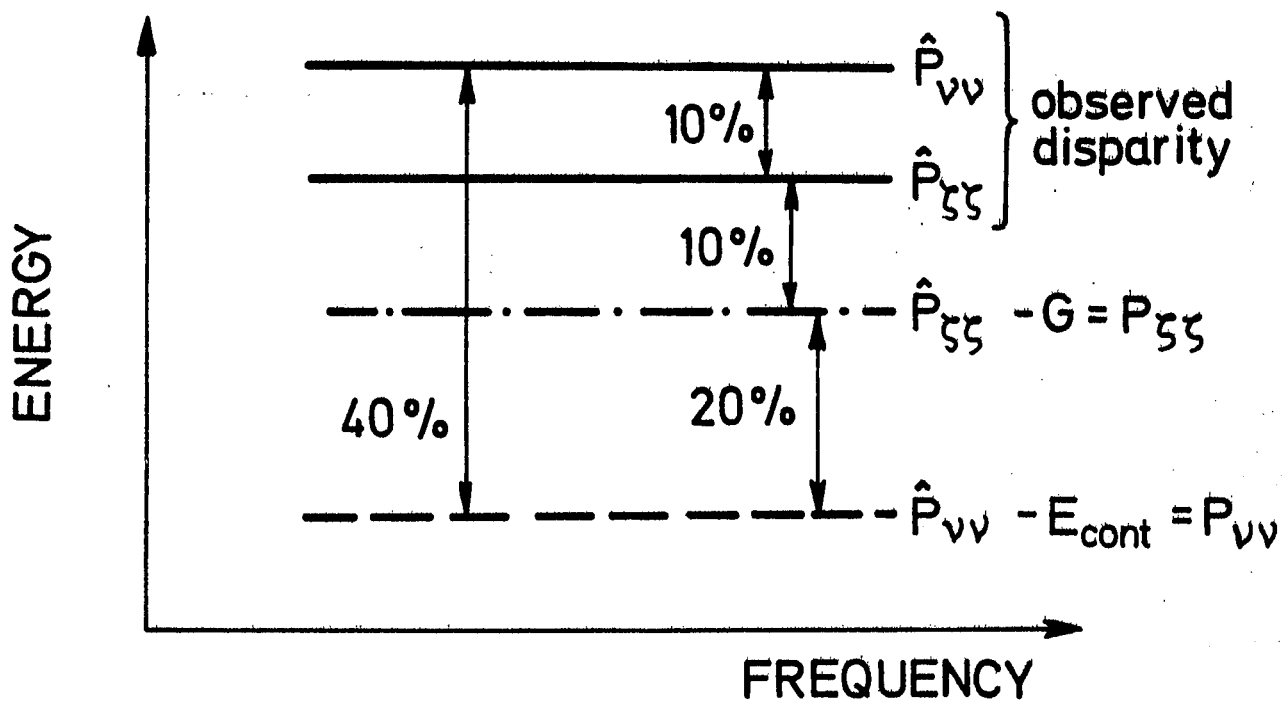


Fig. V.30

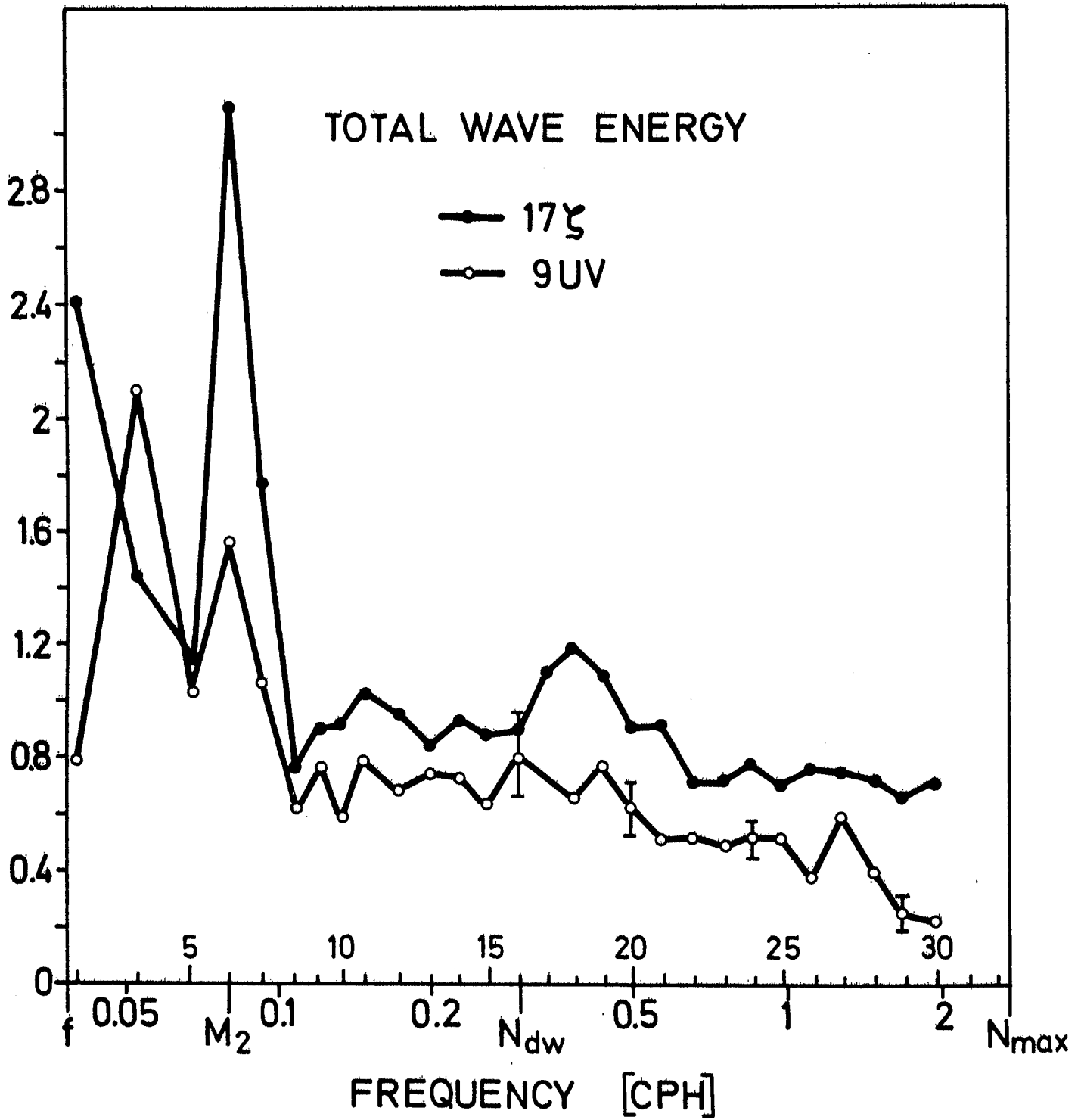


Fig. V.31

# INTERNAL WAVE SPECTRUM

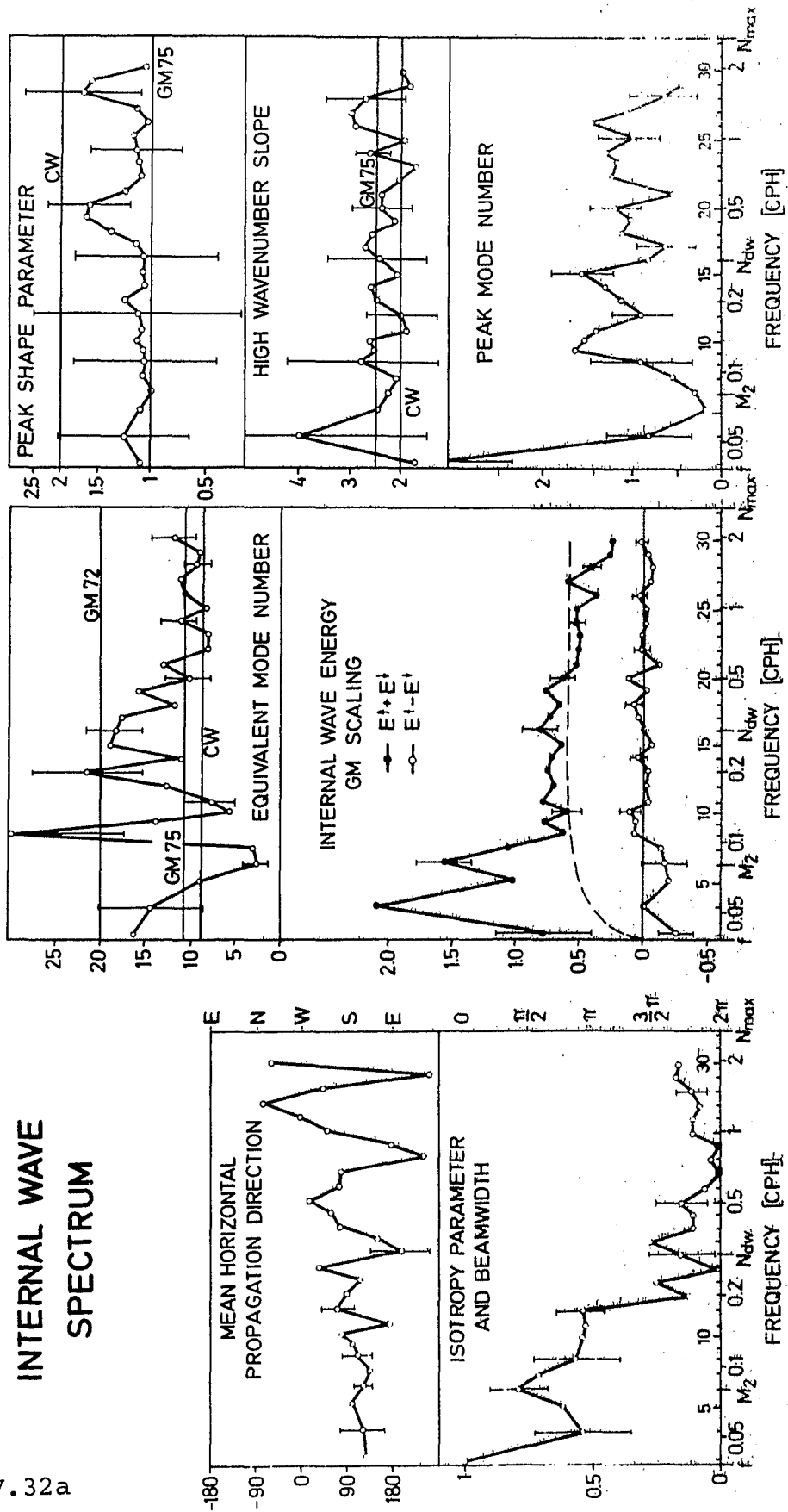


Fig. V.32a

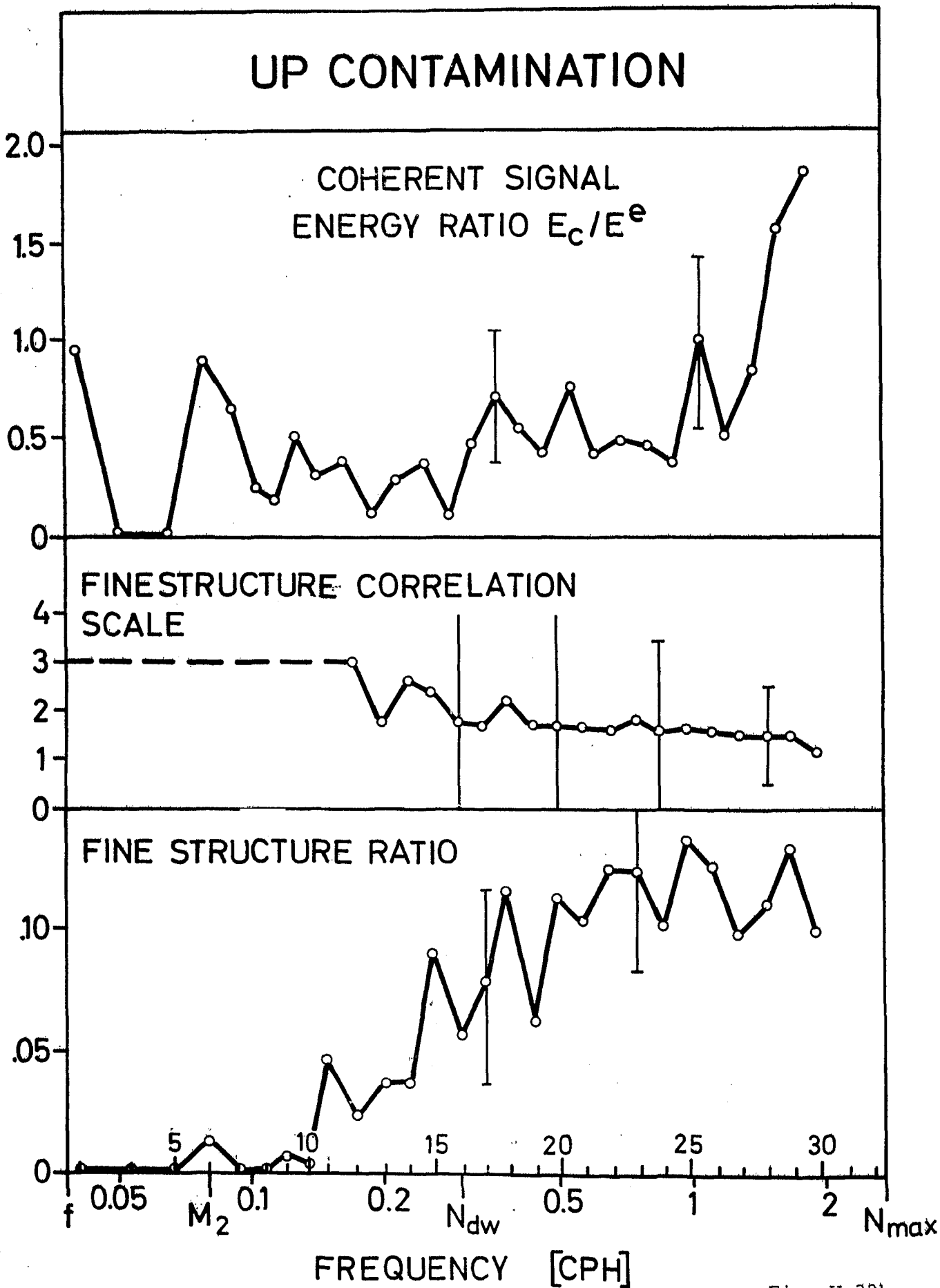


Fig. V.32b

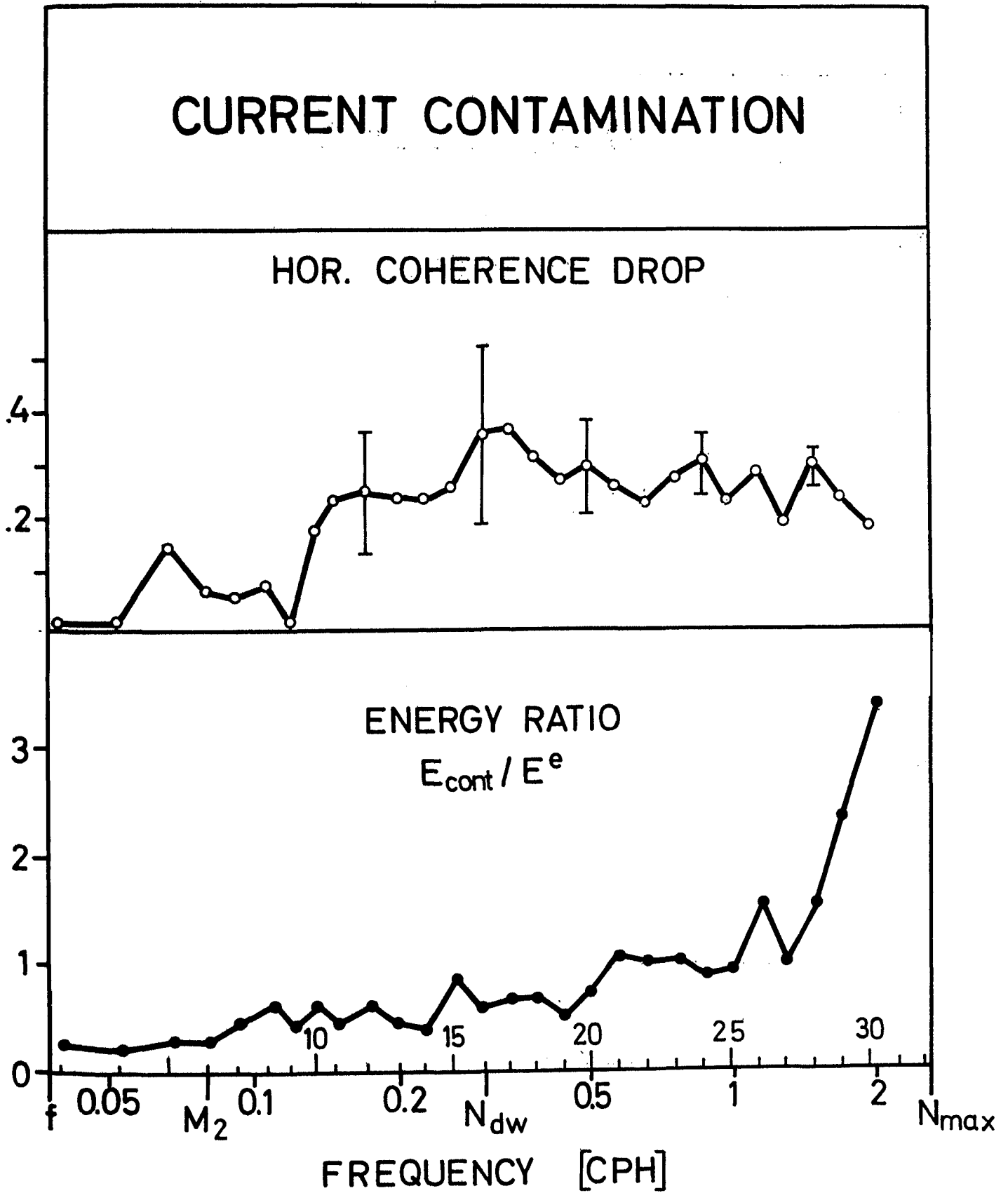


Fig. V.32c

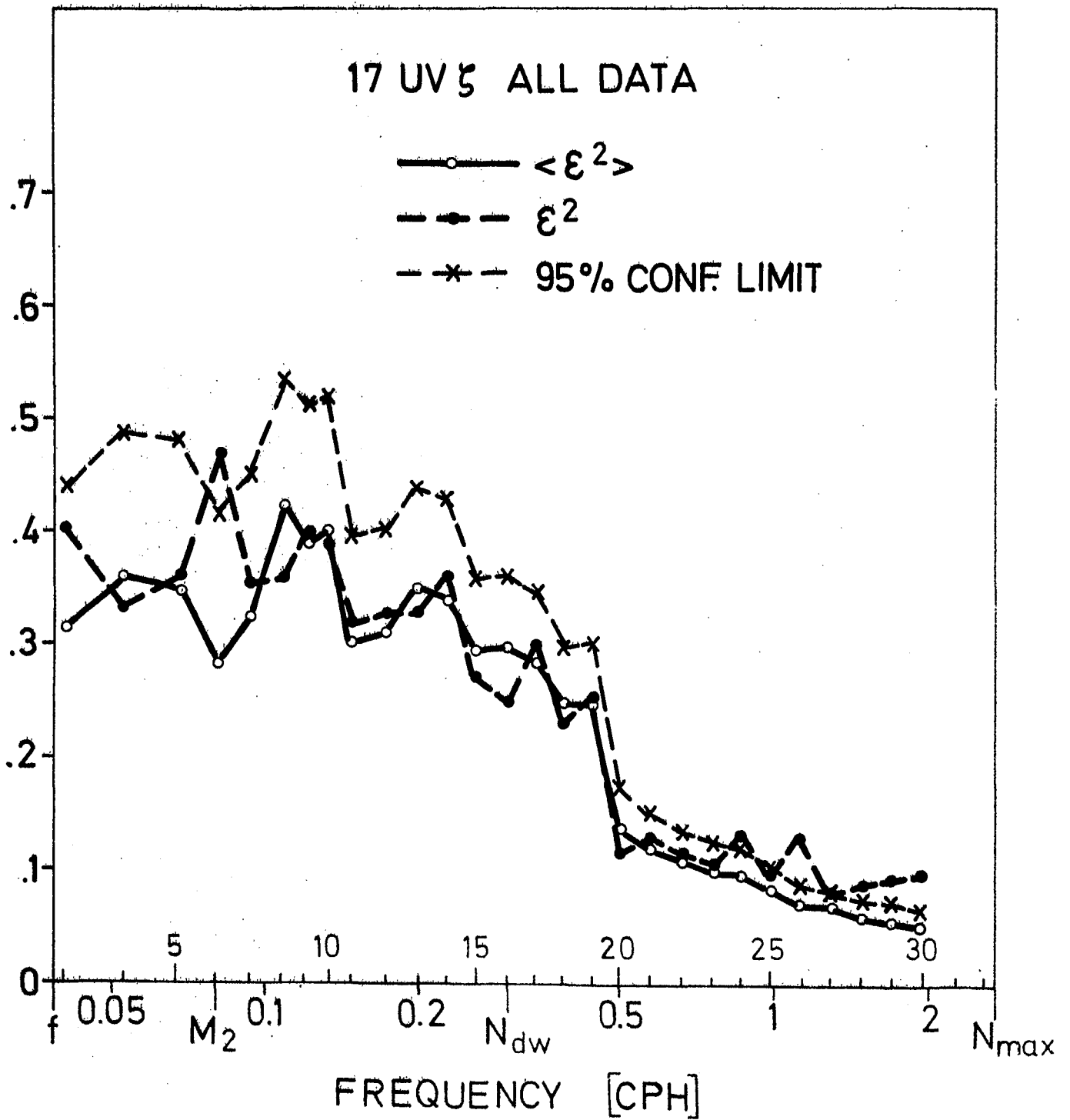


Fig. V.33

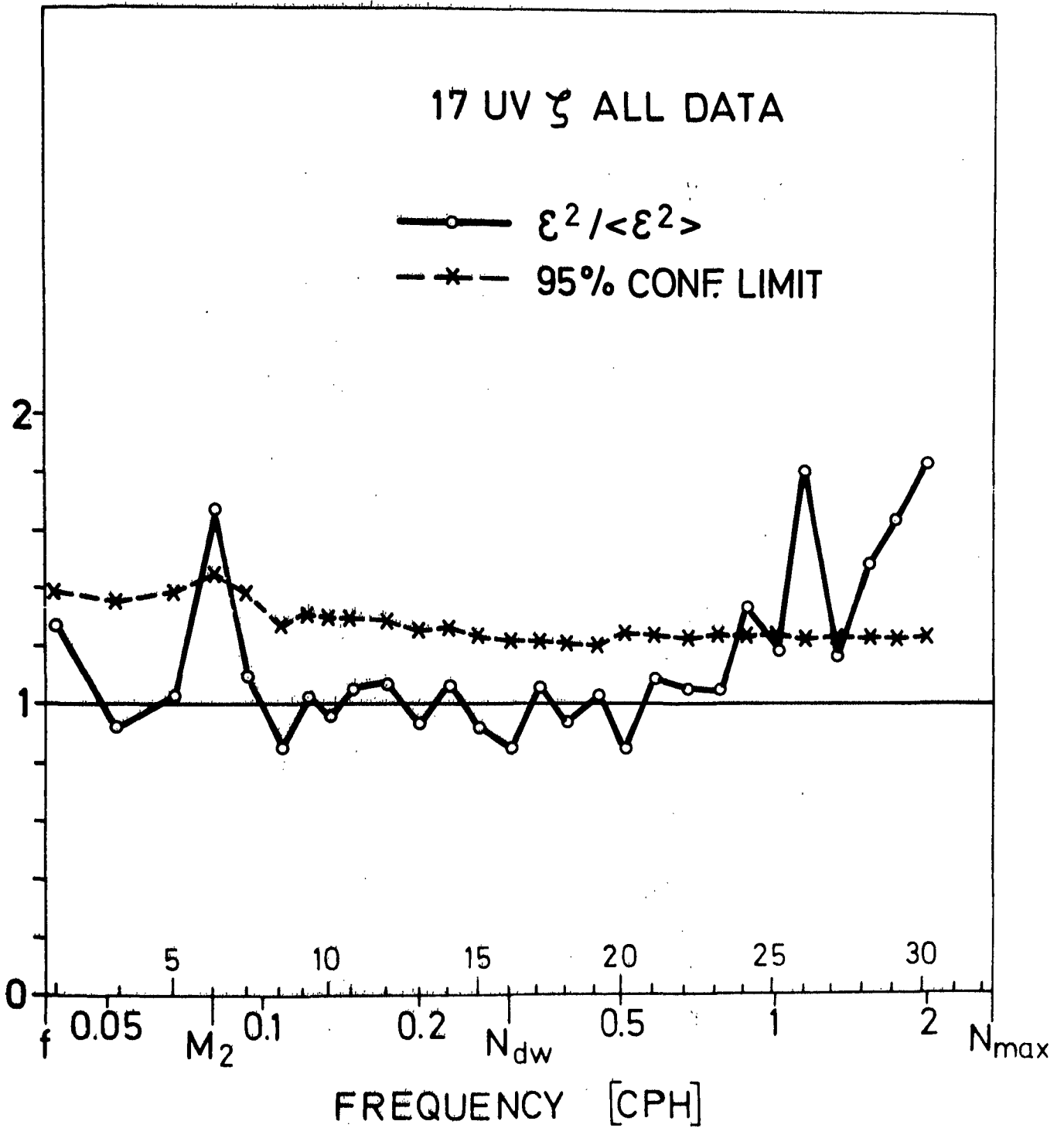


Fig. V.34



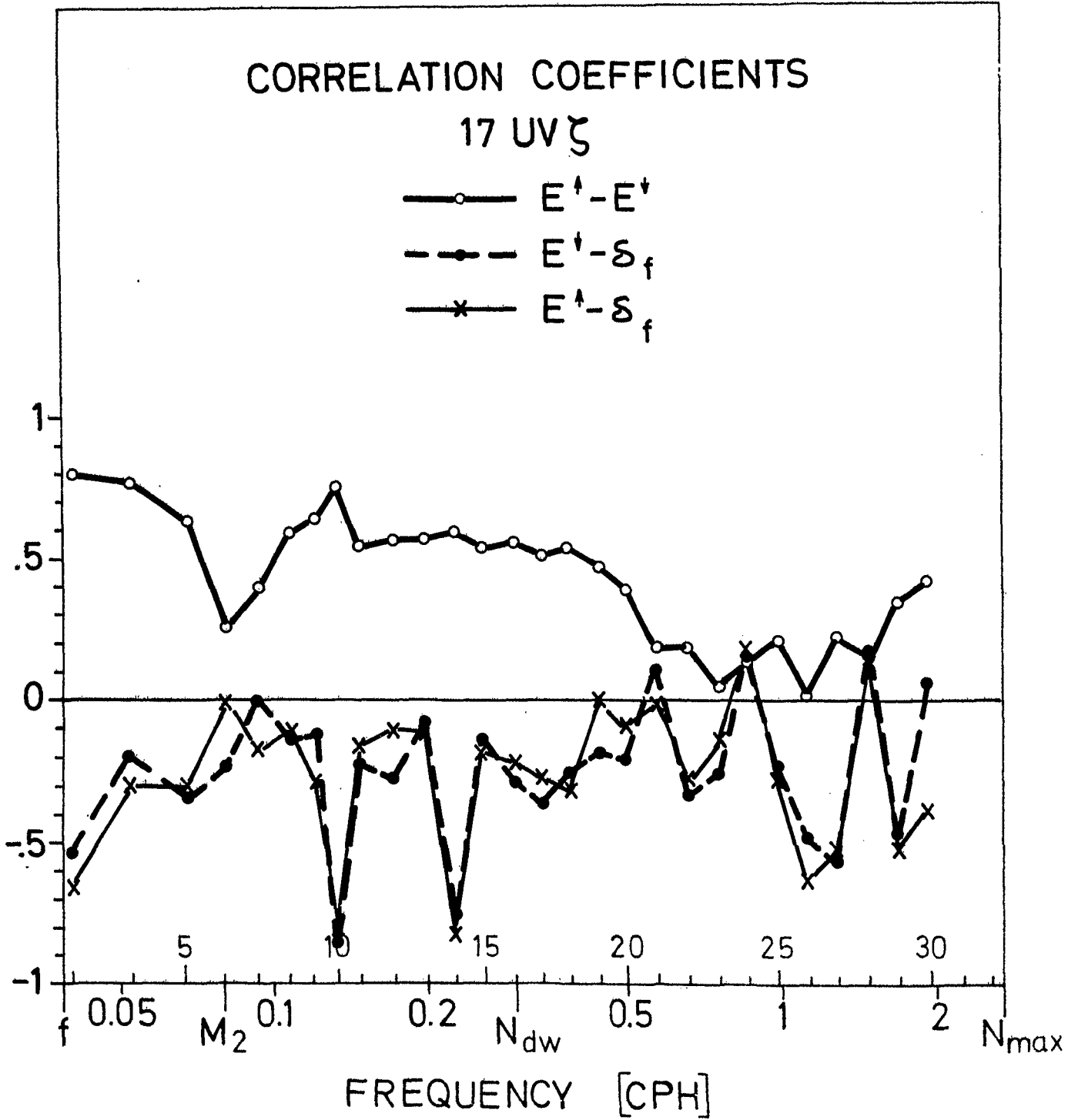


Fig. V.35a

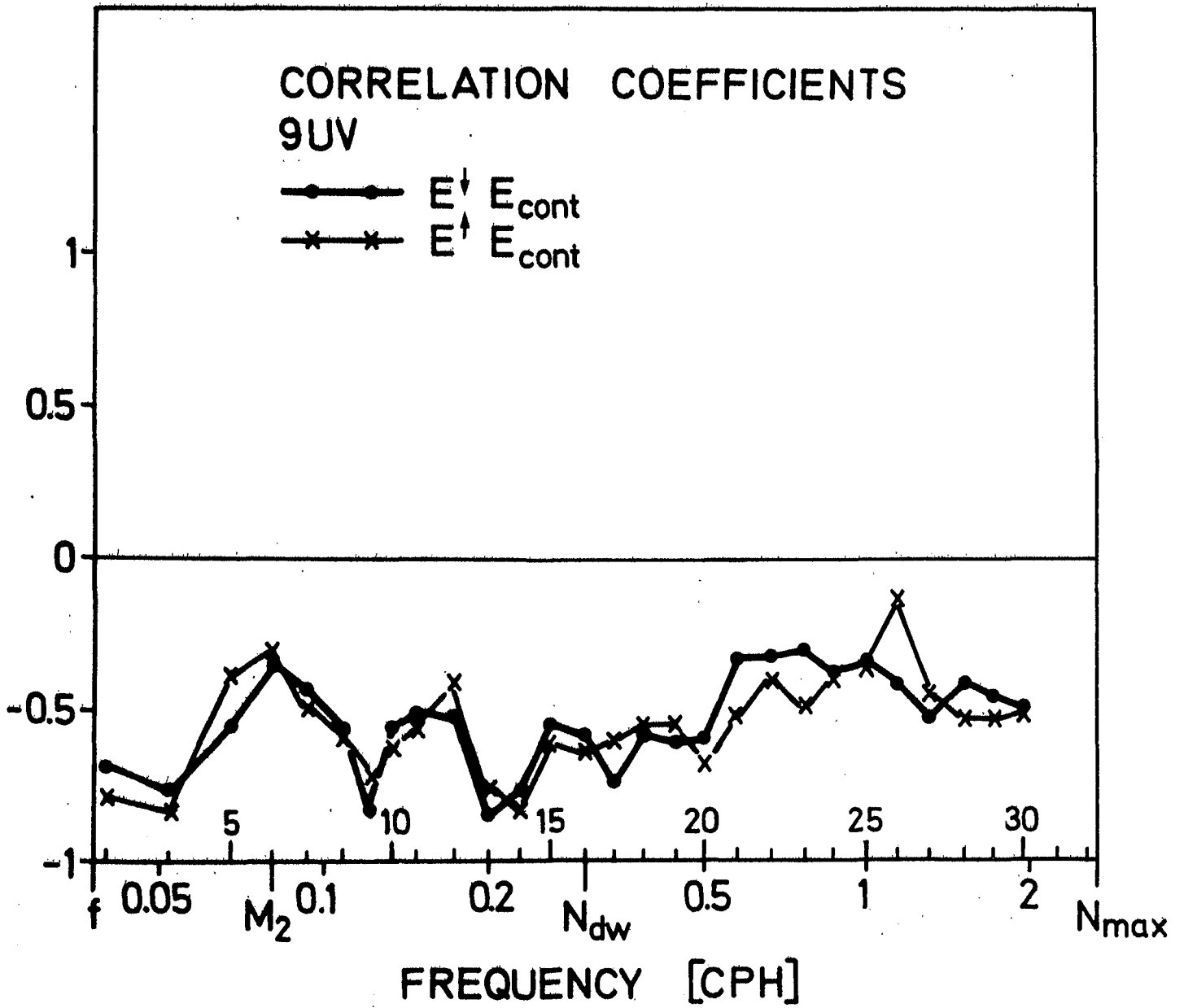


Fig. V.35b

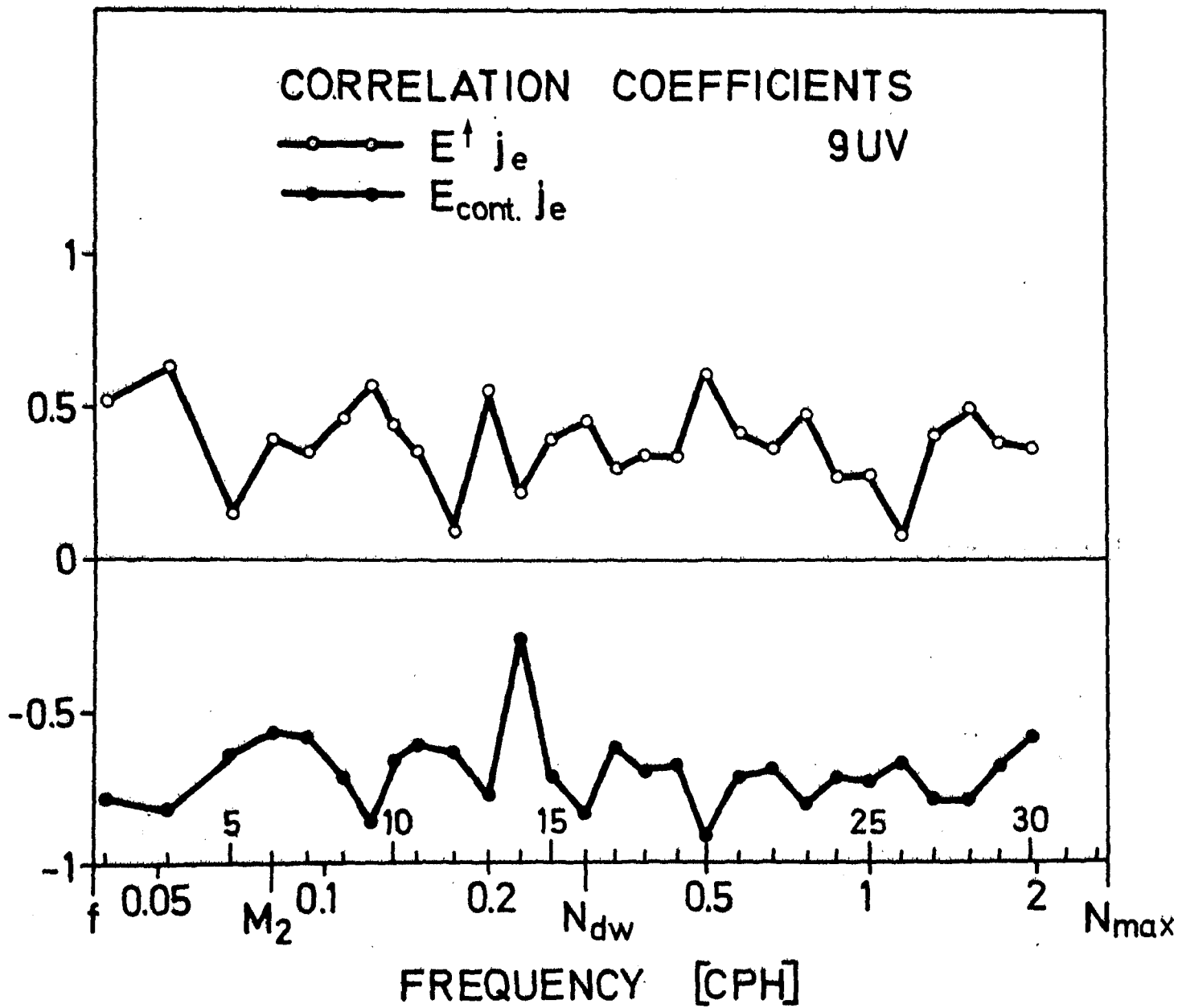


Fig. V.35c

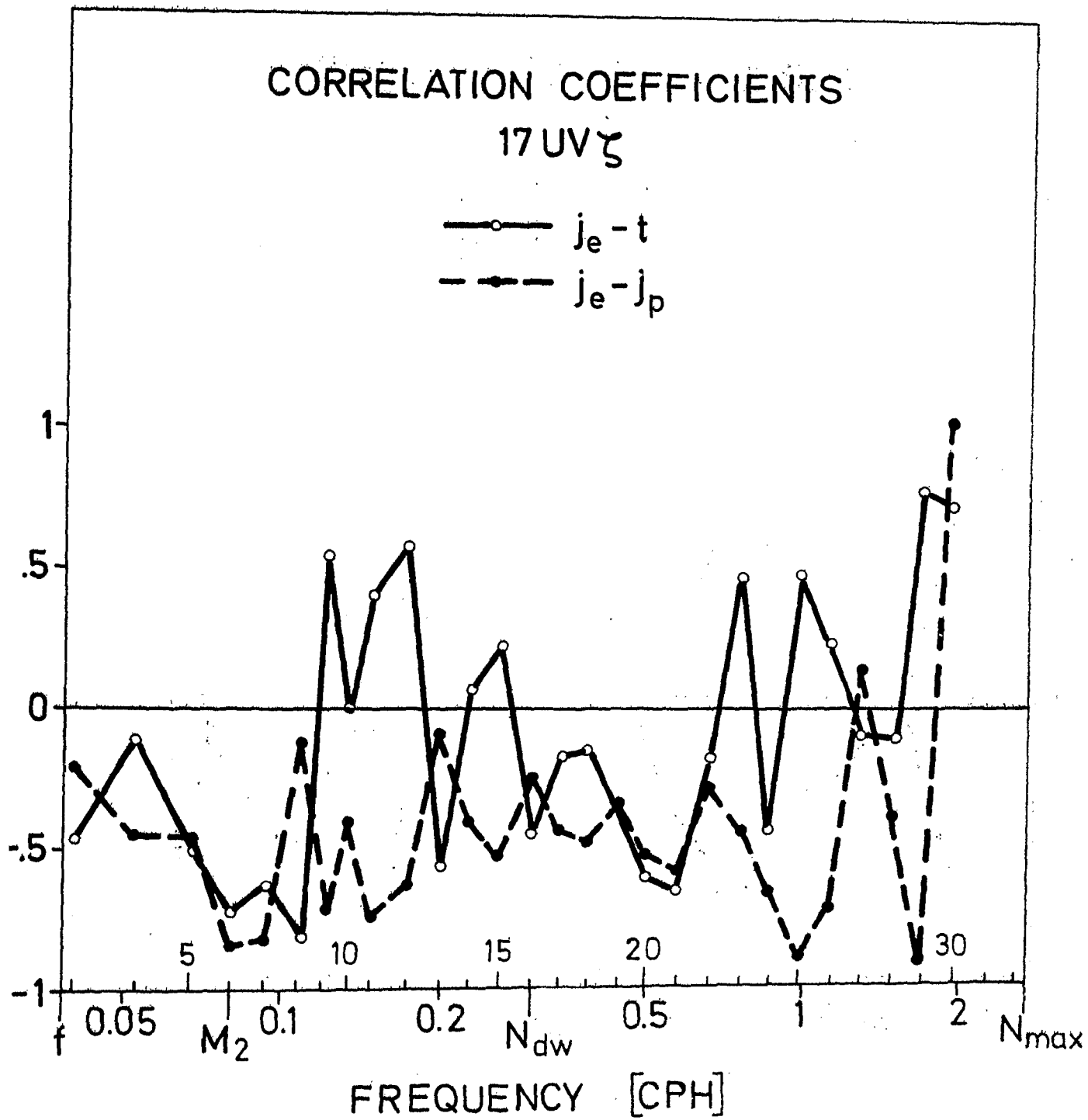


Fig. V.35d

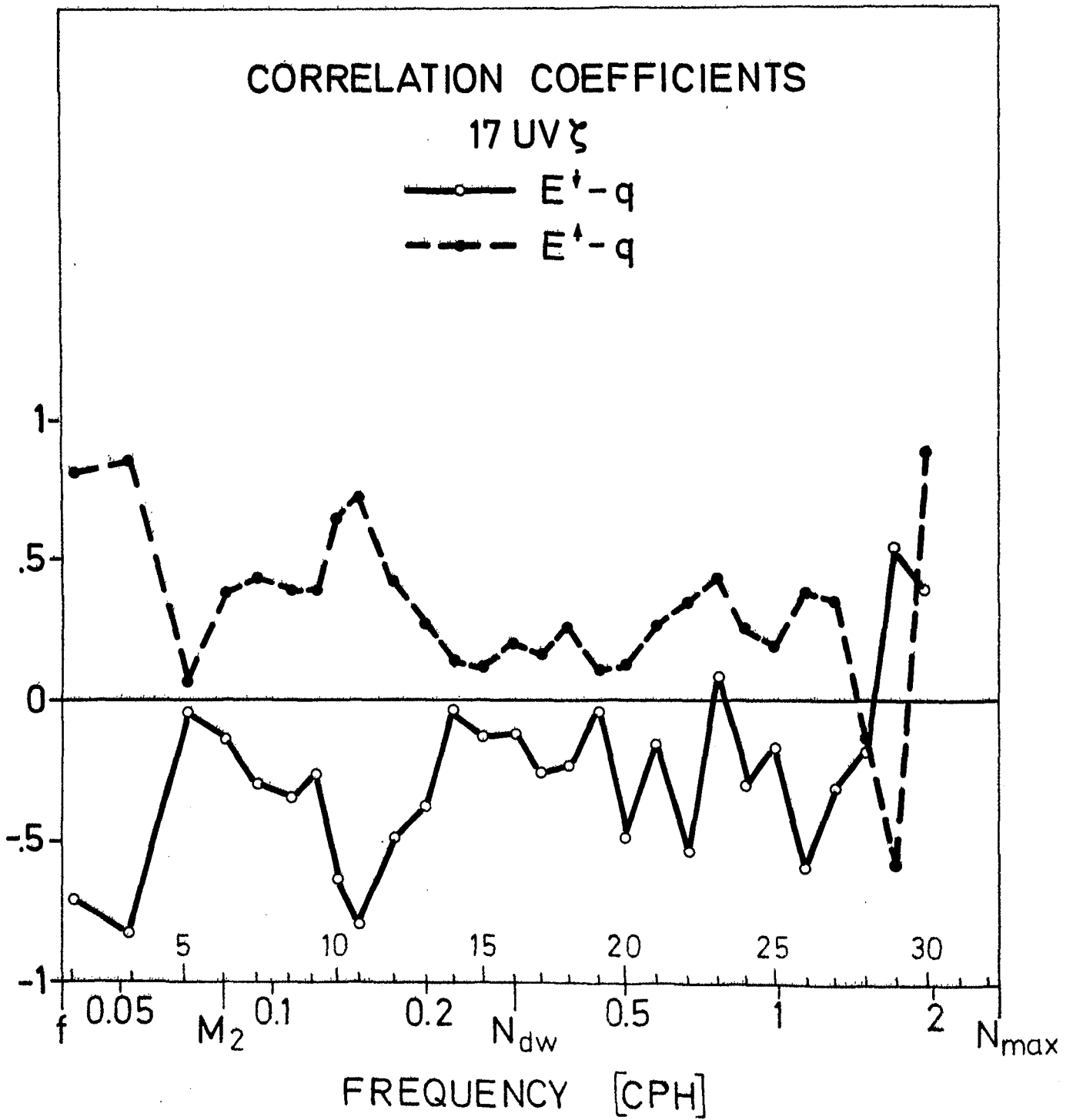


Fig. V.35e

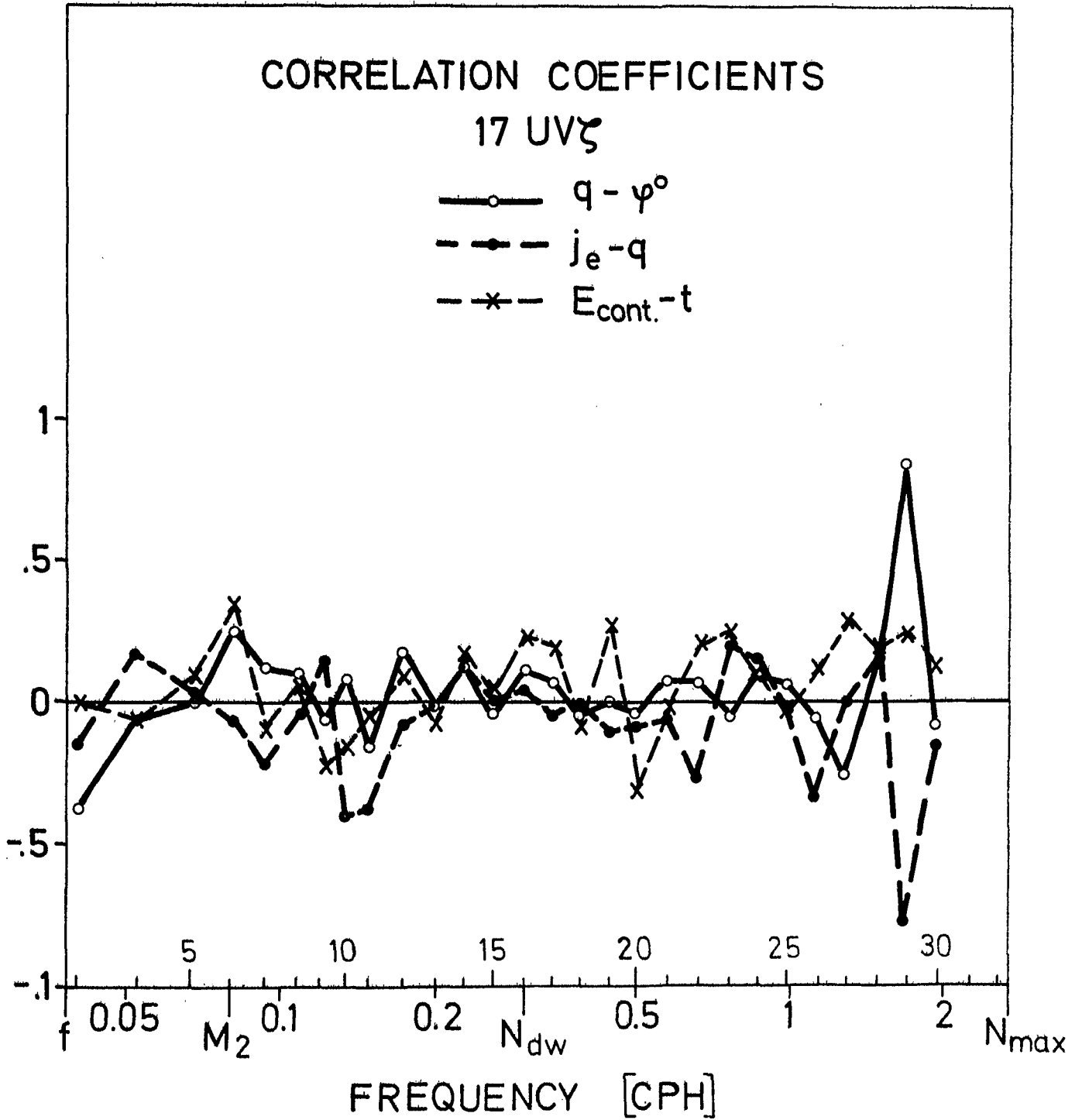


Fig. V.35f

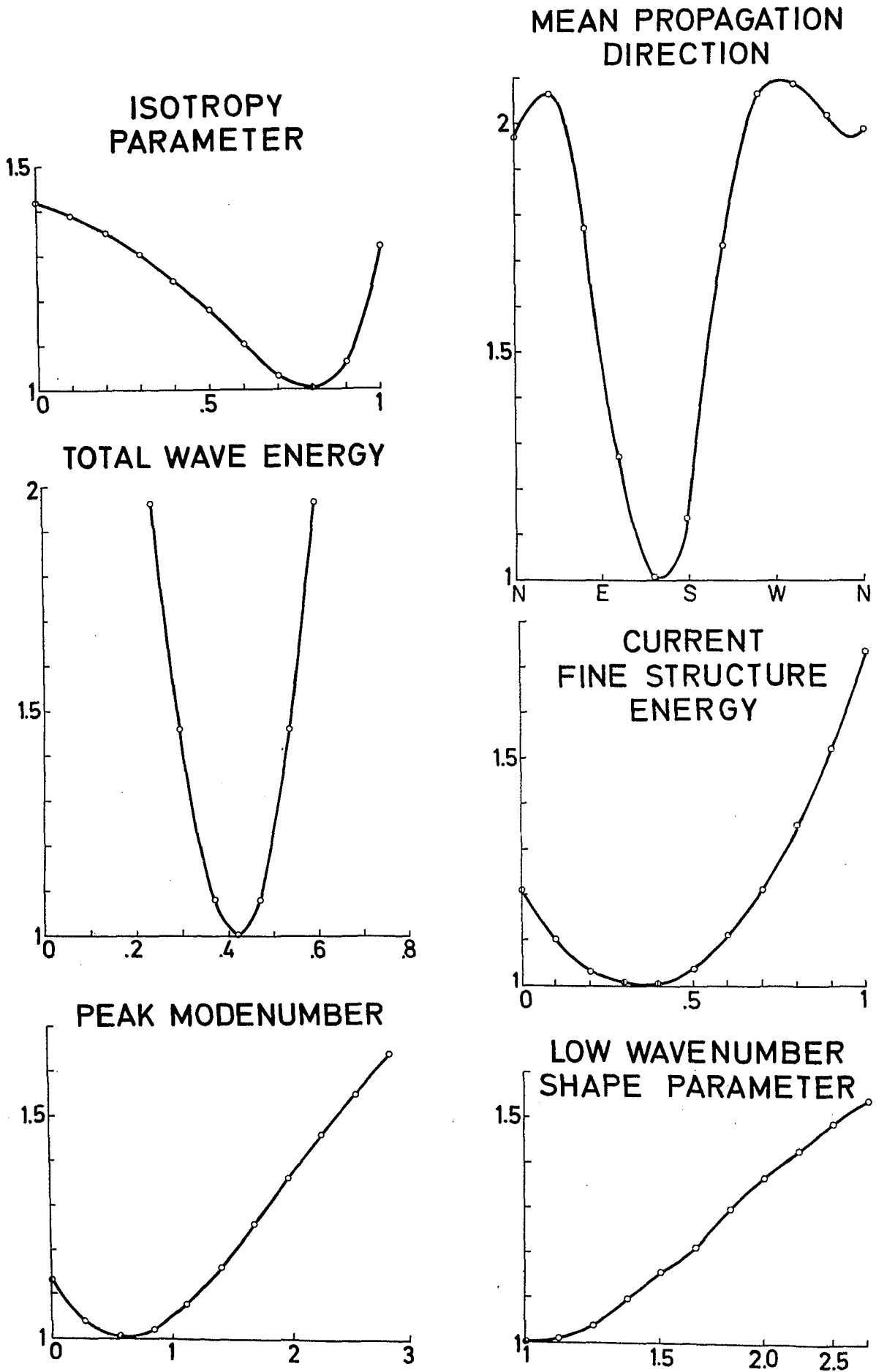


Fig. V.36

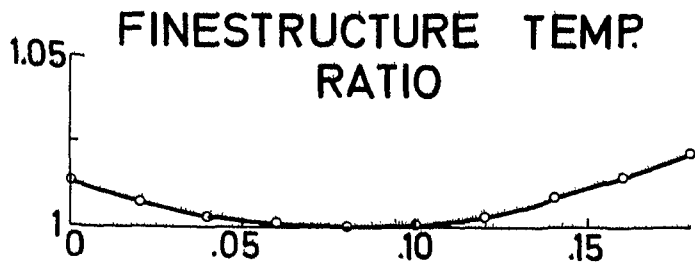
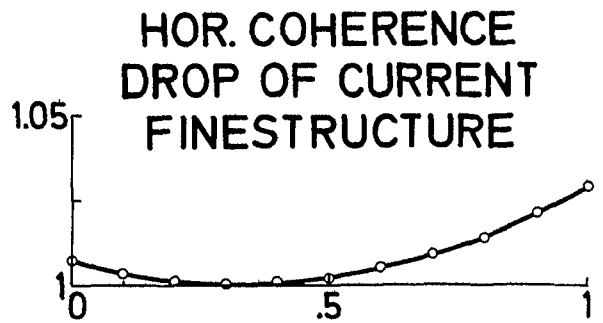
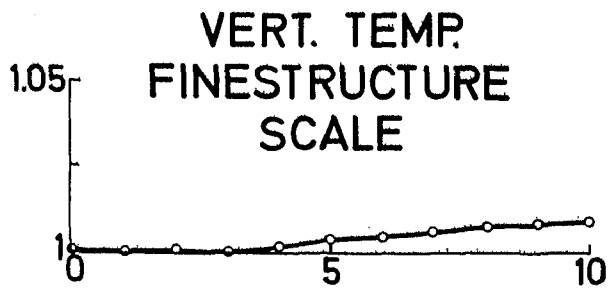
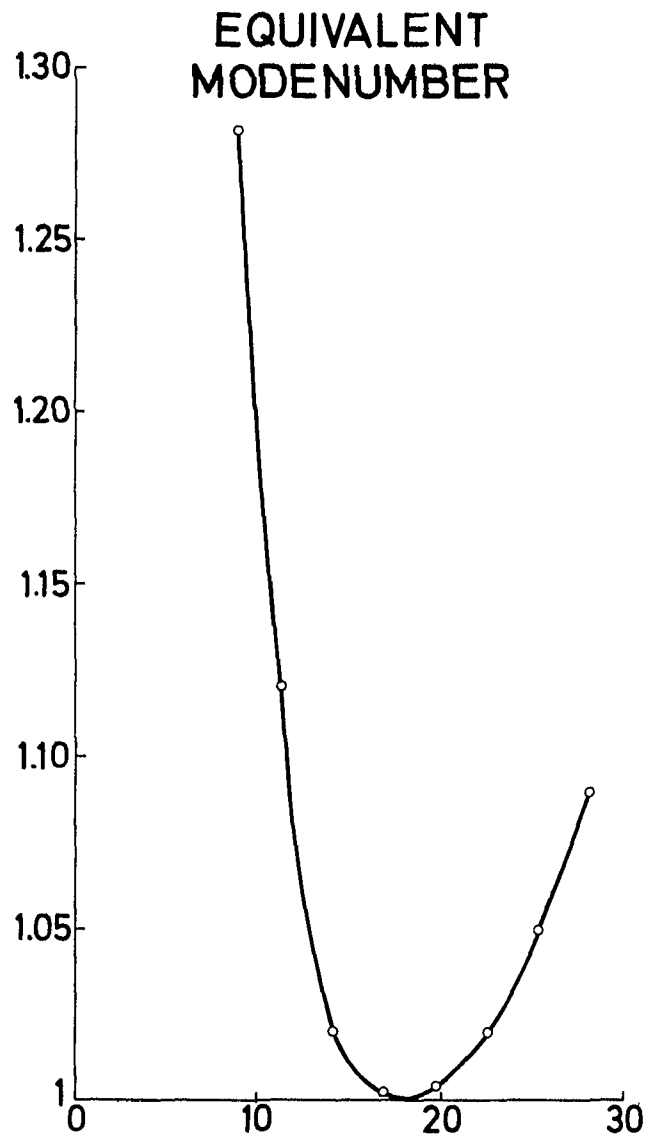
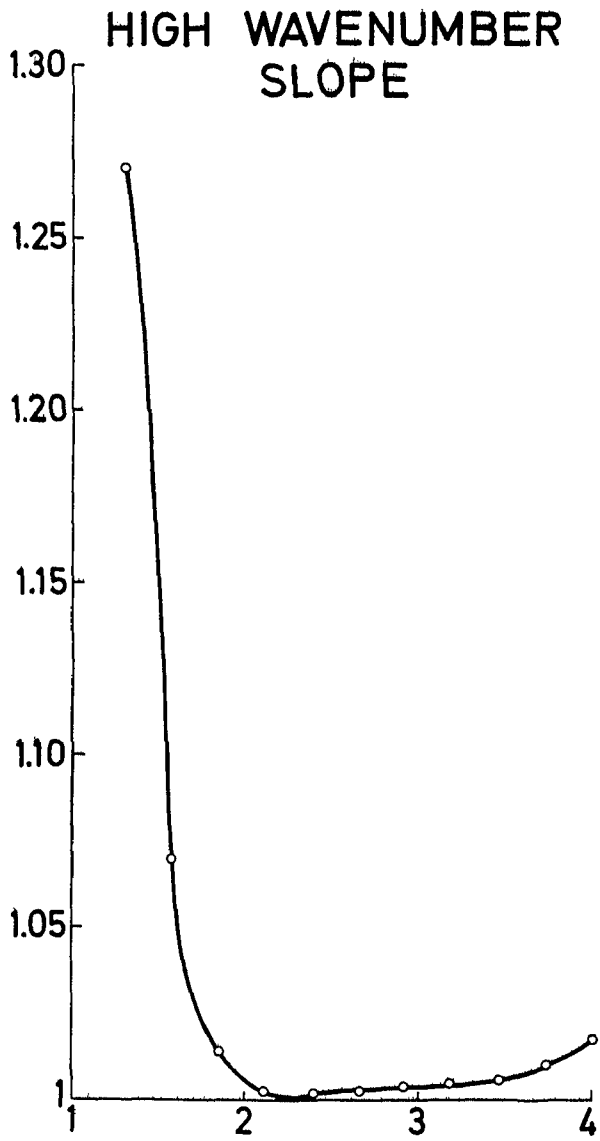


Fig. V.36